AD_____

Award Number: W81XWH-07-1-0368

TITLE: Understanding the Function of Tuberous Sclerosis ComplexGenes in Neural Development: Roles in Synapse Assembly and Axon Guidance

PRINCIPAL INVESTIGATOR: Scott B. Selleck

CONTRACTING ORGANIZATION: The Pennsylvania State University,
University Park, PA 16802-7000

REPORT DATE: February 2012

TYPE OF REPORT: Final Report

PREPARED FOR: U.S. Army Medical Research and Materiel Command
Fort Detrick, Maryland 21702-5012

REPORT DOCUMENTATION PAGE

Form Approved
OMB No. 0704-0188

1. REPORT DATE *(DD-MM-YYYY)*	2. REPORT TYPE	3. DATES COVERED *(From - To)*
February 2012	Final	1 JUL 2007 - 30 NOV 2011

4. TITLE AND SUBTITLE
Understanding the Function of Tuberous Sclerosis Complex Genes in Neural Development: Roles in Synapse Assembly and Axon Guidance

5a. CONTRACT NUMBER

5b. GRANT NUMBER
W81XWH-07-1-0368

5c. PROGRAM ELEMENT NUMBER

6. AUTHOR(S)
Scott B. Selleck

email: sbs24@psu.edu

5d. PROJECT NUMBER

5e. TASK NUMBER

5f. WORK UNIT NUMBER

7. PERFORMING ORGANIZATION NAME(S) AND ADDRESS(ES)
The Pennsylvania State University

University Park, PA 16802-7000

8. PERFORMING ORGANIZATION REPORT NUMBER

9. SPONSORING / MONITORING AGENCY NAME(S) AND ADDRESS(ES)
U.S. Army Medical Research and Materiel Command
Fort Detrick, Maryland 21702-5012

10. SPONSOR/MONITOR'S ACRONYM(S)

11. SPONSOR/MONITOR'S REPORT NUMBER(S)

12. DISTRIBUTION / AVAILABILITY STATEMENT
Approved for public release; distribution unlimited

13. SUPPLEMENTARY NOTES

14. ABSTRACT

The goal of our project was to use the fruitfly *Drosophila melanogaster,* to identify molecular mechanisms affecting nervous system development and behavior that occur as a consequence of Tsc-Tor-Rheb signaling disruption, mimicking the types of changes that are known to occur in human patients with tuberous sclerosis. In our first manuscript we established that hyperactivity of the Tor pathway had several important neurodevelopmental consequences, including misrouting of axon guidance in the visual system and synapse overgrowth at the neuromuscular junction. We showed that synapse overgrowth mediated by *Rheb* was insensitive to rapamycin, a Tor Complex 1 inhibitor, suggesting that other Tor-containing complexes mediate these changes in synapse function.

15. SUBJECT TERMS
Tuberous sclerosis, caloric content, synapse assembly, axon guidance, target of rapamycin, nervous system development, Drosophila

16. SECURITY CLASSIFICATION OF:			17. LIMITATION OF ABSTRACT	18. NUMBER OF PAGES	19a. NAME OF RESPONSIBLE PERSON
a. REPORT	b. ABSTRACT	c. THIS PAGE			USAMRMC
U	U	U	UU	64	19b. TELEPHONE NUMBER *(include area code)*

TABLE OF CONTENTS

INTRODUCTION:

The work supported by the DOD TSCRP examined the molecular basis of nervous system assembly mediated by genes in the signaling pathway that includes tuberous sclerosis 1 and 2 (TSC1 and TSC2). This pathway is fully represented in the fruitfly *Drosophila melanogaster* and we took advantage of the detailed molecular genetic, morphological and physiological methods available in this system to characterize how disruption of this pathway alters nervous system function. Our focus was on two elements of nervous system development, axon pathfinding and synapse assembly. The *Drosophila* visual system provides a beautiful model for tracking axon pathfinding during development and we used this system to demonstrate that signaling via the TOR-TSC pathway is critical for axon guidance. We employed the neuromuscular junction of the larval body wall muscles to investigate how TOR-TSC signaling affects events assembly and function of a glutaminergic synapse, which is the principal excitatory synapse in the vertebrate nervous system. We were able to determine what elements of TOR-TSC signaling govern each of these critical processes in neural development and suggest key regulatory points where an intervention could ameliorate the neurological and behavioral effects of TSC1/2 disruption in humans.

BODY:

The following provides the state of work included in the original grant application.

Task 1. To identify the specific signaling components that mediate axon guidance and synapse assembly in response to TSC signaling.

a. Generate null alleles of Drosophila *raptor* (specific component of TORC1) and *rictor* (specific to TORC2) through imprecise excision of existing P element lines. (Months 1-6)

b. Quantify and characterize photoreceptor axon guidance and motoneuron synapse assembly phenotypes in *raptor* and *rictor* mutant animals, under normal and altered Tsc/Tor signaling. (Months 7-12)

c. In neurons with altered Tsc-Tor signaling, determine the activation state of S6K and Akt, critical targets of TORC1 and TORC2 signaling, respectively. (Months 1-4)

d. Characterize axon guidance and synapse assembly phenotypes under normal and altered Tsc/Tor signaling in *S6k* or *Akt* mutant animals, and in the presence of constitutive S6K or Akt activation. (Months 1-12)

Task 2. To characterize the role of actin cytoskeleton dynamics in Tsc/Tor-dependent axon guidance and synpatogenesis phenotypes.

a. Determine activity and phosphorylation state of candidate cytoskeletal regulators (RhoA, Rac1, Pak, Rok) in *Tsc1* mutant neurons from eye imaginal disc extracts. (Months 12-24)

b. Perform genetic interaction and epistasis analysis between Tsc-Tor pathway components and cytoskeletal regulators Lim1 kinase and cofilin. (Months 12-24)

Task 3. To characterize the physiological and structural alterations at the neuromuscular junction that result from dysregulation of Tsc, Tor, and Rheb function to determine how this pathway affects synaptic function.

a. Assess the number of active zones in synapses with increased altered Rheb, Tsc1,Tsc2 or Tor function.

b. Measure the size of two critical synaptic vesicle pools, the readily releasable pool, and the reserve pool, to determine how loss of Tsc function, and activation of Rheb produce a synapse with enhanced signaling capacity.

What follows is a point-by-point description of our findings pertinent to each of these specific tasks.

Task 1a. Generate null alleles of *Drosophila raptor* (specific component of TORC1) and *rictor* (specific to TORC2) through imprecise excision of existing P element lines. (Months 1-6)
While in the process of generating mutant alleles of *rictor* and *raptor,* two genetic components affecting TORC1 (TOR complex 1) and TORC2 (TOR complex 2) signaling respectively, mutants or RNA interfering constructs (or both) became available through the efforts of other laboratories.

We used these tools to determine how *raptor* and *rictor* signaling affected the two primary phenotypes we examined, disruption of axon guidance in the visual system and synapse growth of the larval neuromuscular junction. The following is the relevant excerpt from the abstract of the paper published describing this and other findings(1):

> "While axon guidance and behavioral phenotypes were affected by altering the function of a Tor complex 1 (TorC1) component, Raptor, or a TORC1 downstream element (S6k), synapse overgrowth was only suppressed by reducing the function of Tor complex 2 (TorC2) components (Rictor, Sin1). These findings demonstrate that different inputs to Tor signaling have distinct activities in nervous system development, and that Tor provides an important connection between nutrient-energy sensing systems and patterning of the nervous system.

These findings showed that axon guidance and synapse growth were separable functions of TOR-TSC signaling, and suggests that both of these pathways must be regulated to insure normal neural development. The experimental methods and detailed findings are found in the attached Appendices.

Task 1b. Quantify and characterize photoreceptor axon guidance and motoneuron synapse assembly phenotypes in *raptor* and *rictor* mutant animals, under normal and altered Tsc/Tor signaling.
Most of our analysis for this task was directed at determining the effect of compromising *raptor* or *rictor* function in the context of hyperactivation of Tor signaling, the situation that occurs in tuberous sclerosis. These findings were published in Dimitroff et al. (2012). Our results were summarized in the following segment of our paper as outlined above: "While axon guidance and behavioral phenotypes were affected by altering the function of a Tor complex 1 (TorC1) component, Raptor, or a TORC1 downstream element (S6k), synapse overgrowth was only suppressed by reducing the function of Tor complex 2 (TorC2) components (Rictor, Sin1). These findings demonstrate that different inputs to Tor signaling have distinct activities in nervous system development, and that Tor provides an important connection between nutrient-energy sensing systems and patterning of the nervous system."

Task 1c. In neurons with altered Tsc-Tor signaling, determine the activation state of S6K and Akt, critical targets of TORC1 and TORC2 signaling, respectively.
This proved a difficult task with the antibody reagents that were available at the time. We wanted to use phospho-S6K and –Akt specific antibodies in whole mount preparations to detect the activated forms of these signaling molecules as well as their physical location in cells. The antibodies available did not provide signal in a whole-mount preparation. They were originally described for use with Western blots and unfortunately did not work with fixed, whole-mount brain preparations.

Task 1d. Characterize axon guidance and synapse assembly phenotypes under normal and altered Tsc/Tor signaling in *S6k* or *Akt* mutant animals, and in the presence of constitutive S6K or Akt activation.

We did an extensive amount of work, primarily on *Akt*. Our initial studies demonstrated that *Akt* had a critical function in the assembly of postsynaptic specializations and we focused our efforts on those findings that resulted in a publication in *Dev Neurobiology (2)*. A summary of our findings is as follows: "The Akt family of serine-threonine kinases integrates a myriad of signals governing cell proliferation, apoptosis, glucose metabolism, and cytoskeletal organization. Akt affects neuronal morphology and function, influencing dendrite growth and the expression of ion channels. Akt is also an integral element of PI3Kinase-target of rapamycin (TOR)-Rheb signaling, a pathway that affects synapse assembly in both vertebrates and Drosophila. Our recent findings demonstrated that disruption of this pathway in Drosophila is responsible for a number of neurodevelopmental deficits that may also affect phenotypes associated with tuberous sclerosis complex, a disorder resulting from mutations compromising the TSC1/TSC2 complex, an inhibitor of TOR (Dimitroff et al., 2012). Therefore, we examined the role of

Akt in the assembly and physiological function of the Drosophila neuromuscular junction (NMJ), a glutamatergic synapse that displays developmental and activity-dependent plasticity. The single Drosophila Akt family member, Akt1 selectively altered the postsynaptic targeting of one glutamate receptor subunit, GluRIIA, and was required for the expansion of a specialized postsynaptic membrane compartment, the subsynaptic reticulum (SSR). Several lines of evidence indicated that Akt1 influences SSR assembly by regulation of Gtaxin, a Drosophila t-SNARE protein (Gorczyca et al., 2007) in a manner independent of the mislocalization of GluRIIA. Our findings show that Akt1 governs two critical elements of synapse development, neurotransmitter receptor localization, and postsynaptic membrane elaboration."

This work established the role of *Akt1* in postsynaptic development and showed the functional separation of its role in elaboration of the specialized post-synaptic membrane, the subsynaptic reticulum (SSR), and the directed localization of the glutamate receptor IIA subunit. We provided a number of lines of evidence that the t-SNARE encoded by *Gtaxin* was required for the Akt1-mediated control of SSR elaboration.

Task 2. We did not work on task 2 on account of interesting findings with Akt and our pursuit of those results.

Task 3. Characterize the physiological and structural alterations at the neuromuscular junction that result from dysregulation of Tsc, Tor, and Rheb function to determine how this pathway affects synaptic function.

The physiological and structural alterations at the NMJ for a number of components of the TOR-TSC-Akt signaling apparatus are described throughout the three papers we have published from the DOD supported work (1-3) using both electrophysiological methods and transmission electron microscopy. However, we did not assess the synaptic pool size using FM1-43, as originally proposed.

A New Task

One important finding that was not originally a proposed task but was nonetheless and important aspect of our DOD-funded work was the discovery that the nutrient and energy-sensing pathway that impinges on TOR-TSC signaling, also influenced phenotypes produced by inappropriate activation of signaling, as occurs in tuberous sclerosis patients. Interestingly, dietary restriction, which could potentially decrease the signaling through this pathway was able to rescue both behavioral and morphological deficits in the nervous system in animals with overexpression of *rheb.* Synapse overgrowth however, was not rescued by the same level of either AMPK expression or dietary restriction (1). This suggests a possible molecular mechanism for the known effects of dietary treatment of seizures, including in patients with tuberous sclerosis. Diets with limited levels of carbohydrate calories (so called ketogenic diets) are known to be effective treatments in some children with intractable seizures.

Statistical Significance.

The work we have described in three manuscripts was all assessed using widely accepted statistical methods to determine the significance of the many findings we have reported. The methods and approaches are all outlined in detail in the refereed and published work provided in the Appendix.

KEY RESEARCH ACCOMPLISHMENTS:

- The goal of our project was to use the fruitfly *Drosophila melanogaster,* to identify molecular mechanisms affecting nervous system development and behavior that occur as a consequence of Tsc-Tor-Rheb signaling disruption, mimicking the types of changes known to occur in human patients with tuberous sclerosis.

- We showed that synapse overgrowth mediated by *Rheb* was insensitive to rapamycin, a Tor Complex 1 inhibitor, suggesting that other Tor-containing complexes mediate these changes in synapse function.

- The second paper established that different Tor-containing complexes (TorC) mediated distinct neurodevelopmental events, allowing us to separate TorC1 and TorC2-dependent processes.

- This work also demonstrated that caloric content was able to affect the severity of behavioral and morphological deficits produced by hyperactivation of the Tor pathway, presumably via the energy or amino acid sensing elements of Tor signaling. This finding was startling to us, and provided a very clear indication that environmental factors, in the form of calorie levels and content, could potentially be used to regulate Tor signaling and the neurological and behavioral consequences of disruptions of that pathway. Our work also suggests that pharmacological intervention of Tor signaling will ultimately need to regulate both TorC1 and TorC2 mediated processes to achieve the best effects.

- The third and final paper describing work supported by the DOD funds, examined a key downstream affector of Tor signaling, *Akt1*. In this work we demonstrated that *Akt1* plays a critical role in two fundamental aspects of synapse assembly, control of neurotransmitter receptor composition and postsynaptic membrane specializations. These findings have implications for a number of behavioral and neurological disorders where Akt function has been implicated, including schizophrenia.

REPORTABLE OUTCOMES:

Three peer-reviewed publications were produced from the DOD grant support.

Pubications resulting from DOD support.

1. Dimitroff B*, et al.* (2012) Diet and energy-sensing inputs affect TorC1-mediated axon misrouting but not TorC2-directed synapse growth in a Drosophila model of tuberous sclerosis. (Translated from eng) *PLoS One* 7(2):e30722 (in eng).
2. Lee HG, Zhao N, Campion BK, Nguyen MM, & Selleck SB (2013) Akt regulates glutamate receptor trafficking and postsynaptic membrane elaboration at the Drosophila neuromuscular junction. (Translated from eng) *Developmental neurobiology* 73(10):723-743 (in eng).
3. Knox S*, et al.* (2007) Mechanisms of TSC-mediated control of synapse assembly and axon guidance. (Translated from eng) *PLoS One* 2(4):e375 (in eng).

Patents, inventions and Research Materials
We do not have any patents or inventions in place or pending based on this DOD sponsored research but all published materials are available to other researchers. For example we receive requests for fly stocks and send out those materials freely. They are all available upon request.

Training supported by DOD award
A number of undergraduate students, PhD students and postdocs have participated in the work supported by the DOD. Individuals who are co-authors on the publications and received training through our work are provided below.

Sarah Knox. Sarah was a postdoctoral fellow in my lab and is now an Assistant Professor at the University of California, San Francisco, Department of Cell & Tissue Biology.

Yi Ren. Yi completed a Master's degree under my direction as is now on staff at the University of Minnesota in the Department of Medicine, Division of Cardiology under the sponsorship of Dr. Garry.

Katie Howe. Katie received her PhD under my direction and now works for the National Marrow Donors Program, with its international headquarters in Minneapolis, MN.

Adrian Watson. Adrian was an undergraduate student in my laboratory at the University of Minnesota and went on to enrolling in the PhD program in Molecular Biology at this institution.

Bridget Campion. Bridget obtained her PhD in my laboratory and is currently teaching at Marquette University in Milwaukee, WI.

H-G. Lee. Dr. Lee was a postdoctoral fellow in my group at Penn State University and is now Research Professor at the Life Science Gwangju Institute of Science and Technology (Gwangju, Republic of Korea).

Na Zhao. Na is currently a PhD student in my group, scheduled to complete her thesis this summer (2014).

CONCLUSION:

When we began this work the prevailing hypothesis was that the neurological manifestations of tuberous sclerosis in humans was the result of the many benign tumors that resulted from loss of *TSC1* or *TSC2* function. There was clinical and pathological data suggesting otherwise, namely that seizures were found in individuals without overt tumors and there was not a correlation between the severity of neurological symptoms and the tumor burden assessed radiologically. We proposed our work to test an alternative hypothesis, that *TSC1/2* affected the signaling of a molecular pathway that alters the development of the nervous system and the function of mature synapses. Our work has contributed to the proof that this is indeed the case, providing a molecular and cellular understanding of this disorder.

Our first paper supported by DOD funds demonstrated that disruption of TOR signaling in the fruit fly *Drosophila* had profound effects on both synapse development and axon guidance. This was one of the initial studies establishing the important of this pathway in fundamental neural development processes. We used a variety of morphological, physiological and genetic methods to establish the phenotypes resulting from disruption of different components of the pathway.

The initial report led us into more mechanistic studies, examining precisely what components of the pathway governed either axon guidance or synapse assembly. Our second paper provided the results from those studies, demonstrating that axon guidance and synapse growth affected by TOR-TSC are molecularly separable processes, governed by two distinct TOR-containing complexes. We also demonstrated that signaling processes that sense energy and nutritional status, and impinge on TOR-TSC signaling, could also affect neurodevelopmental outcomes produced by disruption of TSC. This was in our view a profound result demonstrating the importance of gene-environment interactions in governing the severity of phenotypes produced by a known genetic lesion. It also suggests a mechanism for how the ketogenic diet might control seizures in patients with tuberous sclerosis as well as other epileptic syndromes.

Finally, we examined the function of a key downstream element of TOR-TSC signaling, *Akt1*. Our analysis provided some surprising conclusions, namely that *Akt1* affected the directed targeting of a particular glutamate receptor subunit to the neuromuscular junction. *Akt1* was also required for the normal elaboration of the specialized membrane of the postsynaptic cell. We demonstrated that these two activities are separable, and *Akt1*-mediated control of the t-SNARE *Gtaxin* was likely the mechanism of postsynaptic membrane elaboration. These findings, published in *Developmental Neurobiology,* provided the first evidence that *Akt* is critical for selecting the type and characteristics of neurotransmitter receptors during development and was required for the normal assembly of specialized membrane that organize the synaptic receptor apparatus.

REFERENCES:

1. Dimitroff B, *et al.* (2012) Diet and energy-sensing inputs affect TorC1-mediated axon misrouting but not TorC2-directed synapse growth in a Drosophila model of tuberous sclerosis. (Translated from eng) *PLoS One* 7(2):e30722 (in eng).
2. Lee HG, Zhao N, Campion BK, Nguyen MM, & Selleck SB (2013) Akt regulates glutamate receptor trafficking and postsynaptic membrane elaboration at the Drosophila neuromuscular junction. (Translated from eng) *Developmental neurobiology* 73(10):723-743 (in eng).
3. Knox S, *et al.* (2007) Mechanisms of TSC-mediated control of synapse assembly and axon guidance. (Translated from eng) *PLoS One* 2(4):e375 (in eng).

APPENDICES (attached)

OPEN ACCESS Freely available online

PLoS one

Mechanisms of TSC-mediated Control of Synapse Assembly and Axon Guidance

Sarah Knox[1-], Hong Ge[1-], Brian D. Dimitroff[1,2], Yi Ren[1,2], Katie A. Howe[1,2], Andrew M. Arsham[2], Mathew C. Easterday[1,2], Thomas P. Neufeld[2], Michael B. O'Connor[2], Scott B. Selleck[1,2]*

1 The Developmental Biology Center, Department of Pediatrics, The University of Minnesota, Minneapolis, Minnesota, United States of America, 2 The Developmental Biology Center, Department of Genetics, Cell Biology and Development, The University of Minnesota, Minneapolis, Minnesota, United States of America

Tuberous sclerosis complex is a dominant genetic disorder produced by mutations in either of two tumor suppressor genes, TSC1 and TSC2; it is characterized by hamartomatous tumors, and is associated with severe neurological and behavioral disturbances. Mutations in TSC1 or TSC2 deregulate a conserved growth control pathway that includes Ras homolog enriched in brain (Rheb) and Target of Rapamycin (TOR). To understand the function of this pathway in neural development, we have examined the contributions of multiple components of this pathway in both neuromuscular junction assembly and photoreceptor axon guidance in Drosophila. Expression of Rheb in the motoneuron, but not the muscle of the larval neuromuscular junction produced synaptic overgrowth and enhanced synaptic function, while reductions in Rheb function compromised synapse development. Synapse growth produced by Rheb is insensitive to rapamycin, an inhibitor of Tor complex 1, and requires wishful thinking, a bone morphogenetic protein receptor critical for functional synapse expansion. In the visual system, loss of Tsc1 in the developing retina disrupted axon guidance independently of cellular growth. Inhibiting Tor complex 1 with rapamycin or eliminating the Tor complex 1 effector, S6 kinase (S6k), did not rescue axon guidance abnormalities of Tsc1 mosaics, while reductions in Tor function suppressed those phenotypes. These findings show that Tsc-mediated control of axon guidance and synapse assembly occurs via growth-independent signaling mechanisms, and suggest that Tor complex 2, a regulator of actin organization, is critical in these aspects of neuronal development.

Citation: Knox S, Ge H, Dimitroff BD, Ren Y, Howe KA, et al (2007) Mechanisms of TSC-mediated Control of Synapse Assembly and Axon Guidance. PLoS ONE 2(4): e375. doi:10.1371/journal.pone.0000375

INTRODUCTION

Mutations in TSC1 or TSC2 result in tuberous sclerosis, a human syndrome characterized by formation of benign tumors, or hamartomas, and a range of neurological and behavioral anomalies, including epilepsy and autism. While neurological dysfunction in patients with tuberous sclerosis is clearly linked to structural brain abnormalities in the central nervous system [1], recent work has provided evidence that TSC1/2 may affect neural development by altering neuronal morphology and function. Loss of TSC function produces changes in dendritic architecture of hippocampal neurons and altered synaptic properties [2]. Rats heterozygous for TSC2 mutations show disruption of hippocampal physiology, including long term potentiation, a measure of synaptic plasticity [3]. Mutations in the Drosophila ortholog of TSC2, gigas, have also been shown to produce ectopic axon terminations in addition to the normal projections of sensory neurons [4,5]. It is unclear to what degree neurological deficits associated with tuberous sclerosis complex result from disruptions of cytoarchitecture in specific brain regions or alterations in synaptic function directly.

TSC1 and TSC2 encoded proteins form a complex that regulates a small GTP-binding protein, Ras homolog enriched in brain (Rheb), promoting its endogenous GTPase activity and thereby limiting Rheb signaling. Rheb in turn controls the activity of Target of Rapamycin (TOR), a serine-threonine kinase. The TSC-Rheb-TOR pathway is a critical determinant of growth during development, regulating a number of cellular functions including translation, mRNA turnover, protein stability, and actin organization [6]. It is responsive to growth factors, such as insulin and insulin-like growth factors (ILGFs), and also serves as a nutrient sensor, thus integrating numerous signals related to cell and tissue growth. TOR plays a pivotal role in this signaling pathway, receiving regulatory inputs from Rheb and affecting downstream targets via two distinct molecular complexes. Tor complex 1 (TORC1) includes Raptor and mLST8, and regulates translation via phosphorylation of S6 kinase (S6K) and 4E-binding protein (4EBP). Tor complex 2 (TORC2) includes Rictor in addition to Tor and mLST8; in both yeast and mammalian cells TORC2 influences the actin cytoskeleton. Tor complex 1, but not Tor complex 2, is inhibited by the anti-proliferative and immunosuppressant compound rapamycin, emphasizing that TORC1 and 2 are pharmacologically separable entities. The distinct molecular outputs of TORC1 and 2 have also suggested that TORC2 may be the primary regulator of cell polarity and morphology. It is not known which functions of TSC-Rheb-TOR in the nervous system are mediated by either or both of the two Tor kinase-containing complexes, and if pharmacological intervention in tuberous sclerosis complex patients should best be directed at TORC1, with agents such as rapamycin, or if TORC2-specific agents will also be important.

Academic Editor: Hugo J. Bellen, Baylor College of Medicine, United States of America

Received November 29, 2006; Accepted March 19, 2007; Published April 18, 2007

Funding: This work was supported by NIH contract grant number GM54832-09 to SBS, the Martin Lenz Harrison Endowment to SBS, and NIH grant RO1 GMO62509 to TN. MBO is an investigator with the Howard Hughes Medical Institute.

Competing Interests: The authors have declared that no competing interests exist.

* To whom correspondence should be addressed. E-mail: selle011@umn.edu

- These authors contributed equally to this work.

The fruit fly *Drosophila* has proven to be an important system for understanding the molecular mechanisms of Tsc-Rheb-Tor signaling during development [7]. As in vertebrates, this signaling cascade is a critical regulator of growth. All of the principal elements of this pathway are represented in *Drosophila*, including molecular components upstream of Tsc, such as phosphatidyinositol-3 kinase (Pi3K), Akt, Pten and the insulin receptor ortholog, InR. Likewise, molecules that convey the signal downstream of Tsc, including Rheb, Tor, and S6k serve critical roles in the fruit fly. Mutations affecting all these genes have been identified in *Drosophila*, as well as transgenes that can convey gain-of-function effects. We have used these molecular and genetic tools to explore the function of Tsc-Rheb-Tor signaling in two fundamental processes essential to nervous system development, synapse formation and axon guidance.

The *Drosophila* neuromuscular junction has served as a powerful model for identifying the molecular components required for assembly and plasticity of a defined synapse [8]. This glutamatergic synapse must respond to greater than a 100-fold increase in the size of the muscle target from first to third instar larval stages. Physiological responses of this synapse are well-characterized using single-cell recording techniques, and morphological development with specific molecular markers has been extensively described. We have used this synapse to determine the role of gain or loss of Tsc-Rheb-Tor signaling on synapse assembly and function.

The visual system of *Drosophila* is equally well described in both molecular and genetic terms [9]. Photoreceptors show stereotyped projections to the brain, and genes required for photoreceptor axon projection and termination have been identified in numerous screens. Methods for making somatic cell mosaics have proven particularly powerful in determining what molecules are required in photoreceptors or in cells along their trajectory into the brain. Previous studies have shown that retinal clones mutant for the *Drosophila* Tsc2 ortholog *gigas* generated enlarged ommatidia with increased numbers of synaptic contact sites in the optic lamina [10]. We have taken advantage of this system to examine Tsc-Rheb-Tor requirements for photoreceptor axon guidance and formation of functional synaptic contacts in the brain.

Our results establish that either gain or loss of signaling via the Tsc-Rheb-Tor pathway affects synapse development at the *Drosophila* NMJ. Ectopic activation of the Tsc-Rheb-Tor signaling pathway produced profound synaptic overgrowth with commensurate increases in synaptic function. We show that Rheb-mediated enhancement of synaptic function depends upon bone morphogenetic protein (BMP) signaling mediated by *wishful thinking* (wit), a type II receptor. In the visual system, increased Tsc-Rheb-Tor signaling produced cell autonomous defects in photoreceptor axon guidance. Both genetic and pharmacological evidence suggest that TORC2 serves critical functions in both synapse development and axon guidance in *Drosophila*. Axon guidance phenotypes produced by null mutations in *Pten* and *Tsc1* are distinct, demonstrating that regulation of signaling by these two tumor suppressor genes are not functionally equivalent in the nervous system.

RESULTS

Activation of Tor signaling produces synaptic growth and enhanced synaptic function

Tsc1/2 affect growth by inhibiting Rheb, a small GTP-binding protein that in turn governs Tor activity. Overexpression of Rheb activates the pathway independent of Tsc gene function [11–13]. We have used the Gal4-UAS system to overexpress *Rheb* in either the motoneuron or the muscle of the *Drosophila* third instar larval neuromuscular junction (NMJ), a well-characterized glutamatergic synapse [8] that shows dynamic growth during larval development. Ectopic expression of *Rheb* in the motoneuron of the third instar larval NMJ using a pan-neuronal Gal4 line (*elav-Gal4*) resulted in more than a doubling of synapse size, measured by the number of synaptic boutons/muscle area (Figure 1A–C, quantified in D). Similar results were seen using a motoneuron-specific OK6-Gal4 line (data not shown). We found no evidence of motoneuron axon misrouting at this level of Rheb activation; the motoneuron axon follows the normal trajectory and synapses at the correct location on muscle 6 and 7(data not shown). Indeed, *elav-Gal4 ▪ UAS-Rheb* animals are viable, indicating this degree of pathway activation is considerably more mild than loss of Tsc1 (see below). Expression of Rheb selectively in muscle (*G14-Gal4 ▪ UAS-Rheb*), while producing enlargement of muscle cells, did not increase the proportional size of the synapse (bouton number/muscle area, Figure 1D). Activation of Tor by overexpression of Pi3K in the motoneuron also produced an enlarged synapse, but to a lesser degree than overexpression of Rheb (Figure 1C, D).

Enlargement of the NMJ in *Drosophila* is not always associated with an electrophysiologically competent synapse. For example, *highwire* mutants display large NMJs but markedly compromised synaptic function [14,15]. We therefore assessed the electrophysiological behavior of the NMJ in animals overexpressing Rheb in the motoneuron. This synapse showed nearly a doubling of the quantal content, a measure of the number of synaptic vesicles released per motoneuron firing (Fig 1I). The amplitude of the excitatory junctional potential (EJP), the voltage change in the muscle elicited by a suprathreshold stimulation of the motoneuron, also increased significantly compared to control synapses (Figure 1E, F). Mini-excitatory junctional potentials (mEJPs) are depolarizations of the muscle that result from spontaneous neurotransmitter release and provide a measure of vesicular fusion. While the mEJP frequencies of *Rheb* overexpressing animals showed no significant change (Figure 1G), the mEJP amplitudes were lower than matched controls (Figure 1H). In all, activation of Tor signaling via overexpression of Rheb produced an expanded synapse that was fully functional.

Reduction of Tor signaling produces a small synapse with compromised function

To determine if reduced Tsc-Rheb-Tor signaling compromises synapse growth and function we overexpressed Tsc1 and Tsc2 in the motoneuron, or compromised *Rheb* activity using a combination of hypomorphic *Rheb* alleles previously shown to cause reductions in cell size and number as well as S6k activity [11]. Overexpression of UAS-Tsc1/Tsc2 has been shown to limit growth mediated by Rheb [11–13], and we observed that Tsc1 and 2 overexpression in the motoneuron reduced synapse size compared to controls (Figure 2A, B, quantified in D). Consistent with this finding, *Rheb* hypomorphic mutant larvae showed a significantly reduced number of boutons per unit muscle area compared to heterozygous controls (Fig 2C, D). The NMJs of these animals also revealed significant changes in synaptic function. mEJP frequencies in *Rheb* mutant animals were half that of controls (Fig 2E, G), and EJP amplitudes were significantly reduced (Figure 2F). We also saw a reduction in the quantal content of *Rheb* mutants (Figure 2I), while mEJP amplitude showed no significant change (Figure 2H). Thus, reducing Tor activity by either of two mechanisms, overexpression of Tsc1/2 or partial loss-of-function mutations in *Rheb*, compromised synapse morphological development and function. Electrophysiology of hypomorphic Tor mutants showed a reduction in mEJP frequency similar to what we saw for Rheb mutants (data not shown).

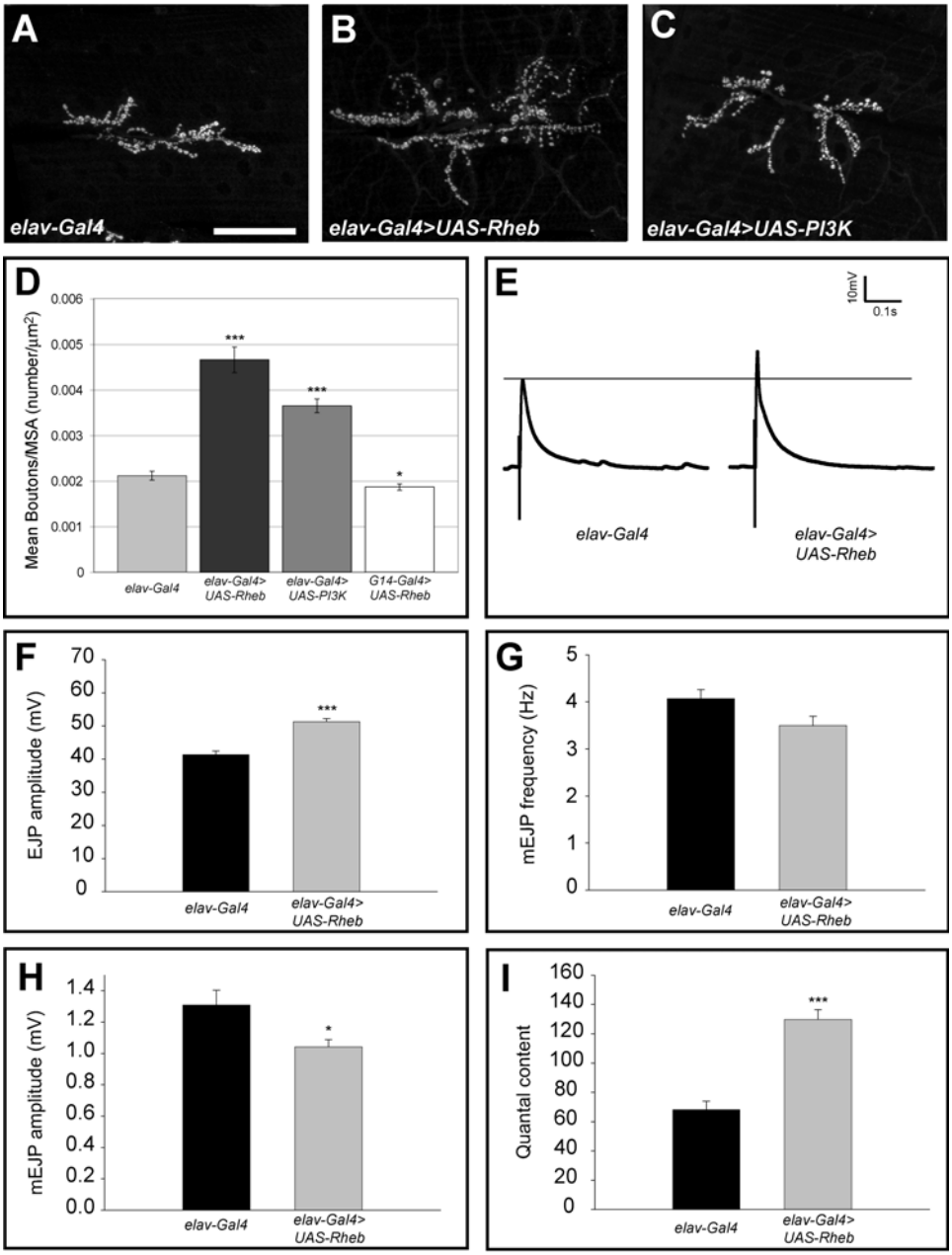

Figure 1. Activation of the Tor pathway produces synaptic growth and enhanced physiological function. The morphology of the third instar larval NMJ was visualized with the presynaptic marker anti-cysteine string protein (CSP) and confocal microscopy. Images shown are stacks of 20 or more optical sections. Neuronal (elav-Gal4) expression of either Rheb (B) or Pi3K (C) increased the size of the synapse compared to control animals bearing the elav-Gal4 transgene alone (A). Numbers of synaptic boutons/muscle area are quantified in D. Expression of either UAS-Rheb (n = 41) or UAS-Pi3K (n = 41) produced a significant increase in the number of boutons/muscle area compared to controls (n = 44), while expression of UAS-Rheb in the muscle (driven by G14-Gal4, n = 18) produced a reduction. Neuron-specific expression of Rheb also produced electrophysiological changes at the NMJ, determined by intracellular recordings from abdominal muscle 6 in third instar larvae. The amplitude of the EJP was significantly increased in animals expressing UAS-Rheb (n = 21) compared to controls with elav-Gal4 alone (n = 12). Examples of EJP voltage traces are shown in E, and mean EJP values are quantified in F. Quantal content, a measure of the number of synaptic quanta released in a single firing of the motoneuron, was nearly doubled by neuron-directed expression of Rheb compared to controls (I). Mini-EJP amplitude was decreased in these animals (H), while mEJP frequency showed no significant change (G). In this and all subsequent figures, *** denotes p-values less than 0.00005 using a student t-test comparison with controls, ** denotes p-values less than 0.005, and * denotes p-values less than 0.05. The scale bar is 50 microns in panel A.
doi:10.1371/journal.pone.0000375.g001

Rapamycin does not inhibit synapse growth mediated by overexpression of Rheb

To evaluate if Rheb overexpression-mediated synapse expansion takes place via known growth regulatory pathways, we grew larvae from hatching to the third instar larval stage on rapamycin-containing food. Rapamycin has been shown to block growth mediated by TORC1 in Drosophila, and we used a concentration that produced clear developmental delay [16]. Culturing larvae bearing elav-Gal4 and UAS-Rheb^{+} transgenes on rapamycin reduced

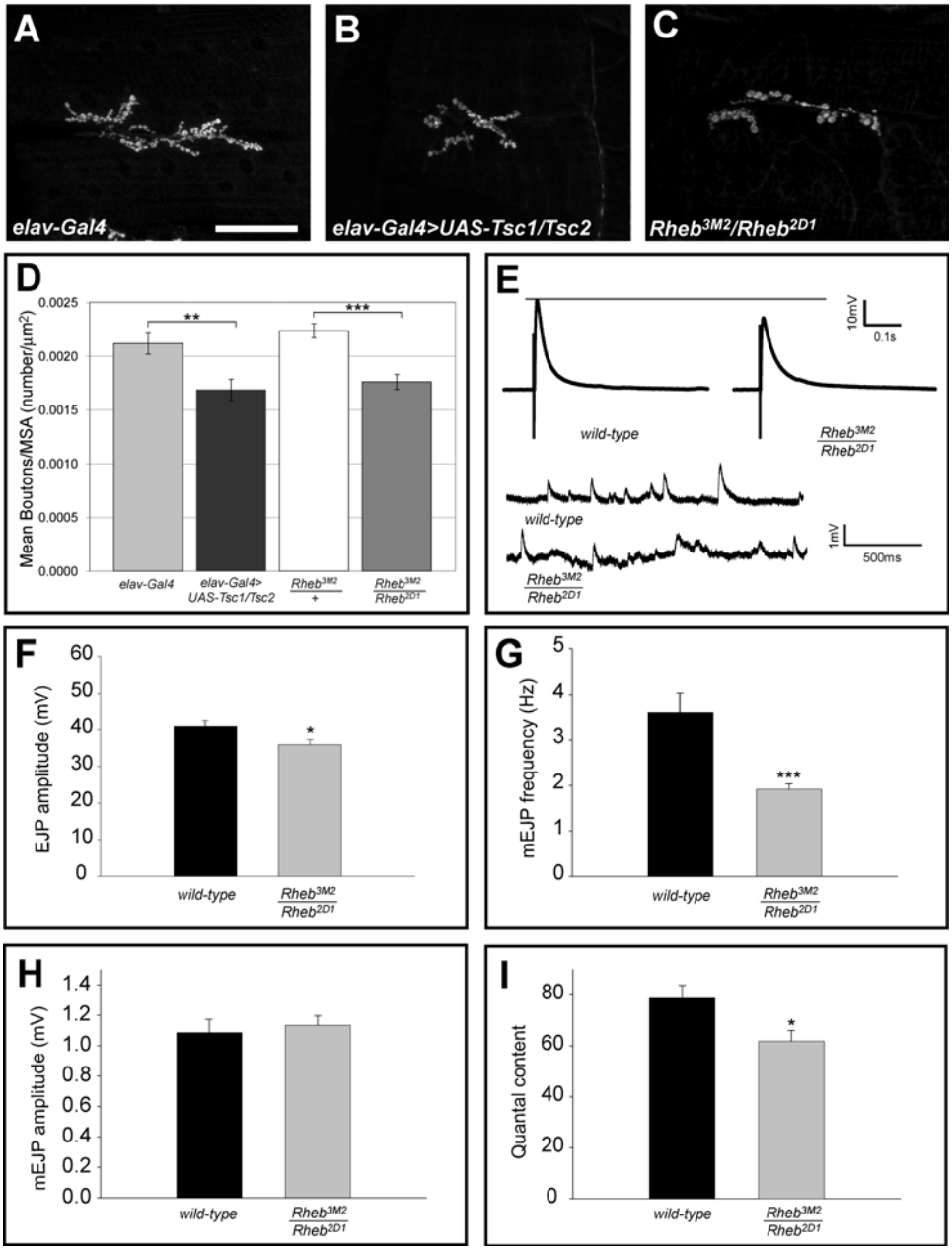

Figure 2. Rheb activity is required for normal synapse assembly. Panels A–C show anti-CSP staining of larval NMJs in a control animal (A, elav-Gal4 driver alone), an animal bearing elav-Gal4 . UAS-Tsc1, UAS-Tsc2 (B), or a Rheb partial loss of function mutant (C). Reduction of Rheb function produced by either neuron-directed expression of Tsc1 and Tsc2 (n = 22) or mutation of Rheb (n = 40) significantly reduced synapse size compared to controls with elav-Gal4 alone (n = 44) or animals heterozygous for a Rheb mutation (n = 17), as measured by the number of synaptic boutons/muscle area (D). Panel E shows sample EJP traces for wild-type and Rheb mutant NMJs, as well as baseline recordings from these preparations showing the size and frequency of mini-EJPs. Panels F, G, and I show reductions in EJP amplitude, mini-EJP frequency, and quantal content for Rheb mutant synapses (n = 29) compared to wild-type controls (n = 10). Mini-EJP amplitude did not show a significant change (H). The scale bar in A is 50 microns.
doi:10.1371/journal.pone.0000375.g002

overall growth, including muscle size, but did not suppress the synaptic enlargement measured either by the number of synaptic boutons/muscle area or the number of motoneuron branches (Figure 3A–C, quantified in D, E). These findings show that Rheb-mediated synaptic growth did not require TORC1 activity, implicating TORC2 and its regulation of the actin cytoskeleton as serving critical functions in synaptic growth control. Interestingly, culturing elav-Gal4 control larvae (without the UAS-Rheb transgene) on rapamycin produced both an increase in the number of boutons per unit muscle area and an in increase in motoneuron branching (Figure 3D, E). This raises the possibility that blocking the activity of TORC1 with rapamycin indirectly influences the activity of other Tor complexes.

The Tsc-Rheb-Tor pathway regulates translation largely by controlling S6k [11–13]. Rheb activation of Tor produces phosphorylation and activation of S6k. The control of translation via S6k represents but one component of regulation affected by this pathway and is molecularly distinct from Tsc-Rheb-Tor-mediated control of the actin cytoskeleton. To evaluate the contribution of S6k to synapse growth we examined the NMJs of

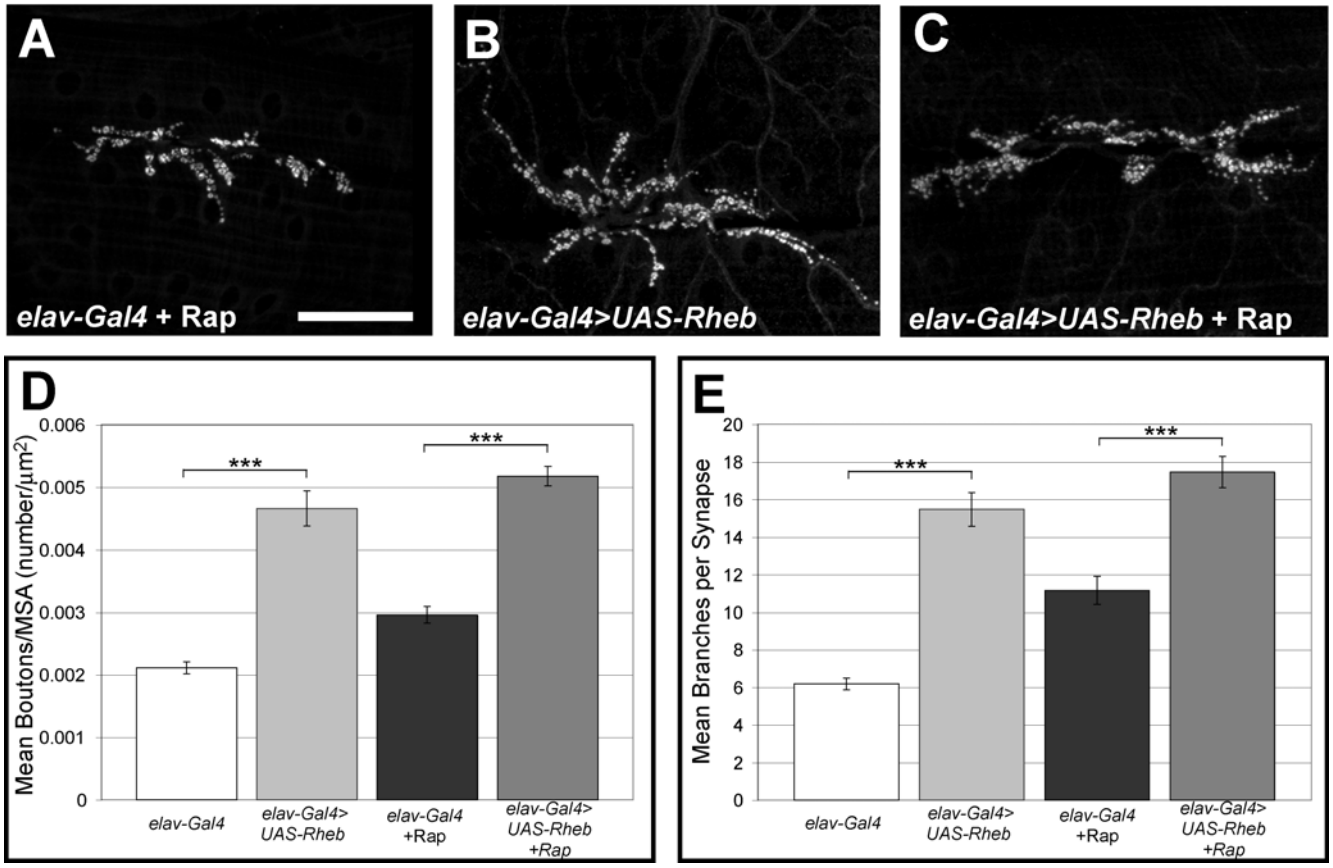

Figure 3. Rapamycin does not block Rheb-mediated synapse growth. Panels A–C show anti-CSP staining of NMJ synaptic boutons, demonstrating that the TORC1 inhibitor rapamycin does not block synapse growth in control animals or in larvae with neuron-directed expression of Rheb (elav-Gal4 ▪ UAS-Rheb). Panels D and E provide quantification of bouton numbers/muscle area and numbers of motoneuron branches, respectively, for elav-gal4 controls (n = 44), animals with neuronal expression of Rheb (n = 41), control animals treated with rapamycin (n = 26), and Rheb expressing animals treated with rapamycin (n = 29). The scale bar is 50 microns.
doi:10.1371/journal.pone.0000375.g003

animals bearing a null mutation in S6k. S6k mutants are small, with a reduced muscle surface area compared to controls. The synapse size, however, as measured by the number of boutons per unit muscle area, is not reduced (data not shown). These findings contrast with the effects of *Rheb* mutations or Tsc1 and Tsc2 overexpression (Figure 2), but are consistent with the finding that rapamycin does not suppress synapse overgrowth (Figure 3). Together, these results suggest that TORC1 and S6k do not contribute significantly to the proportional growth of the NMJ.

Rheb-mediated changes in synapse function require the BMP-signaling receptor encoded by wishful thinking

Growth factor-mediated signaling, including both Wingless (Wg) and BMP pathways, is important for normal NMJ growth in *Drosophila*. Animals bearing mutations in *wishful thinking* (*wit*), a gene encoding a BMP type II receptor, show a very small NMJ with dramatically compromised synaptic function [17–19]. To determine the relationship between Rheb-regulated synaptic growth and BMP-mediated synapse assembly we tested the ability of Rheb overexpression to rescue the synaptic growth defect of wit mutants. While $Rheb^{+}$ expression in the motoneuron was able to restore the number of synaptic boutons to wild-type levels in wit mutant larvae, the number of boutons was significantly less than with Rheb overexpression alone (Figure 4A–E). Rheb overexpression modestly increased mini EJP frequency of wit mutants (Figure 4G), but showed no capacity to rescue either quantal content or EJP amplitudes (Figure 4F–I), therefore wit is clearly required for most Rheb-directed effects on synapse function. While these results do not establish the nature of the communication between Tor-Tsc signaling and the BMP pathway, it does demonstrate that an intact BMP system is necessary for Rheb-directed changes in synapse function.

Tsc-Rheb-Tor signaling is critical for axon guidance in the visual system

Another fundamental aspect of neural development is the correct specification of axon pathfinding and synapse formation with the correct targets. The *Drosophila* visual system offers a powerful experimental model for assessing the function of a signaling system in axon guidance. To evaluate the function of the Tsc-Rheb-Tor signaling pathway in axon guidance we generated genetic mosaic animals where mutant photoreceptor neurons project to a phenotypically wild-type brain. In the fruit fly *Drosophila*, each retinal sensory unit, or ommatidium, is comprised of eight photoreceptors, R1-8. In the third instar larval brain, R1-6 project to the first optic ganglion, the lamina, and terminate to form a discrete plexus where synapses will form later in development (Figure 5A). R7 and R8 project to a deeper level in the brain, the medulla, forming a discrete set of projections seen in both larval and pupal brains. In 40h pupae the R7 and R8 projections terminate in distinct layers

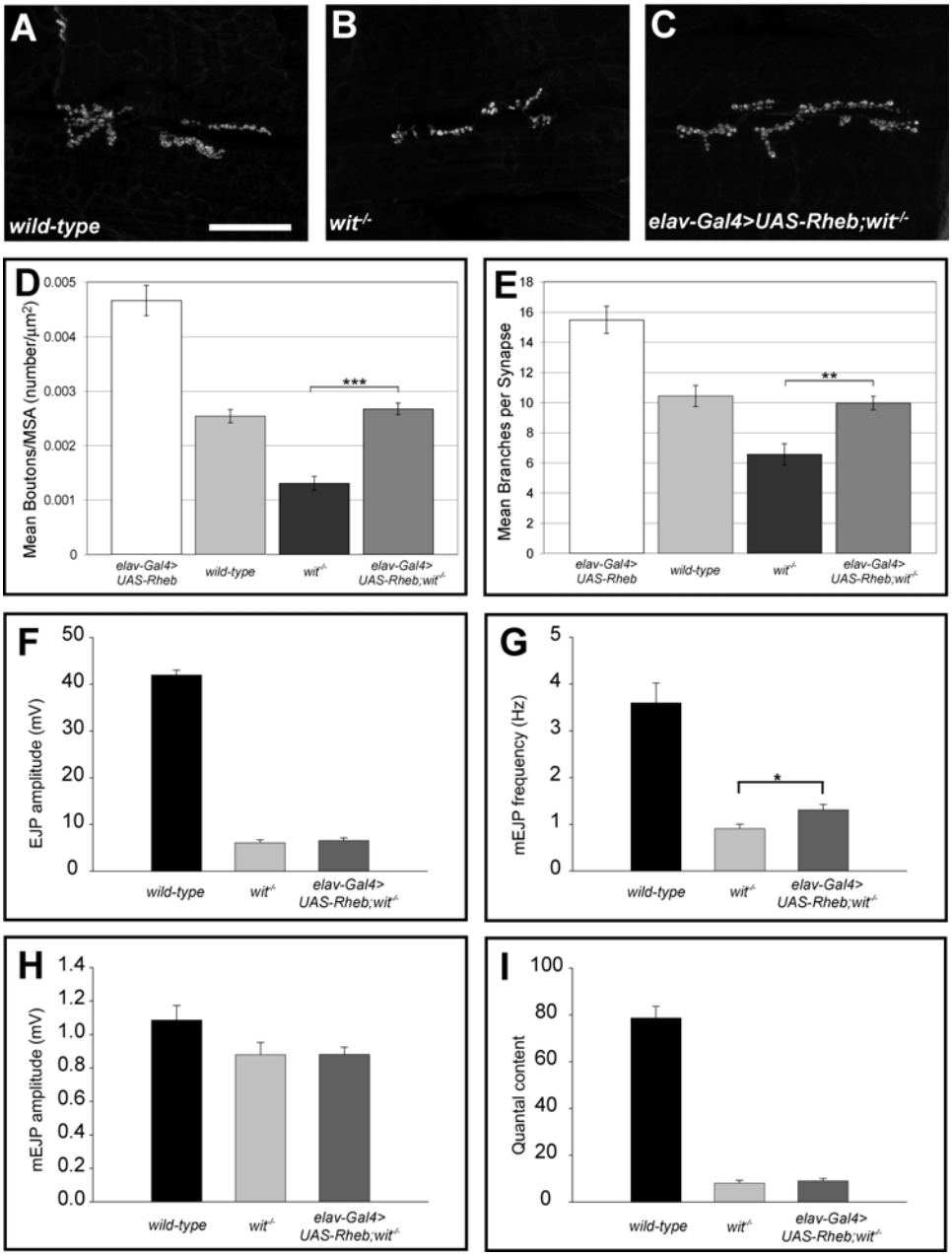

Figure 4. Rheb-mediated synapse expansion and physiological function is BMP-signaling dependent. Anti-CSP staining of synaptic boutons (panels A–C) shows the effects of wit on synapse growth (B), and the effects of neuron-directed expression of Rheb on wit mutant NMJs (C) compared to wild-type (A). Synapse size, measured by either the number of boutons/muscle area (D) or the number of motoneuron branches (E), is dramatically reduced in wit mutants (n = 20) compared to wild-type (n = 12), and is partially rescued by neuron-directed expression of Rheb (elav-Gal4 ▪ UAS-Rheb, n = 24). Reductions in EJP amplitudes (F), mini-EJP amplitudes (H), and quantal content (I) mediated by loss of wit (n = 8) are not rescued by neuron-directed expression of Rheb (n = 16) (n = 10 for wild-type). The decrease in mini-EJP frequency of wit mutants, a measure of spontaneous vesicle release, is rescued to a significant degree by expression of Rheb in the motoneuron (G). The scale bar represents 50 microns.
doi:10.1371/journal.pone.0000375.g004

in the medulla, producing a highly regular and stereotyped pattern (Figure 5E). Loss of Tsc1 function in the retina produces an enlarged eye disc with an increased number of photoreceptors [20–22]. Axon projections from Tsc1 mutant photoreceptors in the brains of third instar larvae and pupae showed severe axon guidance abnormalities (Figure 5B, F, F9, quantified in Table 1). In third instar larvae, R1-6 termination at the lamina plexus is disorganized, producing an irregular termination zone (compare Figure 5A to 5B). R7/R8 terminations within the larval medulla are also abnormal (Figure 5B, arrowhead). At the 40 hr pupal stage we observed gaps in the R7/R8 layers with large axon bundles, or fascicles, that projected past their appropriate termination points (Figure 5F, F9).

To evaluate the degree of pathway activation mediated by pan-neuronal expression of UAS-Rheb, which we used above to evaluate the role of Tor signaling at the NMJ, we examined photoreceptor pathfinding in elav-Gal4 ▪ UAS-Rheb larvae and pupae. These animals survive to adulthood and show disruptions in photoreceptor projections, but to a significantly lesser extent than found in Tsc1 mosaic animals (see Table 1). In elav-Gal4 ▪ UAS-Rheb pupal

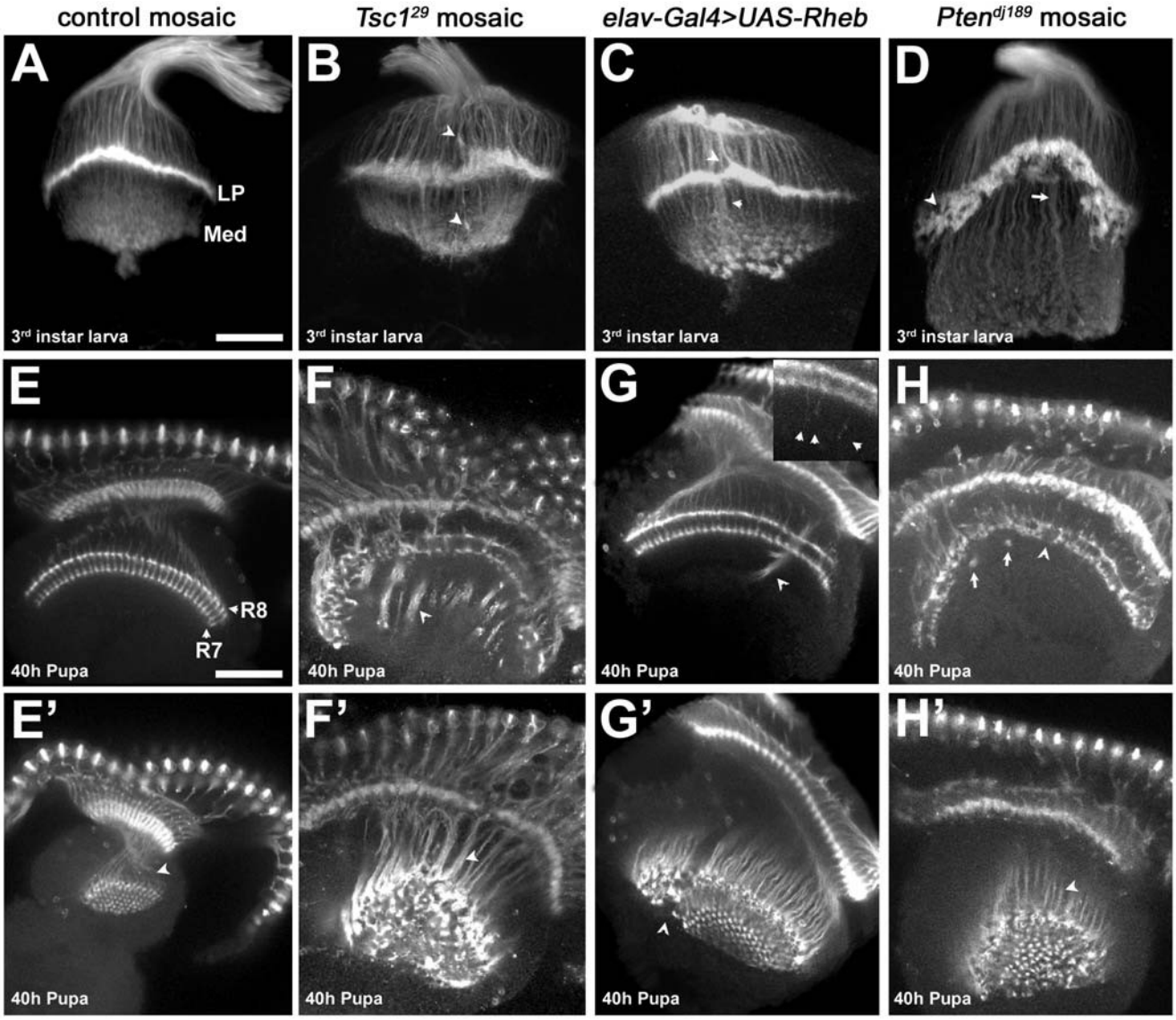

Figure 5. Photoreceptor axon projection defects associated with increased Tor signaling. (A–D) Dorsal-posterior views of third instar optic lobes stained with MAb24B10 to visualize photoreceptor projections. (A) Mitotic clones in an FRT82B control background show proper termination of photoreceptor axons R1-6 at the lamina plexus (LP), and termination of photoreceptors R7 and R8 in the medulla (Med). (B) $Tsc1^{29}$ mutant axons terminate at incorrect positions above and below the lamina (arrowheads) and produce a broadened lamina plexus. (C) Neuronal expression of Rheb creates axon termination defects similar to those seen in Tsc1 mosaics (D) $Pten^{dj189}$ mutant photoreceptors leave gaps and holes (arrowhead) in the lamina plexus, which is broader and noticeably ''peaked.'' The medulla contains axon projections which are thicker and much longer than in controls (arrow). (E–H9) Dorsal view of optic lobes from 40h pupae stained with MAb24B10. E9–H9 are lower optical planes of the optic lobes shown in E–H, respectively. (E, E9) Control photoreceptors R7 and R8 show two distinct layers of termination in the medulla (labels), and are arranged in a highly regular pattern (arrowhead). (F) Animals with $Tsc1^{29}$ mutant photoreceptors show severe disruption of the R7 and R8 termination layers. Instead of terminating at the correct positions, the axons fail to de-fasciculate, forming dense bundles (arrowheads) that project beyond the medulla. (G, G9) Neuron-directed expression of Rheb causes axon bundles to project beyond the medulla in a fashion similar to Tsc1 mosaics (arrowheads), but the phenotype is much less severe. (G, inset) Individual Rheb-overexpressing axons show an intermediate termination defect, stopping several microns beyond their normal targets (arrowheads in inset). (H) $Pten^{dj189}$ mutant axons exhibit gaps and collapses in the R7/R8 termination zone (arrowhead). Thick axon bundles can be seen that bypass their usual stopping points and then loop back to terminate at other locations in the R7/R8 layers (arrows). (H9, F9) Axon bundles in $Pten^{dj189}$ mosaics are not as densely packed as those of $Tsc1^{29}$ mosaics (arrowheads), but are still disorganized. All scale bars are 50 microns.
doi:10.1371/journal.pone.0000375.g005

brains, abnormal bundles of axons that penetrate into deeper brain structures were found, but this phenotype was markedly less severe than in Tsc1 mosaic animals (Figure 5G, G9, Table 1). Close inspection of R7 and R8 endings in the medulla revealed individual photoreceptor axons growing past the correct termination site (Figure 5G inset). R1-6 endings in the larval brain also show irregularities, but the lamina plexus is less disrupted than in Tsc1 mosaics (Figure 5C). These findings indicate that the degree of pathway activation achieved with elav-Gal4 ‗ UAS-Rheb is markedly less than produced by loss of Tsc1. Moreover, these results suggest that there is a continuum of axon pathfinding abnormalities with different levels of pathway activation.

Table 1. Axon guidance defects in animals with altered Tsc-Rheb-Tor signaling

(Percent of optic lobes affected)

						Incorrect Terminations		
3rd instar larvae	Thick LP	Gaps in LP	LP Peaked	Long R7/8	Gaps in Med.	Above LP	Below LP	In Med.
$Tsc1^{29}$ (n = 58)	70	41	7	5	31	45	52	72
$Pten^{dj189}$ (n = 38)	24	100	79	63	29	58	68	95
$Rheb^{3M2/26.2}$ (n = 22)	68	55	0	0	41	32	18	36
Tor^{A948V} (n = 12)	17	17	0	8	0	0	17	33
$S6k^{l-1}$ (n = 49)	29	41	2	0	2	10	14	4
Tor^{A948V} $Tsc1^{29}$ (n = 14)	21	29	0	0	7	7	0	0
$S6k^{l-1}$ $Tsc1^{29}$ (n = 23)	65	83	0	0	70	43	17	43
wild-type +Rap (n = 80)	19	13	0	0	9	21	14	13
$Tsc1^{29}$ +Rap (n = 60)	76	54	2	6	59	46	71	63
40-hour pupae		Pathfinding Defects		De-fasciculation Defects		Termination Laver Defects		
$Tsc1^{29}$ (n = 60)		100		100		100		
elav-Gal4 - UAS-Rheb (n = 23)		83		43		39		
$Pten^{dj189}$ (n = 73)		25		30		8		
$Rheb^{26.2}$ (n = 80)		36		3		19		
$S6k^{l-1}$ (n = 32)		28		9		25		
Tor^{A948V} (n = 20)		35		0		10		
Tor^{A948V} $Tsc1^{29}$ (n = 25)		40		4		16		

*$Tsc1^{29}$, $Pten^{dj189}$, and $Rheb^{26.2}$ are eyFLP mosaics; all others are mutants. LP - lamina plexus; Med. - medulla; Rap - rapamycin

doi:10.1371/journal.pone.0000375.t001

Pten, another negative regulator of cell growth and proliferation, encodes a phosphatase that converts the lipid signaling molecule phosphatidylinositol 3,4,5 triphosphate (PIP_3) to PIP_2, an inactive form, thus antagonizing PI3K activation of the TOR pathway. Like Tsc1, Pten retinal mosaics show eye overgrowth and precocious differentiation [23–27]. To determine if disruptions of Pten function affect axon guidance, we generated mosaic animals. Pten mutant photoreceptor projections showed disorganization of axon termini in the third instar larval brain and were notable for a misshapen and concave lamina plexus with a large number of gaps (Figure 5D, quantified in Table 1). At the pupal stage, Pten mutant projections showed significantly less severe defects than photoreceptors bearing a Tsc1 null mutation (Figure 5H, H9 and Table 1), with fewer projections failing to stop at the normal medulla termination sites. The penetrance of pathfinding, defasciculation, and termination defects in 40h pupae was lower in Pten than in Tsc1 null mutant photoreceptors projecting to a wild-type CNS (Table 1). In sum, Pten and Tsc1 mutant photoreceptor projections show distinct patterns of photoreceptor axon guidance defects, despite the fact that these two inhibitors of Tsc-Rheb-Tor signaling have similar influences on cell size, growth, and differentiation [20–22,24–26,28].

We also observed distinct effects of Tsc1 and Pten retinal mosaics on the differentiation of lamina neurons and visual system glia, detected with anti-Dachshund and anti-Repo antibodies, respectively (Figure S1). Pten mutant retinal projections produced an abnormally large lamina not seen in Tsc1 mosaics (Figure S1A–C). In both Pten and Tsc1 mosaics visual system glia were found in the brain in roughly normal positions (Figure S1D–F), although some disorganization was evident in brains receiving Tsc1 mutant photoreceptor projections. It is possible that this disruption of glial architecture may partially contribute to the axon projection defects observed in Tsc1 mutants.

To evaluate the effects of reduced Tor signaling, we examined axon guidance in animals bearing hypomorphic mutations in Tor and Rheb, as well as a null allele of S6k, a key downstream target of TORC1. In all three of these mutants, mild axon projection defects were observed (Figure 6A–F, Table 1). Third instar larvae had irregular laminas and abnormally thick projections to the medulla (Figure 6A–C, arrowheads). In 40 h pupae, R7 and R8 terminations were largely normal, but there were projections which misrouted and failed to terminate correctly (Figure 6D–F, Table 1). Genetic mosaic analysis of Rheb mutant photoreceptor projections showed the same phenotypes, demonstrating that normal levels of Tor-Tsc signaling in the retina are required for proper photoreceptor targeting (data not shown). These findings establish that reductions in Tor-Tsc signaling also produce axon guidance defects, although quite mild in comparison to activation of the pathway achieved by loss of Tsc1 function. However, only the S6k mutants are null in these experiments, and we cannot therefore fully assess the contributions of Tor or Rheb to axon guidance compared to Tsc1.

To determine if the functional relationships critical for growth control are also in effect for axon guidance, we conducted genetic epistasis experiments between Tsc1 and both Tor and S6k. Tsc1 mosaic pupae show severe axon guidance abnormalities and Tsc1 mutant animals do not survive to the pupal stage; in contrast, animals bearing both a Tsc1 mutation and a hypomorphic Tor allele survived to pupal stages and showed only modest axon guidance abnormalities in larval and pupal brains (Figure 6G, H, Table 1). The gross disruptions of R7/R8 terminations in the medullas of 40h Tsc1 mosaic pupae were almost completely rescued by the presence of a hypomorphic allele of Tor. Genetic mosaics with Tsc1 Rheb double mutant chromosomes also showed dramatic rescue of photoreceptor axon guidance defects (data not

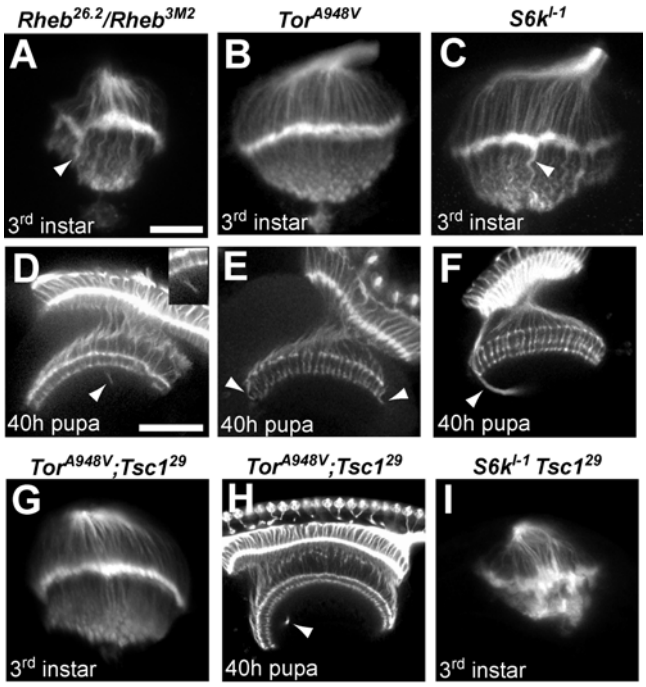

Figure 6. Effects of mutations that downregulate the Tor pathway on photoreceptor axon guidance, and genetic epistasis with Tsc1. Optic lobes from third instar larvae (A–C) and 40h pupae (D–F) stained with MAb24B10. (A) Larvae heteroallelic for a hypomorphic combination of Rheb alleles show abnormal photoreceptor patterning and contain thick axon bundles that extend into the medulla (arrowhead). (D) At the 40 h pupal stage, Rheb mutants display axons that bypass their normal targets in the R7/R8 termination zones (arrowhead). (B) Larvae homozygous for a hypomorphic Tor allele show fairly normal photoreceptor patterning, but at the pupal stage (E) misrouted axons can be seen in the medulla (arrowheads). (C) S6k null homozygous larvae show thick axon bundles projecting past the lamina (arrowhead), while S6k pupae (F) display misrouted axons that initially bypass the R7/R8 termination zone (arrowhead). (G, H) Animals doubly mutant for Tor and Tsc1 do not show the severe photoreceptor defects seen when axons are mutant for Tsc1 alone (compare to Figure 5B, F, F9), although mild defects similar to those in Tor mutants are still apparent (arrowhead). (I) S6k-Tsc1 double homozygous mutants display a severe phenotype dissimilar to mutants for either S6k or Tsc1 alone. The scale bar is 25 microns in panel A, 50 microns in panel D.
doi:10.1371/journal.pone.0000375.g006

shown). In contrast, S6k null mutations did not ameliorate the Tsc1 axon projection defects in the larval brain, and both the lamina plexus and medulla projections were highly disordered (Figure 6I, Table 1). These findings demonstrate that Tor and Rheb, but not S6k, are critical components of the photoreceptor axon guidance signaling system downstream of Tsc1.

In order to evaluate if the growth control functions of Tsc-Rheb-Tor signaling are important for axon guidance, we used rapamycin to inhibit the abnormal growth produced by loss of Tsc1 function. Feeding animals with rapamycin between hatching and the third instar larval stage blocked the retinal cell growth and proliferation defects of Tsc1 mutant photoreceptor mosaics. This was evident in both the overall size of the developing retina and the size of the photoreceptor cell bodies (Figure 7A–C). While the growth defects of Tsc1 mosaics were rescued by rapamycin treatment, photoreceptors from these animals still showed severe axon guidance abnormalities in the third instar larval brain, with an irregular and disrupted lamina plexus, as well as disorganized projections to the medulla (Figure 7E, Table 1). Treatment of wild-type controls with rapamycin produced only mild defects in the lamina plexus (Figure 7D, Table 1) supporting the hypothesis that Tsc1-mediated regulation of axon guidance operates largely via a rapamycin-insensitive function of Tor. We noted that the excessive growth of Pten mutant retinas was not rescued by rapamycin treatment, in contrast to the effects of this TORC1 inhibitor on Tsc1 mosaics. While the growth and differentiation phenotypes of Pten and Tsc1 mutant retinas are comparable, the difference in their rapamycin responses highlights how disruption of signaling by these two regulators is distinct.

DISCUSSION

Tsc-Rheb-Tor signaling in neural development

The Tsc-Rheb-Tor pathway is critical for integrating a variety of signals that govern cellular and organismal growth. Inappropriate activation of the pathway also leads to severe neurological and behavioral abnormalities, including mental retardation, autism, and epilepsy [1,6]. While TSC mutations produce hamartomatous growths in the brain, recent evidence has suggested that these benign tumors may not be solely responsible for the nervous system dysfunction that is a hallmark of tuberous sclerosis complex. Loss of TSC2 in hippocampal neurons produces changes in neuronal morphology and synaptic transmission [2]. Heterozygosity for TSC2 in the rat compromises several measures of hippocampal long term potentiation [3]. Loss of Pten, an important upstream regulator of Tsc-Rheb-Tor signaling, in a limited set of neurons also affects neuronal morphology and socialization

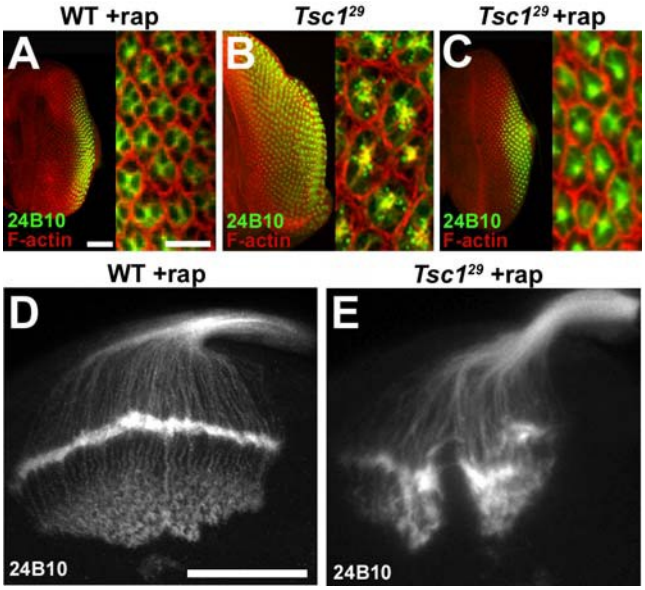

Figure 7. Axon guidance defects in Tsc1 mosaics are not suppressed by blocking growth. (A–C) Third instar eye discs from wild type and Tsc1 mosaic larvae raised with or without rapamycin (rap). Ommatidial units, comprised of eight photoreceptors, were visualized with phalloidin (red) that detects F-actin, and MAb24B10 (green). Phalloidin staining is strongest at the perimeter of each ommatidium, outlining each sensory unit. Rapamycin treatment of Tsc1 mosaic eye discs (C) restored eye disk size and cell size compared to wild type (A). (D and E) Rapamycin treated third instar larval brains stained with MAb24B10. Rapamycin treatment blocked abnormal growth of the retina and the increase in photoreceptor cell size, but did not ameliorate the abnormal axon projections also characteristic to untreated Tsc1 ^{29} mosaics. The scale bars in panel A represent 50 microns in the left image, 10 microns in the right image. The scale bar is 50 microns in panel D.
doi:10.1371/journal.pone.0000375.g007

behavior [29]. These findings collectively provide evidence that Tsc-Rheb-Tor signaling is critical for the morphological and functional development of the nervous system. It is not clear, however, if the entire Tsc-Rheb-Tor signaling network is critical for nervous system development, or if neural function is strictly a consequence of altered growth regulation. It is also not known if loss of signaling is as detrimental to neuronal development as inappropriately elevated signaling, such as occurs with loss of TSC function. We have taken advantage of the genetic and molecular tools available in the fruit fly *Drosophila* to address these questions. Our findings demonstrate that appropriate levels of Tsc-Rheb-Tor signaling are critical for both NMJ development and for axon guidance in the visual system. In both these contexts, effects are independent of growth, implicating TORC2 rather than TORC1 as the complex mediating Tsc-Rheb-Tor signaling influences in the nervous system.

Tsc-Rheb-Tor effects on neural development are independent of growth regulation

Given the importance of Tsc-Rheb-Tor signaling in regulating cellular and tissue growth, it was important to determine if disruption of this pathway affects neural development via its effects on growth or through signaling components independent of those that govern cellular size and growth. To address this issue we used both pharmacological and genetic methods to block the increased growth produced by pathway activation. The immunosuppressant rapamycin is a TORC1-specific inhibitor that prevents activation of S6k and blocks growth mediated by loss of Tsc1. Rapamycin treatment retarded growth in larvae with pan-neuronal expression of *Rheb*, but failed to reduce the synapse expansion characteristic of these animals. Similarly, while rapamycin effectively reduced the retinal overgrowth of Tsc1 mosaic animals, it failed to suppress the photoreceptor axon guidance defects seen in the visual system. Loss of S6k function also failed to ameliorate axon guidance defects in Tsc1 mosaic animals. This contrasts with effects of Tor partial loss-of-function mutations, which effectively rescued axon guidance defects of Tsc1 mutants. Collectively, these findings demonstrate that the role of Tsc-Rheb-Tor signaling in synapse assembly and axon guidance is largely independent of TORC1, S6k, and their effects on growth. Indeed, while animals bearing null alleles of S6k have some axon pathfinding defects, the effects are relatively modest compared to Tsc1 mosaics, indicating that S6k does not provide the critical outputs affecting axon guidance.

Our findings parallel recent work in the mouse, where neuronal hypertrophy produced by loss of *Pten* in granule neurons of the cerebellum and dentate gyrus was not rescued by loss of S6k1 [30]. It is also of note that some but not all Tsc1/2-mediated changes in dendritic morphology of hippocampal neurons in organotypic cultures were suppressed by rapamycin treatment [2]. Our findings suggest that inhibition of growth regulatory components in tuberous sclerosis patients, such as achieved with rapamycin and related agents, may not affect all processes that are deranged in the nervous system.

Recent studies of Pi3 kinase, Akt and InR in *Drosophila* have shown that activation of signaling upstream of Tsc1/2 also produces increases in synapse size, both at the NMJ as well as central synapses [31]. Expression of these components in adult neurons demonstrated that Pi3 kinase-mediated synaptogenesis was age-independent, and therefore not a developmentally restricted phenomenon. In agreement with studies reported here, the expanded NMJs produced by activation of Pi3 kinase were functional, with increased stimulus-induced EJPs. Overexpression of the *Drosophila* ortholog of the epidermal growth factor receptor (EgfR) in central neurons increased neuronal cell size, without an increase in synapse number. These results are consistent with those reported here where we have been able to directly suppress growth mediated by Tsc-Rheb-Tor pathway activation without altering effects on synapse formation or axon guidance.

Recent studies have also demonstrated a link between Tsc1/Tsc2 and *highwire*, a gene known to effect synapse size and functionality in *Drosophila* [32]. The *highwire* ortholog Pam was shown to bind Tsc2 in pull-down assays, and it has been suggested that Pam may function as an E3 ubiquitin ligase to regulate the intracellular levels of the Tsc1/Tsc2 complex. This concept of Highwire as a negative regulator of Tsc levels is consistent with our findings, since *highwire* mutants have been shown to possess enlarged NMJs similar to what we see for Rheb overexpression [14]. Despite this, the enlarged synapses of *highwire* mutants display compromised synaptic function which is contrary to what we found when overexpressing Rheb, so Highwire is likely to have multiple functions at the synapse besides simply the regulation of Tsc.

Contributions of TORC1 versus TORC2 in synapse assembly and axon guidance

Tor has a number of molecular outputs that influence many cellular processes; notable among these are cellular growth and cellular morphology. TORC1, which contains Raptor and is sensitive to the anti-proliferative agent rapamycin, is a major contributor to the regulation of cellular growth, in large measure due to its effects on protein synthesis. TORC2, which includes Rictor, is implicated in the control of cell morphology mediated by regulation of the actin cytoskeleton [33]. Both pharmacological and genetic studies presented here argue in favor of Tor complex 2 providing an essential regulatory component of both synapse growth and axon guidance in *Drosophila*. Our results support recent work showing that changes in dendritic morphology of hippocampal neurons produced by loss of Tsc1 required regulation of the actin-depolymerizing factor Cofilin [2], implicating TORC2-mediated processes. There is a considerable body of work demonstrating that control of the actin cytoskeleton is critical for NMJ growth and function [34–36] and TORC2 may provide an important component of that control. Regulation of actin is also essential for axon guidance in the visual system (reviewed in [37,38]), and disruption of Tor-mediated control of actin may be the underlying molecular deficit in Tsc1 mosaics.

Either gain or loss of Rheb signaling compromises neuromuscular junction assembly and axon guidance

A number of studies have suggested that TOR activation produced by loss of TSC1/2 affects neuronal morphology and synaptic function. Our findings support these observations; elevated Rheb activity produces synaptic enlargement and enhanced physiological function at the *Drosophila* NMJ. However, it was not evident from earlier studies whether loss of signaling through Rheb and Tor is also important for neural development. We provide evidence that this is the case. Partial loss-of-function mutations in *Rheb* compromise NMJ growth and function, as well as photoreceptor axon targeting in the visual system. Overexpression of Tsc1 and Tsc2 in the motoneuron also limited synaptic growth, supporting the conclusion that depressed levels of Rheb activity compromise synapse development.

Rheb-mediated synaptic development is dependent on a functional BMP signaling system

The capacity of Tsc-Rheb-Tor signaling to affect neuronal morphology and synapse function begs the question of whether

these effects are dependent on signaling systems known to be critical for synapse development. At the Drosophila NMJ, BMP signaling is critical for normal growth and function. Mutations in wit, a gene encoding a type II BMP receptor, produce a small and poorly functioning NMJ [17,19]. These deficits can be rescued by motoneuron expression of wit^{+}, demonstrating that BMP signaling in the motoneuron is critical for synaptic expansion during larval growth. To determine if Rheb-mediated synaptic growth required BMP signaling, we placed elav-Gal4 and UAS-Rheb transgenes into a wit mutant background. While overexpression of Rheb and the accompanying activation of the Tor pathway partially rescued the defect in synapse growth produced by loss of wit function, it was unable to restore a normal EJP response or rescue quantal content. These findings establish that Tsc-Rheb-Tor mediated effects on synapse morphology are partially dependent on BMP signaling, and are fully dependent on BMP activity for a physiologically competent synapse. Our findings also establish that the functional deficits in wit mutants are not simply the result of reduced synapse size, since restoration of synapse size by expression of UAS-Rheb does not restore physiological function. Intersection of BMP, and Akt/PTEN/TOR signaling has been noted for other systems, and our results indicate the relationship between these pathways is important for synapse growth and plasticity as well [39].

Loss of function mutations in Tsc1 and Pten have different effects on axon guidance

Previous analysis of gigas/Tsc2 mutants demonstrated that loss of this gene in mechanoreceptors affects axon targeting, producing projections to novel areas in the CNS in addition to innervation of normal targets [5]. We have used genetic mosaics to evaluate the function of Tsc-Rheb-Tor signaling in photoreceptor axon guidance. Animals homozygous for Tsc1 in the retina showed grossly aberrant photoreceptor projections to both the lamina and medulla. R7 and R8 projections to the medulla in 40h pupae failed to terminate correctly and projected beyond normal targets to inappropriate regions within the brain. Somatic mosaics bearing retinal neurons mutant for Pten also showed photoreceptor axon guidance defects, but to a notably lesser degree. Since both Tsc1 and Pten alleles used for this analysis were nulls and show comparable effects on cellular growth and differentiation [23], it follows that Pten is not as critical for axon guidance as Tsc1. The distinctions between axon guidance phenotypes of Pten and Tsc1 null mutants indicate that altered timing of differentiation is not critical for axon guidance and that control of this pathway at the level of Pten or Tsc1 is not functionally equivalent. Our findings that rapamycin arrests retinal overgrowth produced by loss of Tsc1 but not Pten in the retina supports earlier work demonstrating that retinal overgrowth mediated by loss of Tsc1, but not Pten, can be suppressed by reductions in S6k activity [40]. Those results were interpreted as demonstrating that Pten is largely a regulator of Akt activity, whereas Tsc1/2 serves as a tumor suppressor and inhibitor affecting principally S6k. Our results support these relationships and emphasize that in the nervous system regulation of Tsc1/2 targets other than S6k are critical.

Graded activation of the Tsc-Rheb-Tor signaling axis produces graded effects on axon guidance

We have used two different genetic methods for activating the Tsc-Rheb-Tor pathway in the visual system; generating retinal mosaics with a loss of function allele of Tsc1, and pan-neuronal expression of Rheb using elav-Gal4 and UAS-Rheb. The comparison of these methods revealed that overexpression of Rheb produced milder axon guidance phenotypes in the visual system than complete loss of Tsc1 function. Of interest is that the degree of activation achieved with elav-Gal4 - UAS-Rheb, a level that did not produce lethality, did result in discernable axon targeting defects in the visual system. This suggests that axon guidance controlled by Tsc-Rheb-Tor is sensitive to incremental changes in signaling. The range of neurological and behavioral phenotypes associated with loss of one copy of TSC1 or TSC2 is consistent with this model, where other environmental or genetic factors may affect signaling levels, producing a range of deficits. Our findings indicate that Drosophila can serve as a useful model for identifying how graded changes in signaling can produce a spectrum of defects in neural development.

MATERIALS AND METHODS

Drosophila strains

UAS-$Rheb^{EP50.084}$/TM6B Tb [11], UAS-$DP110^{WT}$ [41], and y w hsFLP; UAS-Tsc1 UAS-Tsc2 [21] were crossed to elav-Gal4/CyO P[w^{+}; ubi-GFP] [42] or OK6-Gal4 [17] for expression in neurons, and to G14-Gal4/CyO P[w^{+}; ubi-GFP] (from C. Goodman) for expression in muscles. Stocks used for mutant analysis and genetic interaction studies were y w; $Rheb^{3M2}$/TM6B Tb y^{+} [11], $Rheb^{2D1}$/TM6B Tb [11], b w; wit^{B11}/TM6B Tb [19], w; wit^{A12}/TM6B Tb [19], $S6k^{l-1}$/TM6B Tb [43], and $Tor^{2.1/Ala948Val}$/CyO P[w^{+}; ubi-GFP] [44]. Eye-specific mosaics were generated using the FLP-FRT technique [45] by crossing y w eyFLP GMR-lacZ; FRT82B I(3)cl-R3/TM6B Tb [45] or y w eyFLP GMR-lacZ; I(2)cl-L3 w^{+} FRT40A/CyO y^{+} [45] to w; FRT82B $Tsc1^{29}$/TM6B Tb [20], w; FRT82B $Rheb^{26.2}$/TM6B Tb y^{+} [11], y w hsFLP; FRT40A $Pten^{dj189}$/SM6-TM6B [24], y w eyFLP GMR lacZ; FRT82B [45], or y w eyFLP GMR lacZ; FRT40A [45]. Using this mosaic method, heterozygous cells have a growth disadvantage since they bear a Minute and cell-lethal mutation [l(3)cl-R3 or l(2)cl-L3]. For all retinal mosaics, we assessed the degree of mosaicism by examining the adult retina where mutant cells could be identified by loss of the w+ marker. In Tsc1, Pten and Rheb mosaics, mutant cells comprised the vast majority of the adult retina (~90%). Wild-type strains were y w, Oregon-R, or Canton-S.

Immunohistochemistry

For visualization of neuromuscular junction synapses, third instar larvae were filleted in PBS and fixed in 4% formaldehyde before staining with Anti-Cysteine String Protein mAB49 at 1:1000 (a generous gift from Zinsmaier and Buchner) and FITC-conjugated Anti-HRP at 1:50 (Jackson Labs). Bouton numbers were determined by a combination of CSP and HRP image data. Muscle surface area measurements were performed using ImageJ data analysis software (NIH) and represent the combined area of the second abdominal segment muscles 6 and 7. Third instar larvae and 40hr pupae were fixed, stained, and mounted as described [46] for photoreceptor analysis. Antibodies from the Developmental Studies Hybridoma Bank were used at 1:25 for mouse anti-Chaoptin (MAb24B10), 1:10 for mouse anti-Repo (MAb8D12), and 1:25 for mouse anti-Dachshund (MabDac2-3). Secondary antibodies were from the AlexaFluor series (Invitrogen). Texas Red-phalloidin was used at 0.165 mM (Invitrogen). All images were acquired on a Nikon C1 upright laser confocal.

Rapamycin Treatment

Flies were raised on standard laboratory food supplemented with rapamycin (Sigma) to a final concentration of 3 mM for NMJ analysis or 2 mM for eye disks. Rapamycin treated $Tsc1^{29}$ mosaic animals with eye discs similar in size to control animals were selected for photoreceptor projection analysis.

Electrophysiology

Excitatory junctional potential (EJP) recordings were taken from muscle 6 in the second abdominal hemisegment of 3rd instar larvae. Dissections were done in Ca^{++}-free saline and recordings were performed in HL3 following published protocols [47]. Recordings were acquired with an Axoclamp 2B amplifier and pClamp9 software (Axon Instruments). EJP amplitudes and mini-EJP amplitudes were measured with MiniAnalysis software from Synaptosoft.

SUPPORTING INFORMATION

Figure S1 Patterning of lamina precursor cells and glia in Pten or Tsc1 mosaic animals. (A–F) Dorsal-posterior views of third instar larval optic lobes stained with anti-Dachshund (lamina precursor cell marker) or anti-Repo (glial cell marker). (A–C) Pten mosaic animals show a significantly larger lamina compared to control animals. This is not seen to the same extent in Tsc1 mosaics. (D–F) Glial cells successfully differentiate and migrate in both Pten and Tsc1 mosaics, however mild patterning defects are apparent and could possibly contribute to the photoreceptor patterning abnormalities observed. All scale bars are 50 microns.
Found at: doi:10.1371/journal.pone.0000375.s001 (1.32 MB TIF)

ACKNOWLEDGMENTS

We thank Hoda Pourhassan for assistance with data collection and analysis, the Bloomington Drosophila stock center for fly stocks, and the Developmental Studies Hybridoma Bank for antibodies.

Author Contributions

Conceived and designed the experiments: SS MO MO SK AA TN. Performed the experiments: SK HG BD YR KH AA ME. Analyzed the data: SS MO MO SK HG BD YR ME TN. Wrote the paper: SS.

REFERENCES

1. Ess KC (2006) The neurobiology of tuberous sclerosis complex. Semin Pediatr Neurol 13: 37–42.
2. Tavazoie SF, Alvarez VA, Ridenour DA, Kwiatkowski DJ, Sabatini BL (2005) Regulation of neuronal morphology and function by the tumor suppressors Tsc1 and Tsc2. Nat Neurosci 8: 1727–1734.
3. von der Brelie C, Waltereit R, Zhang L, Beck H, Kirschstein T (2006) Impaired synaptic plasticity in a rat model of tuberous sclerosis. Eur J Neurosci 23: 686–692.
4. Acebes A, Ferrus A (2001) Increasing the number of synapses modifies olfactory perception in Drosophila. J Neurosci 21: 6264–6273.
5. Canal I, Acebes A, Ferrus A (1998) Single neuron mosaics of the drosophila gigas mutant project beyond normal targets and modify behavior. J Neurosci 18: 999–1008.
6. Inoki K, Corradetti MN, Guan KL (2005) Dysregulation of the TSC-mTOR pathway in human disease. Nat Genet 37: 19–24.
7. Neufeld TP (2004) Genetic analysis of TOR signaling in Drosophila. Curr Top Microbiol Immunol 279: 139–152.
8. Prokop A, Meinertzhagen IA (2006) Development and structure of synaptic contacts in Drosophila. Semin Cell Dev Biol 17: 20–30.
9. Mast JD, Prakash S, Chen PL, Clandinin TR (2006) The mechanisms and molecules that connect photoreceptor axons to their targets in Drosophila. Semin Cell Dev Biol 17: 42–49.
10. Meinertzhagen IA (1994) The early causal influence of cell size upon synaptic number: the mutant gigas of Drosophila. J Neurogenet 9: 157–176.
11. Stocker H, Radimerski T, Schindelholz B, Wittwer F, Belawat P, et al. (2003) Rheb is an essential regulator of S6K in controlling cell growth in Drosophila. Nat Cell Biol 5: 559–565.
12. Zhang Y, Gao X, Saucedo LJ, Ru B, Edgar BA, et al. (2003) Rheb is a direct target of the tuberous sclerosis tumour suppressor proteins. Nat Cell Biol 5: 578–581.
13. Saucedo LJ, Gao X, Chiarelli DA, Li L, Pan D, et al. (2003) Rheb promotes cell growth as a component of the insulin/TOR signalling network. Nat Cell Biol 5: 566–571.
14. Wan HI, DiAntonio A, Fetter RD, Bergstrom K, Strauss R, et al. (2000) Highwire regulates synaptic growth in Drosophila. Neuron 26: 313–329.
15. McCabe BD, Hom S, Aberle H, Fetter RD, Marques G, et al. (2004) Highwire regulates presynaptic BMP signaling essential for synaptic growth. Neuron 41: 891–905.
16. Zhang H, Stallock JP, Ng JC, Reinhard C, Neufeld TP (2000) Regulation of cellular growth by the Drosophila target of rapamycin dTOR. Genes Dev 14: 2712–2724.
17. Aberle H, Haghighi AP, Fetter RD, McCabe BD, Magalhaes TR, et al. (2002) wishful thinking Encodes a BMP Type II Receptor that Regulates Synaptic Growth in Drosophila. Neuron 33: 545–558.
18. Marques G, Haerry TE, Crotty ML, Xue M, Zhang B, et al. (2003) Retrograde Gbb signaling through the Bmp type 2 receptor wishful thinking regulates systemic FMRFa expression in Drosophila. Development 130: 5457–5470.
19. Marques G, Bao H, Haerry TE, Shimell MJ, Duchek P, et al. (2002) The Drosophila BMP type II receptor Wishful Thinking regulates neuromuscular synapse morphology and function. Neuron 33: 529–543.
20. Gao X, Pan D (2001) TSC1 and TSC2 tumor suppressors antagonize insulin signaling in cell growth. Genes Dev 15: 1383–1392.
21. Potter CJ, Huang H, Xu T (2001) Drosophila Tsc1 functions with Tsc2 to antagonize insulin signaling in regulating cell growth, cell proliferation, and organ size. Cell 105: 357–368.
22. Tapon N, Ito N, Dickson BJ, Treisman JE, Hariharan IK (2001) The Drosophila tuberous sclerosis complex gene homologs restrict cell growth and cell proliferation. Cell 105: 345–355.
23. Bateman JM, McNeill H (2004) Temporal control of differentiation by the insulin receptor/tor pathway in Drosophila. Cell 119: 87–96.
24. Gao X, Neufeld TP, Pan D (2000) Drosophila PTEN regulates cell growth and proliferation through PI3K-dependent and -independent pathways. Dev Biol 221: 404–418.
25. Huang H, Potter CJ, Tao W, Li DM, Brogiolo W, et al. (1999) PTEN affects cell size, cell proliferation and apoptosis during Drosophila eye development. Development 126: 5365–5372.
26. Goberdhan DC, Paricio N, Goodman EC, Mlodzik M, Wilson C (1999) Drosophila tumor suppressor PTEN controls cell size and number by antagonizing the Chico/PI3-kinase signaling pathway. Genes Dev 13: 3244–3258.
27. Scanga SE, Ruel L, Binari RC, Snow B, Stambolic V, et al. (2000) The conserved PI3'K/PTEN/Akt signaling pathway regulates both cell size and survival in Drosophila. Oncogene 19: 3971–3977.
28. Ito N, Rubin GM (1999) gigas, a Drosophila homolog of tuberous sclerosis gene product-2, regulates the cell cycle. Cell 96: 529–539.
29. Kwon CH, Luikart BW, Powell CM, Zhou J, Matheny SA, et al. (2006) Pten regulates neuronal arborization and social interaction in mice. Neuron 50: 377–388.
30. Chalhoub N, Kozma SC, Baker SJ (2006) S6k1 is not required for Pten-deficient neuronal hypertrophy. Brain Res 1100: 32–41.
31. Martin-Pena A, Acebes A, Rodriguez JR, Sorribes A, de Polavieja GG, et al. (2006) Age-independent synaptogenesis by phosphoinositide 3 kinase. J Neurosci 26: 10199–10208.
32. Murthy V, Han S, Beauchamp RL, Smith N, Haddad LA, et al. (2004) Pam and its ortholog highwire interact with and may negatively regulate the TSC1.TSC2 complex. J Biol Chem 279: 1351–1358.
33. Wullschleger S, Loewith R, Hall MN (2006) TOR signaling in growth and metabolism. Cell 124: 471–484.
34. Eaton BA, Fetter RD, Davis GW (2002) Dynactin is necessary for synapse stabilization. Neuron 34: 729–741.
35. Ang LH, Chen W, Yao Y, Ozawa R, Tao E, et al. (2006) Lim kinase regulates the development of olfactory and neuromuscular synapses. Dev Biol.
36. Coyle IP, Koh YH, Lee WC, Slind J, Fergestad T, et al. (2004) Nervous wreck, an SH3 adaptor protein that interacts with Wsp, regulates synaptic growth in Drosophila. Neuron 41: 521–534.
37. Rao Y (2005) Dissecting Nck/Dock Signaling Pathways in Drosophila Visual System. Int J Biol Sci 1: 80–86.
38. Luo L (2002) Actin cytoskeleton regulation in neuronal morphogenesis and structural plasticity. Annu Rev Cell Dev Biol 18: 601–635.
39. He XC, Zhang J, Tong WG, Tawfik O, Ross J, et al. (2004) BMP signaling inhibits intestinal stem cell self-renewal through suppression of Wnt-beta-catenin signaling. Nat Genet 36: 1117–1121.
40. Radimerski T, Montagne J, Hemmings-Mieszczak M, Thomas G (2002) Lethality of Drosophila lacking TSC tumor suppressor function rescued by reducing dS6K signaling. Genes Dev 16: 2627–2632.
41. Leevers SJ, Weinkove D, MacDougall LK, Hafen E, Waterfield MD (1996) The Drosophila phosphoinositide 3-kinase Dp110 promotes cell growth. Embo J 15: 6584–6594.
42. Luo L, Liao YJ, Jan LY, Jan YN (1994) Distinct morphogenetic functions of similar small GTPases: Drosophila Drac1 is involved in axonal outgrowth and myoblast fusion. Genes Dev 8: 1787–1802.
43. Montagne J, Stewart MJ, Stocker H, Hafen E, Kozma SC, et al. (1999) Drosophila S6 kinase: a regulator of cell size. Science 285: 2126–2129.
44. Zhang Y, Billington CJ Jr, Pan D, Neufeld TP (2006) Drosophila target of rapamycin kinase functions as a multimer. Genetics 172: 355–362.

45. Newsome TP, Asling B, Dickson BJ (2000) Analysis of Drosophila photoreceptor axon guidance in eye-specific mosaics. Development 127: 851–860.
46. Blair SS (2000) Imaginal Discs. In: Sullivan W, Ashburner M, Hawley RS, eds (2000) Drosophila Protocols. Cold Spring Harbor, New York: Cold Spring Harbor Laboratory Press. pp 159–173.
47. Rawson JM, Lee M, Kennedy EL, Selleck SB (2003) Drosophila neuromuscular synapse assembly and function require the TGF-beta type I receptor saxophone and the transcription factor Mad. J Neurobiol 55: 134–150.

Diet and Energy-Sensing Inputs Affect TorC1-Mediated Axon Misrouting but Not TorC2-Directed Synapse Growth in a Drosophila Model of Tuberous Sclerosis

Brian Dimitroff[1,3], Katie Howe[2-], Adrienne Watson[1-], Bridget Campion[2-], Hyun-Gwan Lee[3], Na Zhao[3], Michael B. O'Connor[1], Thomas P. Neufeld[1], Scott B. Selleck[1,2,3]*

1 Department of Genetics, Cell Biology and Development, Developmental Biology Center, University of Minnesota, Minneapolis, Minnesota, United States of America, 2 Graduate Program in Neuroscience, University of Minnesota, Minneapolis, Minnesota, United States of America, 3 Department of Biochemistry and Molecular Biology, The Pennsylvania State University, University Park, Pennsylvania, United States of America

Abstract

The Target of Rapamycin (TOR) growth regulatory system is influenced by a number of different inputs, including growth factor signaling, nutrient availability, and cellular energy levels. While the effects of TOR on cell and organismal growth have been well characterized, this pathway also has profound effects on neural development and behavior. Hyperactivation of the TOR pathway by mutations in the upstream TOR inhibitors TSC1 (tuberous sclerosis complex 1) or TSC2 promotes benign tumors and neurological and behavioral deficits, a syndrome known as tuberous sclerosis (TS). In Drosophila, neuron-specific overexpression of Rheb, the direct downstream target inhibited by Tsc1/Tsc2, produced significant synapse overgrowth, axon misrouting, and phototaxis deficits. To understand how misregulation of Tor signaling affects neural and behavioral development, we examined the influence of growth factor, nutrient, and energy sensing inputs on these neurodevelopmental phenotypes. Neural expression of Pi3K, a principal mediator of growth factor inputs to Tor, caused synapse overgrowth similar to Rheb, but did not disrupt axon guidance or phototaxis. Dietary restriction rescued Rheb- mediated behavioral and axon guidance deficits, as did overexpression of AMPK, a component of the cellular energy sensing pathway, but neither was able to rescue synapse overgrowth. While axon guidance and behavioral phenotypes were affected by altering the function of a Tor complex 1 (TorC1) component, Raptor, or a TORC1 downstream element (S6k), synapse overgrowth was only suppressed by reducing the function of Tor complex 2 (TorC2) components (Rictor, Sin1). These findings demonstrate that different inputs to Tor signaling have distinct activities in nervous system development, and that Tor provides an important connection between nutrient-energy sensing systems and patterning of the nervous system.

Citation: Dimitroff B, Howe K, Watson A, Campion B, Lee H-G, et al. (2012) Diet and Energy-Sensing Inputs Affect TorC1-Mediated Axon Misrouting but Not TorC2-Directed Synapse Growth in a Drosophila Model of Tuberous Sclerosis. PLoS ONE 7(2): e30722. doi:10.1371/journal.pone.0030722

Editor: Edward Giniger, National Institutes of Health (NIH), United States of America

Received March 22, 2011; Accepted December 21, 2011; Published February 3, 2012

Funding: This study was funded by the Department of Defense Congressionally Directed Medical Research Program for Tubersous Sclerosis, the Harrison Endowment fund to SBS, and the University of Minnesota Autism Initiative. The funders had no role in study design, data collection and analysis, decision to publish, or preparation of the manuscript.

Competing Interests: The authors have declared that no competing interests exist.

* E-mail: sbs24@psu.edu

- These authors contributed equally to this work.

Introduction

The TOR signaling pathway is critical for a broad range of biological processes. TOR, a serine-threonine kinase, is best recognized for its role as a central regulator of cell and tissue growth [1], but recently it has been found to have other important activities independent of its effects on cell size and rates of cell division. TOR signaling influences development of the nervous system, controlling cell migration, synapse growth, and axon guidance [2,3]. Disruption of the TOR pathway has profound consequences on neural development, as evidenced by the effects of abnormally elevated TOR signaling in humans with tuberous sclerosis [4]. Tuberous sclerosis (TS) is a dominant disorder produced by mutations affecting one of two proteins, TSC1 or TSC2. These proteins form a heteromeric complex that negatively regulates TOR activity, and mutations which impair the function of either component result in a high incidence of benign tumors, chronic seizures, and behavioral abnormalities such as attention deficit hyperactivity disorder (ADHD) and autism spectrum disorder (ASD) [5]. The physiological basis of these behavioral disorders is not known in detail, although studies in model organisms have shown that disruption of TOR signaling can affect synapse function, axon guidance, dendritic arborization, and cell migration during cortical assembly [6,7,8,9].

In both humans and Drosophila, TOR associates with other proteins in the cell to form distinct TOR-containing complexes. TOR Complex 1 (TORC1) contains Raptor (Regulatory associated protein of mTOR), and is sensitive to the drug rapamycin. It is primarily involved in regulating protein translation through phosphorylation of the downstream targets S6-Kinase (S6K) and 4E Binding Protein (4EBP) [10]. TOR complex 2 (TORC2) contains Rictor (Rapamycin-insensitive companion of mTOR)

and Sin1 (Stress-activated-protein-kinase-interacting protein 1). TORC2 is not affected by rapamycin, a TORC1-inhibitor and immunosuppressant, and in addition to having a role in actin dynamics [11], functions as the long-searched-for ''PDK2'', capable of phosphorylating AKT at a key regulatory site. AKT is a serine-threonine kinase [12,13] that not only inhibits TSC2 activity directly, but also influences apoptosis, metabolism, cell proliferation, and growth [14,15]. Although much is known about the upstream inputs that control TORC1 activity, very little is known about regulation of TORC2 [16]. We are interested in examining the relative contribution of these two distinct complexes to the neurodevelopmental events governed by TOR, and in testing whether inputs that are important for regulating TOR-mediated growth will also play a role in regulating the effects of TOR on nervous system development and function.

As a key regulator of growth, TOR activity is controlled by a variety of inputs from nutrient and energy sensing systems, as well as a number of different growth factors [10]. Nutrient sensing is largely mediated by amino acid availability, however until recently it remained a mystery exactly how amino acids were able to influence TOR pathway activity. Recent studies have shed light on this question by identifying a family of molecules known as Rag GTPases, which are able to modify TOR activity in response to amino acid levels [17,18,19]. They most likely achieve this by facilitating increased interaction between TOR and Rheb (Ras homolog enriched in brain), a small GTPase directly downstream of TSC1/2 and directly upstream of TOR [20]. Cellular energy in the form of ATP is sensed by AMPK (AMP-activated Protein Kinase) [21]. When ATP levels are low, AMPK reduces the activity of the TOR pathway by promoting the inhibitory functions of TSC1/2. Growth factors, such as insulin and IGF-1 (Insulin-like growth factor 1), regulate TOR activity through the class I Phosphatidylinositol 3-kinase (PI3K) [14,22]. Activation of PI3K produces the charged lipid molecule PIP_3 (phosphatidylinositol (3,4,5)-triphosphates), which in turn activates a signaling cascade of kinases that governs the function of the TSC1/2 complex. A principal step in this cascade is the phosphorylation of AKT by PDK1 (Protein-dependent kinase 1), which occurs at a conserved site on AKT separate from the site of TORC2-mediated phosphorylation. Discovering how these various nutrient sensing, energy sensing, and growth factor mediated inputs to TOR differ in their effects on neurodevelopment is a key step towards understanding the overall processes that direct neural patterning and function. This knowledge will also aid in identifying possible candidates for pharmacological intervention in treating diseases where TOR signaling is misregulated, such as tuberous sclerosis.

Because TOR activity is greatly affected by nutritional and energy sensing inputs, we have an avenue for manipulating the function of this pathway through strictly environmental influences, such as diet composition and caloric intake. This provides a unique opportunity for evaluating gene-environment interactions, a fundamental component of disease susceptibility [23]. The degree to which environmental dietary factors affect normal development is largely an open question. Instead, we have focused on the relationship between diet and neural development in the context of TOR misregulation, such as occurs in humans with tuberous sclerosis. The possibility that dietary restriction could be a treatment option for patients with TS is not unprecedented. Dietary regimes such as the ketogenic diet, where total calories are reduced and lipids become the primary source of caloric intake, are already effectively being used to treat seizures, including those exhibited by individuals with TS [24].

Our study seeks to understand the neurological and behavioral abnormalities produced by hyperactivation of the TOR pathway using *Drosophila* as a model system. Complete loss-of-function of either Tsc1 or gigas, the *Drosophila* Tsc2 homolog, is lethal [25,26], so we have created a model of TS in the fruit fly using neuron-directed overexpression of Rheb, the GTP-binding protein that is the immediate upstream activator of Tor. This provides a more modest activation of the pathway [27] and more accurately reflects the partial loss-of-function found in patients with TS, where heterozygosity for either TSC1 or TSC2 produces the disease. In *Drosophila* we have identified three different neurodevelopmental and behavioral phenotypes that result from *Rheb* overexpression: photoreceptor axon guidance abnormalities in the brain, deficits in normal phototaxis behavior, and increased size and hyperactivity of synapses at the neuromuscular junction (NMJ). We examined the influence of various genetic and environmental inputs to these Tor-misregulation abnormalities and tested their abilities to rescue each of the different phenotypes. Rheb and Pi3K showed distinct and separable roles in neural development, with Rheb hyperactivity producing a broader spectrum of abnormalities. Changes in diet, both nutrient composition and caloric content, affected neural patterning and behavioral responses, as did genetic manipulations of the critical energy sensor AMPK. Synaptic phenotypes responded differently compared to axon guidance and behavioral phenotypes, and we show that this is due to a dependence on different downstream Tor complexes. Taken together, these findings demonstrate that Tor signaling provides a critical link between metabolic factors and neural development, and that environmental influences such as diet can effect neural patterning and function.

Results

The TSC-TOR signaling system

The complex signaling system that includes Tsc1/Tsc2, Rheb, and Tor is outlined in Figure 1A [10]. Tor activity is controlled by a number of critical inputs, including growth factor signaling pathways mediated through Pi3K, metabolic energy regulators such as AMPK, and direct measures of amino acid availability. Nutrient-rich conditions that favor growth promote activation of Tor, while dietary or energy limitations reduce Tor activity [28]. In the cell, Tor associates with other proteins to form at least two unique Tor-containing complexes, TorC1 and TorC2, each with its own distinct binding partners and targets. TorC1, which contains Raptor, affects protein translation via S6k and 4EBP, while TorC2, which contains both Rictor and Sin1, influences actin organization and phosphorylates Akt, a critical regulator of several different cellular processes. The immediate upstream components most directly involved in regulating Tor activity are Rheb and Tsc1/Tsc2.

A Drosophila model of TS

In *Drosophila*, overexpression of *Rheb* results in hyperactivation of the Tor pathway. The level of activation achieved in this manner is more modest than generating Tsc1 or gigas knockouts, and more accurately reflects the levels of TOR activation seen in humans with TS, where heterozygosity for TSC1 or TSC2 mutations produces symptoms. Systemic overexpression of *Rheb* causes a high degree of lethality, so we used the Gal4-UAS system [29] to selectively express *Rheb* in neurons. This resulted in behavioral, morphological, and physiological abnormalities in the nervous system.

Positive phototaxis responses were used as a sensitive behavioral measure of nervous system function in this *Drosophila* model of TS.

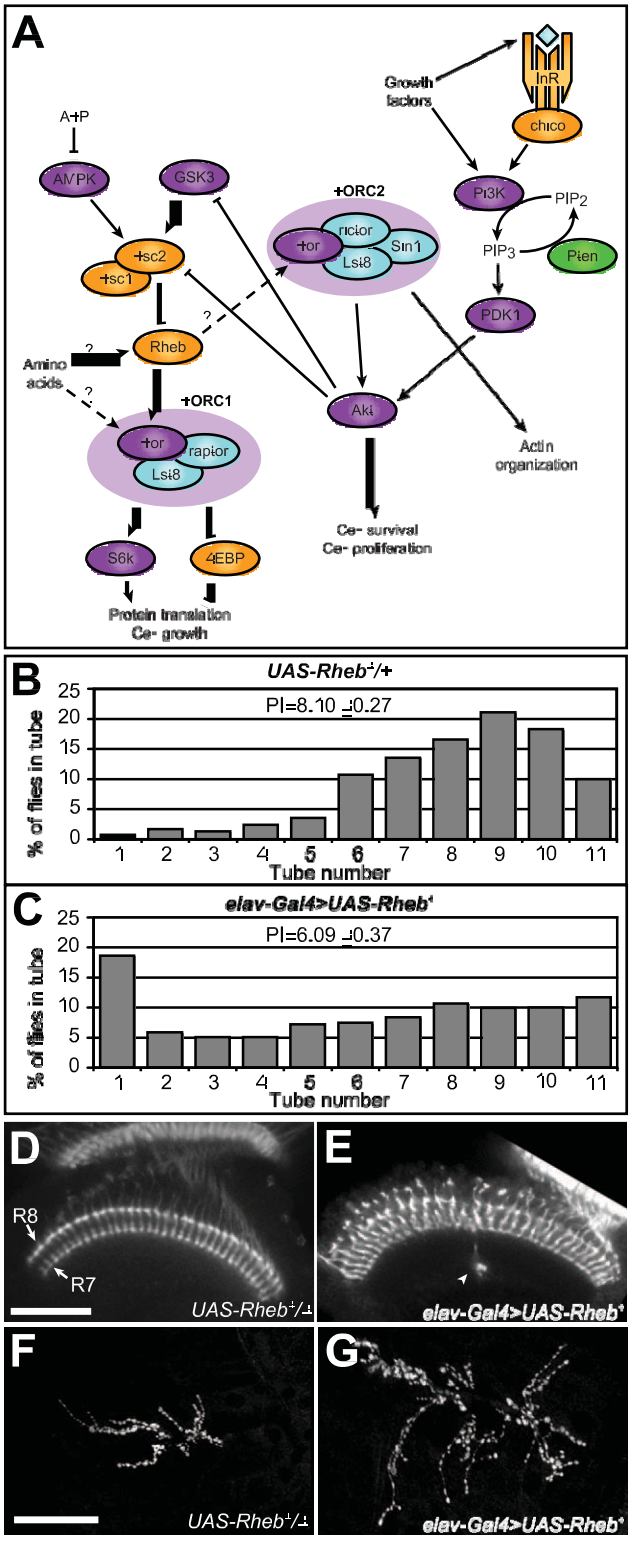

Figure 1. Rheb overexpresion causes defects in behavior, axon guidance, and synapse morphology. (A) Schematic diagram of the Tor pathway. Kinases are purple, Tor-complex components are blue, phosphatases are green, and other components are orange. The Tsc1/2 heterodimer inhibits Rheb, which in turn controls the activity of two Tor-containing complexes, TORC1 and TORC2. Relationships which are not fully-understood or could have multiple intermediary steps are shown as dashed arrows with question marks. (B, C) Phototaxis measurements in flies overexpressing Rheb in all neurons (elav-Gal4 > UAS-Rheb$^+$, n = 416) compared to control flies that have UAS-Rheb$^+$ transgenes but lacked the neuron-specific Gal4 driver (UAS-Rheb$^+$/+, n = 531). The percentage of flies in each tube of the phototaxis apparatus after 10 trials is shown, along with the phototaxis index (PI), a cumulative score where higher numbers indicate a stronger phototaxis response. (D, E) Optic lobes of pupal brains oriented with retinas toward the top of the photos. Visualization of photoreceptor projections with Anti-Chaoptin antibody staining reveals that R7 and R8 photoreceptor neurons form two highly-structured parallel rows of terminations in the medulla (arrows), with no axon bundles projecting beyond the R7 termination layer in controls. (E) Rheb overexpression in neurons caused some axon bundles to continue growing beyond their proper R7/R8 termination targets to eventually stop elsewhere within the medulla (arrowheads). (F, G) Anti-CSP (Cysteine string protein) staining at the larval NMJ reveals synaptic active zones known as boutons. Neuron-specific overexpression of Rheb resulted in neuromuscular synapses approximately 50% larger than corresponding synapses in animals lacking a Gal4 driver. Scale bars are 50 microns.
doi:10.1371/journal.pone.0030722.g001

The phototaxis assay, developed by Seymour Benzer, provides a measure of responses to light in repeated trials of adult flies where 10 successive trials are conducted using a single apparatus [30]. Flies that show positive phototaxis for all ten trials end up in the 11th tube of the phototaxis apparatus. The distribution of flies in the 11 tubes is therefore a measure of their phototaxis behavior (see Fig. 1B). The phototaxis index (PI) provides a consolidated measure of responses across an entire test group [31]. Neuronally-directed overexpression of Rheb produced phototaxis deficits and a significantly lower phototaxis index (PI = 6.1 in Rheb overexpressing flies, versus 8.1 in control flies lacking a Gal4 driver, $p < 0.001$ by Student's t-test).

Overexpression of Rheb in neurons had other neurodevelopmental consequences as well. Elevated signaling through the Tor pathway, mediated by either loss of Tsc1 or increased levels of Rheb, resulted in axon guidance defects in the brain [27]. Drosophila have eight distinct photoreceptor neurons, R1–R8, and during development these project axons to specific termination sites in the brain [32]. By 40-hours after pupal formation (APF), the R7 and R8 photoreceptor axons terminate in a highly reproducible pattern in the medulla region. When viewed in optical cross-section, these terminations appear as regularly spaced rows of processes (Fig. 1D). Neuronal overexpression of Rheb resulted in a failure of some R7 and R8 photoreceptors to terminate at their proper locations (Fig. 1E, arrowheads). Sometimes these aberrant axon bundles looped back to terminate elsewhere in the medulla, while in some animals the axons simply stopped outside of the normal termination zone. The photoreceptor termination defects in transgenic flies overexpressing Rheb were relatively moderate compared to mosaic animals where a majority of retinal cells were homozygous mutant for Tsc1 [27].

In addition to the photoreceptor axon guidance defects, we observed that hyperactivation of Tor signaling also greatly affected synapse development. Overexpression of Rheb in neurons caused substantial synaptic overgrowth at the neuromuscular junction (Fig. 1F, G), altering the balance between the number of synaptic boutons and the size of the underlying muscle, a tightly controlled relationship during normal growth and development [27,33]. Animals bearing elav-Gal4 > UAS-Rheb$^+$ transgenes sometimes showed more than a two-fold enlargement of NMJ synapses and were on average approximately 50% larger [27].

Rheb activity is mediated through Tor

Although Rheb is known to be directly upstream of Tor [34], we wanted to verify that these Rheb overexpression phenotypes were the result of increased Tor activation. Complete loss of Tor is

lethal, so Tor function was reduced by 50% by creating animals heterozygous for a Tor null mutation. Reducing Tor function in the context of neuronal Rheb overexpression rescued phototaxis behavior almost to the level of controls (Fig. 2A). To assess the degree of photoreceptor axon misrouting, the widths of all axon bundles that failed to terminate at their proper locations were measured and averaged across the total number of optic lobes examined. The average width of misrouted axons in wild-type controls was essentially zero (data not shown). Heterozygosity for a Tor null mutation almost completely rescued Rheb-induced axon guidance abnormalities (Fig. 2B).

At the NMJ, overexpression of Rheb produced large synapses. The size of the synapse was measured by immunostaining with anti-Cysteine String Protein (CSP), a critical presynaptic component, and determining the number of pixels with staining above a background threshold. These ''bouton pixel'' counts were then divided by the surface areas of the underlying muscles, a method used for normalizing the size of the motoneuron process to the size of its target. This method of measuring synapse size is comparable to traditional bouton counts, but can be more quantitative when boutons are very small or indistinct, as is the case in animals with Rheb overexpression (see Methods). Reducing Tor function by 50% caused a significant rescue of the synapse overgrowth phenotype (Fig. 2C). Taken together with the phototaxis behavior and axon guidance results, it is evident that the range of neurodevelopmental deficits produced by Rheb overexpression all require Tor activity, demonstrating that this is a good model for studying the consequences of TOR signaling hyperactivation, as occurs in TS.

Pi3K and Rheb have distinct activities in neural development

Pi3K and Rheb constitute two different upstream regulators of Tor, and their relative contributions to distinct neurobehavioral phenotypes were examined. At the larval NMJ, Pi3K and Rheb have been shown to have largely equivalent effects in promoting both NMJ expansion and increases in physiological responses to motoneuron stimulation [27]. While Rheb is immediately upstream of Tor, Pi3K conveys signaling information from growth factor receptors at the cell surface via multiple intermediates [14,22]. The similar effects of Rheb and Pi3K expression at the NMJ prompted an analysis of the influence these two critical Tor signaling components have on other neurodevelopmental phenotypes, namely phototaxis and photoreceptor axon guidance. Consistent with previous reports, expressing Rheb or PI3K with an elav-Gal4 transgene specific to neurons produced similar levels of synaptic expansion (Fig. 3A–C) and comparable increases in EJP amplitudes with either combination (Fig. 3D). However, using these same Gal4-UAS transgenes, Rheb and Pi3K overexpression produced very different effects on photoreceptor axon guidance and phototaxis. Whereas overexpression of Rheb caused substantial axon termination errors, Pi3K had virtually no effect on axon guidance in the visual system, even when expressed from a constitutively active transgene $Pi3K^{CAAX}$ [35](Fig. 3E–G). Similarly, Pi3K overexpression had no effect on phototaxis behavior, in contrast to the deficits observed when Rheb was overexpressed (Fig. 3H). These results demonstrate that despite having similar effects on the synapse, Rheb and Pi3k have distinct roles within the full spectrum of Tor-mediated neurodevelopmental events.

Dietary rescue of behavioral deficits

TOR was originally identified as a key regulator of cell and tissue growth in response to nutrition [1]. Conditions of plentiful nutrient and calorie availability are known to activate the TOR pathway and promote growth, whereas conditions of low food availability inhibit TOR and restrict growth. Nutrient availability is also a potentially important environmental modulator of neural development. As the behavioral, morphological, and physiological defects in our Drosophila model of TS are dependent on elevated Tor signaling, we examined the capacity of dietary restriction to modulate these effects. Flies were reared on four different diets: (1) a rich, high-calorie diet (high-calorie or HC, 1203 kcal/L), (2) a diet low in yeast, the primary source of lipids and amino acids, which also provides 28% fewer calories as a result (yeast-restricted or YR, 861 kcal/L), (3) a diet isocaloric to the yeast-restricted diet, but reduced instead for sugar, the primary source of carbohydrates (sugar-restricted or SR, 863 kcal/L), and (4) a diet restricted for both yeast and sugar, providing a low caloric content (calorie-restricted or CR, 521 kcal/L) [36]. Both the yeast-restricted (YR) and calorie-restricted (CR) diets significantly rescued phototaxis deficits in Rheb-overexpressing flies, with the YR food restoring this behavior to nearly wild-type levels (Fig. 4A). These changes in behavior were not a consequence of the dietary changes alone, since these diets had no effect in the absence of the Gal4 transgene necessary for producing overexpression of Rheb (Fig. 4B). Control experiments with animals bearing elav-Gal4 and a GFP-tagged transgene (UAS-mCD8-GFP) showed that these diets did not affect Gal4-directed expression levels measured at either the NMJ or in the third instar larval CNS (data not shown). We also examined the possibility that diet did not show an effect on wild-type fly behavior since these animals had such a robust phototaxis response that any enhancements from dietary changes were obscured. To test this possibility we assessed the effects of dietary change in a fly stock with a much lower baseline phototaxis score. Early studies in Drosophila established that different wild-type strains display varying degrees of positive phototaxis [37], and one strain with a particularly low level of phototaxis is Oregon-R (Ore-R). We raised Ore-R flies on each of the four diets and found no evidence of enhanced phototaxis behavior (Fig. 4B). In these tests a small, yet significant, decrease in performance was observed with the calorie-restricted diet, but there was no evidence of any improvement of behavior such as we observed in animals overexpressing Rheb. Therefore, the improvement in phototaxis performance observed in elav-Gal4 $\cdot$ UAS-$Rheb^{+}$ flies is mediated by caloric restriction and represents a specific gene and environment interaction (Rheb overexpression and diet).

Dietary rescue of Tor-mediated axon guidance abnormalities

Our results thus far demonstrate that a behavioral aspect of nervous system dysfunction produced by Tor hyperactivation can be corrected by dietary restriction, but what about a morphological deficit? Rheb overexpression in the nervous system produced a moderate defect in photoreceptor axon targeting, and the capacity of caloric restriction to ameliorate this developmental deficit was examined. Elevated levels of Tor signaling caused R7 and R8 photoreceptor axons to grow past their intended targets in the brain (Fig. 5A, arrows). To quantify the severity of this defect, the widths of all aberrant axon bundles that failed to terminate were measured (as indicated by the red bars in Fig. 5A, insets), and the total width of misrouted axons was determined for each brain. Compared to control animals raised on the high-calorie (HC) diet, Drosophila raised on the yeast-restricted (YR) diet displayed a shift away from the more severe defects and a corresponding increase in the proportion of milder defects (Fig. 5B). This rescue is more readily seen by comparing the mean total widths of all misrouted axons within each group (Fig. 5C). Interestingly, when Rheb was expressed at this moderately high level, all three diet-restricted

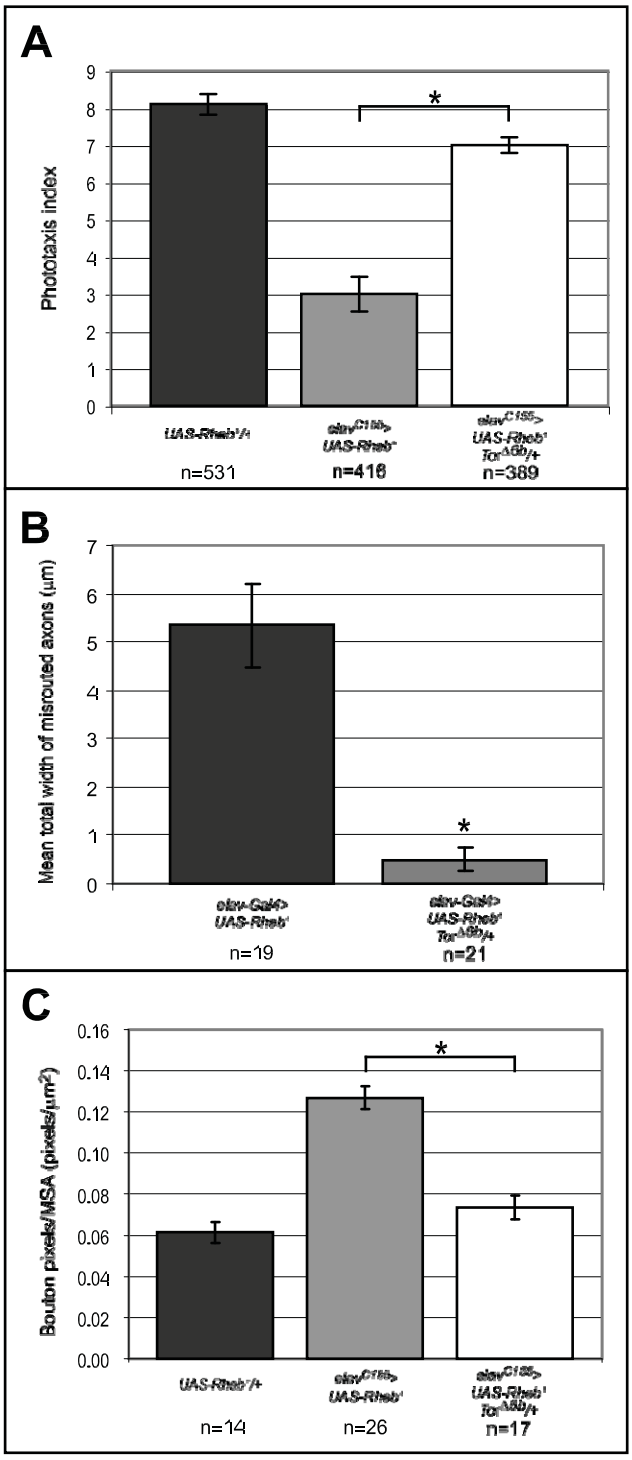

Figure 2. Rheb overexpression defects are Tor-dependent. (A–C) Heterozygosity for a Tor null mutation, Tor^{D6B}, rescued Rheb-directed deficits in phototaxis behavior, axon guidance, and synapse expansion. (A) Neuronally-directed expression of Rheb ($elav^{C155}$-UAS-$Rheb^{+}$) caused a substantial drop in phototaxis response compared to controls (UAS-$Rheb^{+}$/+). Heterozygosity for a Tor null allele ($elav^{C155}$-UAS-$Rheb^{+}$ Tor^{D6B}/+) almost completely rescued this defect. (B) Measures of axon guidance misrouting showed a significant decrease in severity when Tor function was reduced by 50%. (C) Reduced Tor function rescued synapse overgrowth to nearly wild-type levels in animals with neuronally-directed (elav-Gal4) expression of Rheb (MSA = "Muscle Surface Area"). Asterisks denote $p > 0.05$ using a two-tailed student's t-test. Note that different neuronal-directed Gal4 drivers were used for assessing the influence of Tor function on Rheb-directed axon misrouting and synapse expansion. These two different Gal4 drivers were selected for producing phenotypes at a penetrance and expressivity where Tor-dependence could readily be assessed.
doi:10.1371/journal.pone.0030722.g002

foods showed a significant capacity to rescue the axon guidance phenotype.

The capacity of different diets to provide rescue of axon guidance was explored further using conditions where the degree of misrouting was less severe. It seemed possible that any differences between these diets might only be observed at modest levels of Tor activation, where smaller changes in Tor signaling would have a more detectable effect. To produce lower levels of Tor activation, flies were reared at a reduced temperature (21uC versus 25uC) where the Gal4 transcriptional activator protein is less active and therefore directs a lower level of Rheb expression. This technique resulted in an approximately 5-fold reduction in the severity of axon guidance defects (compare HC diets in Fig. 5C to 5D). Within this context, the yeast-restricted and calorie-restricted diets still showed a significant capacity to rescue, but the sugar-restricted diet did not (Fig. 5D). Both YR and CR diets limit lipids and amino acids, whereas SR is specifically limiting for carbohydrates. Since the YR and SR diets contain equal amounts of calories, these results suggest that for this level of Tor pathway activation it is the composition of each diet that is the key determinant of rescue, rather than the overall caloric content.

Since the experiments described thus far restrict caloric input by altering the food content, it was important to determine if the rates of food consumption and absorption were equivalent across all diets. A radioactive label was seeded into the food, and third instar larvae were allowed to ingest the labeled food for a 6-hour interval. The levels of radioactivity incorporated into the larvae were then determined, which provides a measure of both food ingestion and nutrient absorption [38]. No significant differences in the rates of food uptake were observed for any of the four different diets (Fig. S1), thus the effects of diet on behavioral and morphological development were not confounded by differing levels of food consumption.

Effects of diet on Tor-mediated synapse abnormalities

In addition to testing the effects of diet restriction on phototaxis deficits and axon patterning defects, the influence of dietary inputs on the synaptic abnormalities produced by Rheb overexpression was also examined. Hyperactivation of the Tor pathway resulted in substantial overgrowth of synapses at the neuromuscular junction (Fig. 6A, B), as visualized by staining for the presynaptic marker Cysteine-String Protein (CSP). Despite its ability to rescue other Rheb-overexpression phenotypes, diet restriction showed no capacity to rescue synaptic overgrowth (Fig. 6B–D). Animals raised on YR or CR diets showed the same degree of bouton-per-muscle-area expansion as flies raised on the high-calorie diet. Flies raised on the sugar-restricted diet actually showed an increase in synaptic overgrowth. Control experiments showed that reducing caloric content was also unable to limit synapse growth in animals without overexpression of Rheb in the nervous system (elav-Gal4-UAS-mCD8-GFP; data not shown).

Hyperactivation of Tor signaling also caused changes in the electrophysiological function of the NMJ. Suprathreshold stimulation of the motoneuron evokes a depolarization at the muscle known as the excitatory junctional potential (EJP) [33,39](see Fig. 6F). Overexpression of Rheb caused an abnormal increase in the magnitude of this response, and raising flies on YR food was not able to rescue this defect (Fig. 6E, F). The inability of dietary

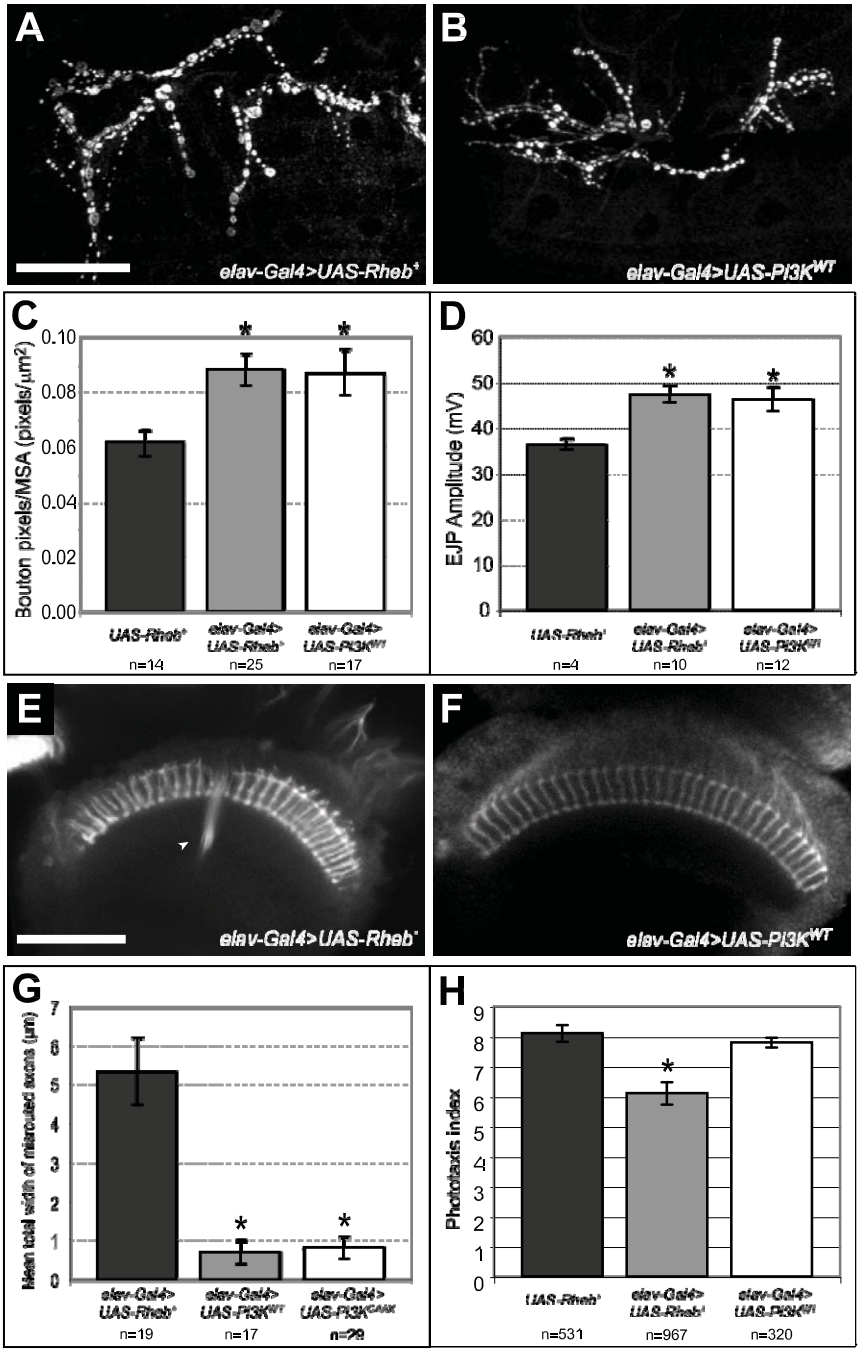

Figure 3. Pi3K and Rheb have similar effects on synapse size and function, but not on axon guidance or phototaxis behavior. (A–C) Neuronal expression of either Pi3K or Rheb had equivalent effects on synapse size, as measured by anti-CSP staining. (D) Suprathreshold electrical stimulation of the motoneuron produces synaptic transmission and depolarization of the underlying muscle known as an excitatory junctional potential (EJP) [33]. This physiological measurement provides a reproducible readout of synapse functionality. Compared to control animals lacking a neuron-specific Gal4 driver, Pi3K expression and Rheb expression both caused similar increases in EJP amplitudes at the neuromuscular junction. (E–G) Anti-Chaoptin staining of photoreceptor axons revealed that, contrary to the axon guidance defects observed in animals overexpressing Rheb (arrowhead), axon guidance misroutings in Pi3K-expressing animals were extremely rare, even when we expressed the constitutively-activated transgene UAS-Pi3K^{CAAX}. (H) Neuronal overexpression of Pi3K did not cause deficits in phototaxis behavior, unlike what was observed when flies overexpressed Rheb. Asterisks denote $p \gtrsim 0.05$ compared to control UAS-Rheb^{+}/+ animals using a two-tailed student's t-test statistic. Scale bars are 50 microns.

doi:10.1371/journal.pone.0030722.g003

restriction to affect either the NMJ growth or the physiological changes mediated by hyperactivation of Tor indicates that nutritional signals have a smaller impact on these Rheb-mediated outcomes.

Effects of activated AMPK on Tor misregulation

Given the ability of dietary changes to alter the behavioral and axon guidance deficits of Tor hyperactivation, we examined whether genetically manipulating an energy-sensing input to Tor

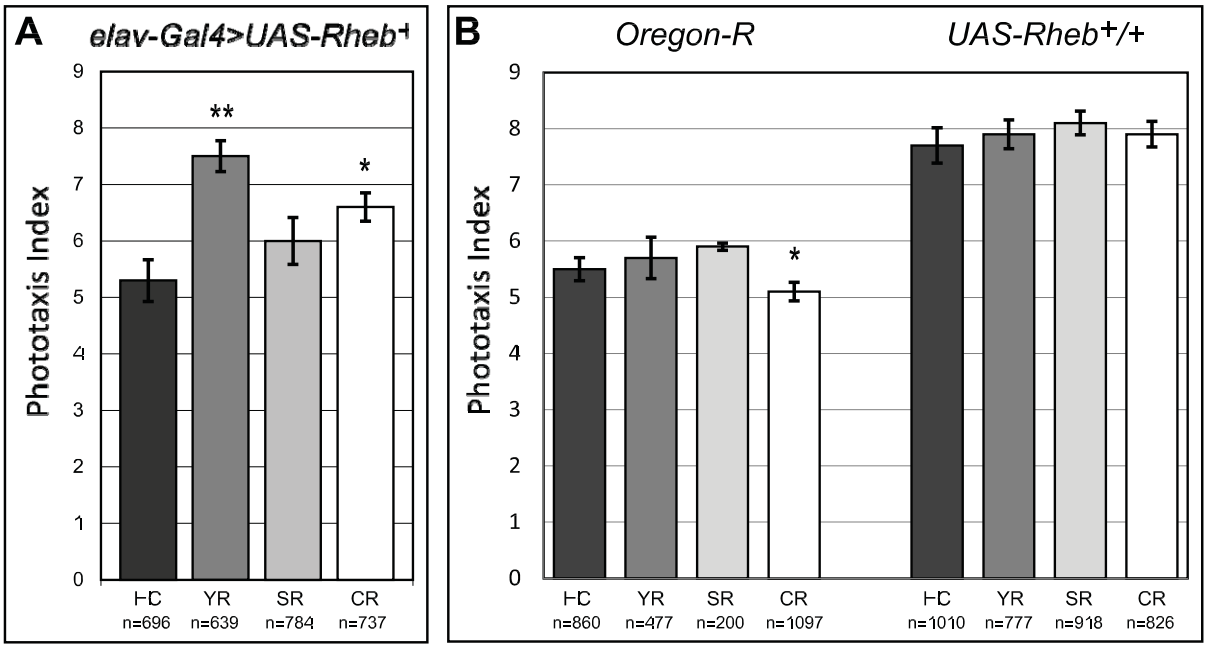

Figure 4. Changes in diet can rescue phototaxis behavior. (A) Yeast-restricted (YR) and calorie restricted (CR) diets significantly rescued phototaxis behavioral deficits in Rheb-overexpressing flies, compared to identical flies raised on a diet of rich, high-calorie (HC) food. Flies raised on a diet restricted only for sugar (SR) showed a slight trend toward improvement, but the results were not significant. (B) Oregon-R, a wild-type strain of Drosophila which phototaxes poorly but has normal levels of Tor pathway activity, did not show any improvement of phototaxis responses due to dietary changes. A small, statistically significant decrease in phototaxis performance was seen as a result of the calorie-restricted (CR) diet. Dietary changes did not affect phototaxis behavior in control flies which lacked a Gal4 driver, and therefore did not overexpress Rheb. The number of animals (n) in each group is indicated. In all graphs, one asterisk denotes $p < 0.05$ using a two-tailed student's t-test (compared against the HC diet) and two asterisks denotes $p < 0.001$.
doi:10.1371/journal.pone.0030722.g004

signaling, AMPK, could rescue the Rheb overexpression abnormalities we previously observed. In the cell, AMPK assess the ratio between the high-energy molecule ATP and its low-energy counterpart ADP [21]. Under low-energy conditions, AMPK positively regulates Tsc1/2 activity and causes a corresponding decrease in Tor pathway activity (see Fig. 1). Expressing a constitutively activated form of AMPK, $AMPK^{TD}$ [21], in neurons provided signals indicative of a low energy status. When $AMPK^{TD}$ and $Rheb^{+}$ were co-expressed in neurons there was a significant rescue of Rheb-mediated axon guidance and phototaxis abnormalities compared to animals with neuronal expression of $Rheb^{+}$ alone (Fig. 7 A–D). In previous experiments, dietary restriction was not able to rescue Tor-misregulation defects at the synapse, and a similar result was found for AMPK. Not only did $AMPK^{TD}$ expression fail to rescue the synaptic abnormalities (Fig. 7 E–I), it actually enhanced Rheb-mediated synapse overgrowth (Fig. 7H). Expression of $AMPK^{TD}$ alone, under the direction of elav-Gal4, did not affect NMJ size or EJP responses. It would appear, therefore, that the synaptic effects of AMPK are dependent on the baseline activity of Rheb and Tor.

Identifying downstream components of Rheb-overexpression phenotypes

To determine how different inputs that influence Tor activity (calorie levels, AMPK, Rheb, Pi3K) affected some Rheb-overexpression phenotypes but not others, a series of experiments were undertaken to modulate Tor-containing complexes downstream of Rheb. Previous studies have established that nutrient levels, and in particular amino acids, regulate the growth control functions of TOR primarily by modulating the activity of TORC1, the Raptor-containing complex that affects translation, ribosome biogenesis, and autophagy [10,20]. Because the axon guidance defects produced by Rheb overexpression were sensitive to changes in dietary composition, TorC1 was a logical signaling complex to test that could be essential for photoreceptor axon misrouting abnormalities. This hypothesis was examined by testing the ability of an RNAi construct targeted against raptor, a critical component of TorC1 [16,40], to suppress the effects of neuronally-directed Rheb expression. Using the pan-neuronal driver elav-Gal4, $Rheb^{+}$ was co-expressed along with a raptor RNAi transgene. Knockdown of raptor resulted in almost complete rescue of Rheb-mediated axon guidance defects (Fig. 8A, C), suggesting that this is indeed a TorC1-dependent output of Tor hyperactivation. RNAi knockdown of S6k, a major downstream target of TorC1-signaling, also significantly reduced the axon misroutings produced by overexpression of $Rheb^{+}$ in neurons, supporting the conclusion that this phenotype is largely a TorC1-directed process (Fig. 8B, C). To rule out the possibility that the presence of two UAS-containing transgenes titrated the level of Gal4 protein, and produced rescue by simple reduction of Rheb expression, we determined the level of synapse expansion mediated by elav-Gal4 - UAS-Rheb when a second UAS-mCD8-GFP was present in the stock. In this case we observed a 3-fold expansion of the NMJ (data not shown), a level comparable to previously published findings from our group (2.2 fold) [41]. We have also conducted control experiments where we examined the expression levels of two tagged UAS-transgenes, either when only one (UAS-mCD8-GFP) or both (UAS-mCD8-GFP and UAS-RFP) were present in the animal bearing the elav-Gal4 driver. Expression of UAS-mCD8-GFP at the NMJ was unaffected by the presence of the second UAS-transgene (data not shown), indicating that titration of Gal4 protein was not a confounding factor in these experiments.

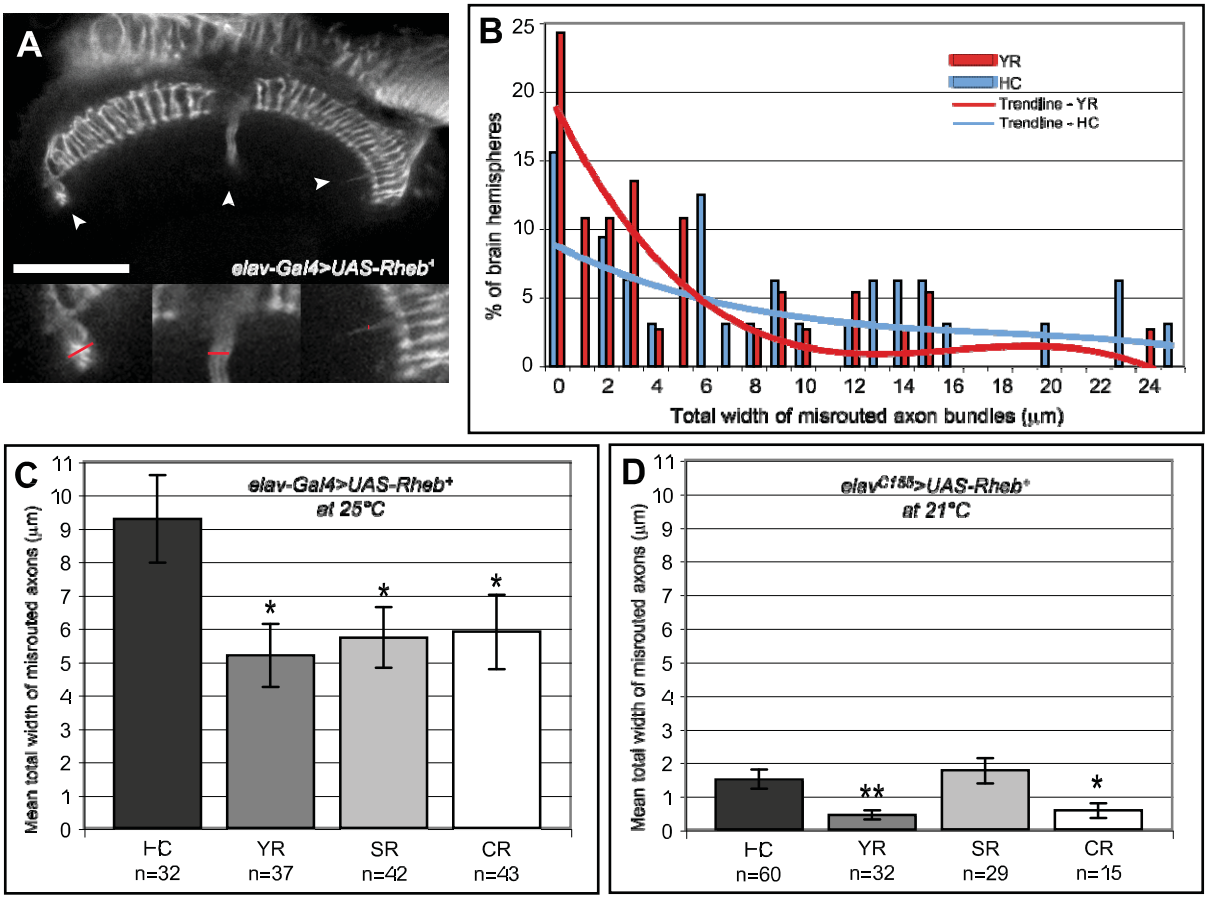

Figure 5. Dietary changes can rescue axon misrouting defects in photoreceptor neurons. (A) In pupal brains with neuronally-directed overexpression of Rheb (elav-Gal4 ‐ UAS-Rheb^{+}), anti-Chaoptin staining revealed photoreceptor axon bundles that failed to stop at their proper targets and continued to grow into other areas of the brain (arrows). The inset images at the bottom of this panel (2✕ magnified) contain red bars that illustrate our technique for measuring across the width of these misrouted axon bundles. By adding these measurements together we achieved a semi-quantitative measure for the severity of axon guidance defects within each individual brain hemisphere. (B) Dietary restriction in Rheb-overexpressing animals shifted the distribution of brains with axon guidance problems away from the more severe defects and towards more mild phenotypes (compare YR and HC diets). This was measured by the percentage of brain hemispheres (penetrance) with wider bundles of axon misroutings versus the percentage of brains with smaller misroutings or no misroutings at all. (C) Averaging the width of misrouted axon bundles across all the brains in a particular group provides an alternative measure of axon misrouting severity. The restricted diets significantly rescued axon guidance defects in Rheb-overexpressing animals compared to the same flies raised on rich, high-calorie (HC) food. (D) We greatly reduced the level of Rheb overexpression by using a different neuron-specific Gal4 driver, elav^{C155}, and rearing the flies at a temperature that limits Gal4 activity, 21uC. Under these conditions, axon misrouting defects were much milder and could only be rescued by the YR and CR diets, both of which are restricted in their levels of yeast, the primary source of lipids and amino acids. Reducing sugar alone (the SR diet) had no effect. In all graphs, one asterisk denotes $p < 0.05$ using a two-tailed student's t-test (compared against the HC diet) and two asterisks denotes $p < 0.001$. Scale bar is 50 microns.
doi:10.1371/journal.pone.0030722.g005

TorC2 is a regulator of actin dynamics, cell morphological changes, and dendritic arborization [9,11]. Mutations compromising the function of Sin1 and rictor, two unique TorC2 components, have been described and provide a means of selectively compromising this signaling entity. Null mutations in either of these genes are viable, allowing these alleles to be placed in the context of a fly with neuronally-directed Rheb^{+} expression. Null mutations in either rictor or Sin1 failed to show a statistically significant effect on Rheb-mediated axon guidance defects (Fig. 8D–E), indicating that TorC2 is not involved in this particular output of elevated Tor signaling.

In contrast to axon guidance defects, the synapse overgrowth phenotypes of Rheb overexpression were not suppressed by diet restriction or AMPK activity. To further explore these findings, TorC1 activity was inhibited with the same neuronally-directed raptor and S6k RNAi constructs that were effective in suppressing axon guidance defects mediated by Rheb. Neither the S6k nor raptor RNAi transgene was able to rescue Rheb-mediated synaptic overgrowth (Fig. 9A–D). To evaluate the role of TorC2 in Rheb-directed synapse overgrowth, sin1 and rictor mutants were crossed into elav-Gal4 ‐ UAS Rheb^{+} flies. Both sin1 and rictor mutations were able to suppress the overgrowth of the NMJ mediated by overexpression of Rheb (Fig. 9E–J). sin1 mutants also showed a significantly smaller synapse compared to controls (Fig. 9I), suggesting that TORC2 does play a role in the NMJ growth during normal development.

Discussion

The TOR signaling pathway, long known for influencing growth control and tumor formation, has more recently been identified as an important pathway in nervous system development, controlling such cellular events as cell migration, axon

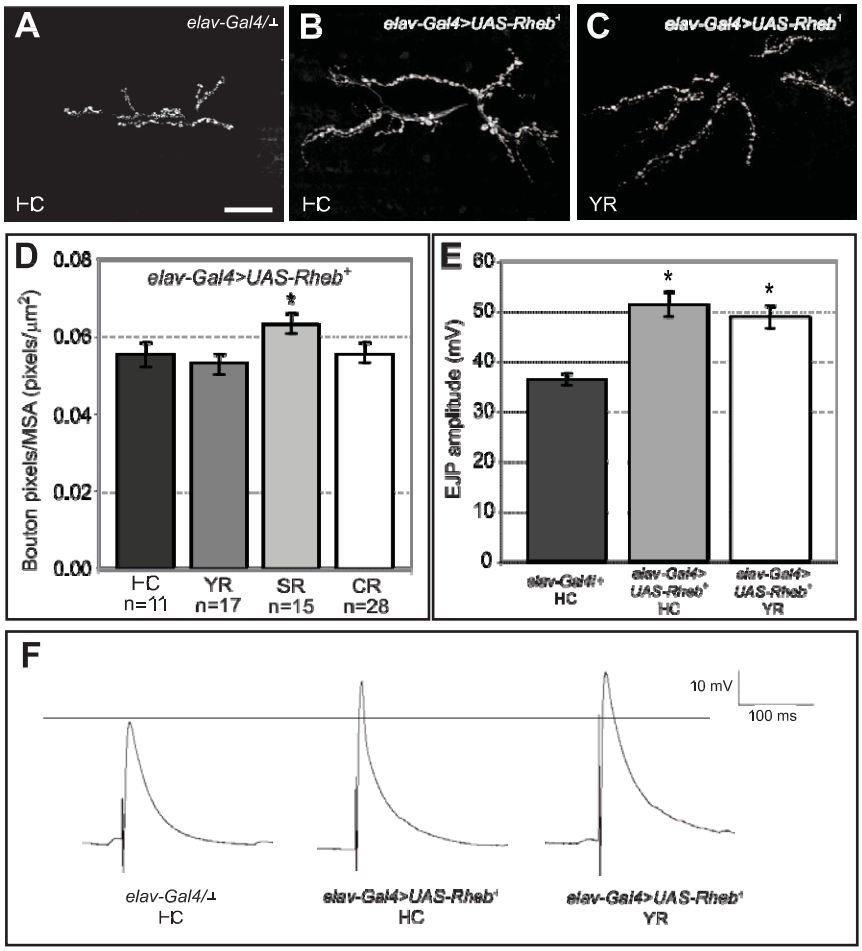

Figure 6. Dietary restriction does not rescue Rheb-mediated overgrowth or electrophysiological changes at neuromuscular synapses. (A, B) Rheb overexpression caused an increase in the CSP-expressing pixels (boutons) in larval motoneurons at the neuromuscular junction, as shown by anti-CSP staining. (C, D) Dietary restriction showed no significant rescue of the Rheb-overexpression phenotype at the NMJ, and restriction of sugar (SR) actually caused a modest increase in the CSP-stained regions of the boutons, corrected for muscle size (by dividing by the muscle-surface-area). (E) The hyperfunctional excitatory junctional potential (EJP) responses seen in Rheb-overexpressing animals could not be rescued by a dietary regime that was particularly effective at rescuing both phototaxis behavior and axon misrouting (compare elav-Gal4 ∴ UAS-Rheb$^+$ animals raised on the YR diet, n = 11, to elav-Gal4 ∴ UAS-Rheb$^+$ animals raised on the HC diet, n = 11. For elav-Gal4/+ control animals raised on HC food, n = 7). (F) Representative traces of recorded EJP measurements clearly illustrate the elevated amplitudes observed when Rheb is overexpressed, regardless of diet. Asterisks denote p ∴ 0.05 using a two-tailed student's t-test compared against the HC diet in D, and against elav-Gal4/+ control animals in E. Scale bar is 50 microns.
doi:10.1371/journal.pone.0030722.g006

guidance, synaptic expansion, and dendritic arborization [3,7,9,42,43,44]. The central role of TOR as an integrator of signals from different metabolic and growth factor inputs has been well established with regards to growth control, but how these inputs affect TOR-directed neural development had not been previously examined. The TOR signaling pathway is rather unique in serving a critical role in both the regulation of metabolism and the control of developmental patterning. The fact that dietary influences are able to affect the morphological and physiological processes controlled by this system emphasizes that energy availability is not simply a ''stop'' or ''go'' input to development. Rather, neural patterning and metabolism are linked via this critical growth regulatory pathway.

Pi3K and Rheb have distinct activities in neural patterning

We tested multiple upstream inputs to Tor signaling and found each one to have a varying ability to affect Tor-hyperactivation phenotypes (summarized in Fig. 10). For example, growth factor inputs through Pi3K produced the same level of synapse expansion as overexpression of Rheb, however Pi3K had no effect on axon misrouting or phototaxis behavior. This fits with earlier work from our group where we found that loss of Pten, an antagonist of Pi3K activity, in the Drosophila retina produced much milder photoreceptor misrouting defects compared to loss of Tsc1, the primary inhibitor of Rheb [27]. Rheb activates Tor directly, whereas Pi3K influences Tor through a series of molecular intermediaries, most notably Akt and Tsc1/Tsc2 [22]. Pi3K signaling certainly does play an important role in Tor pathway events such as responding to insulin signals and mediating inhibitory feedback mechanisms, yet Pi3K signaling also has a number of other downstream targets independent of Tor. It would seem that in photoreceptor axon guidance and phototaxis behavior Pi3K has only a modest impact on Tor signaling.

Dietary and AMPK-mediated rescue of Rheb-induced axon guidance defects

Manipulation of metabolic inputs provided significant rescue of Tor-mediated axon guidance and phototaxis deficits. The most

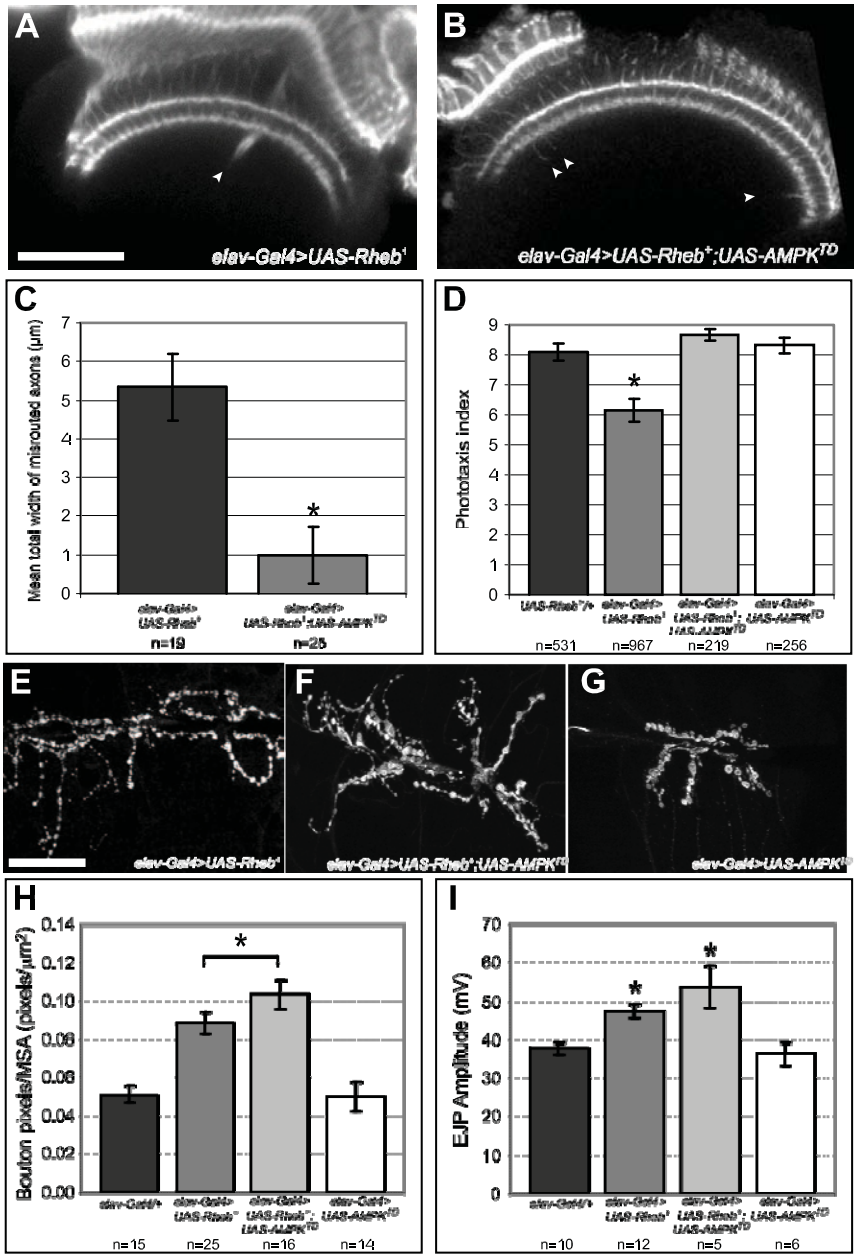

Figure 7. Constitutively active AMPK rescues Rheb-mediated axon guidance and phototaxis deficits, but not NMJ overgrowth or amplified EJP responses. (A–C) Expression of a constitutively activated AMPK transgene together with Rheb^{+} greatly decreased the severity of the axon misrouting defects (arrows) normally seen in Rheb–overexpressing animals. (D) Co-expression of both AMPK^{TD} and Rheb^{+} in neurons also rescued the phototaxis deficits normally present in Rheb-expressing animals. When we expressed AMPK^{TD} on its own, we did not see any change in phototaxis performance compared to controls or any measurable axon misrouting (data not shown). (E–H) At the larval NMJ, co-expression of a constitutively-activated AMPK in Rheb-overexpressing neurons did not rescue Rheb-mediated synaptic overgrowth, and in fact, caused an even greater increase in synapse size, despite the fact that AMPK^{TD} had no effect on synapse growth when expressed on its own. (I) Similarly, co-expression of AMPK^{TD} in Rheb-overexpressing neurons failed to rescue the elevated EJP amplitudes and, in fact, further exacerbated this defect. AMPK^{TD} had no effect on synaptic response when expressed alone. Asterisks denote a two-tailed Student's t-test statistic of $p > 0.05$. Scale bars are 50 microns.
doi:10.1371/journal.pone.0030722.g007

substantial rescue of Rheb overexpression phenotypes by diet came from the ones lowest in lipids and amino acids, namely YR and CR. This suggests caloric levels and content both affect Tor activity in the context of neural patterning. Indeed, different amino acids are known to have varying degrees of effect on TOR pathway activity. For example, restricting the level of either leucine or arginine alone results in nearly the same degree of TORC1 inactivation as restricting all amino acids [28]. These observations are relevant toward designing diets that are optimally suited for diminishing the effects of TOR hyperactivation. We note that more severe disruption of Tor signaling produced by complete loss of Tsc1 function in the retina of a genetic mosaic animal was not rescued by dietary restriction (data not shown), indicating that an intact Tsc-Rheb-Tor axis is required for dietary

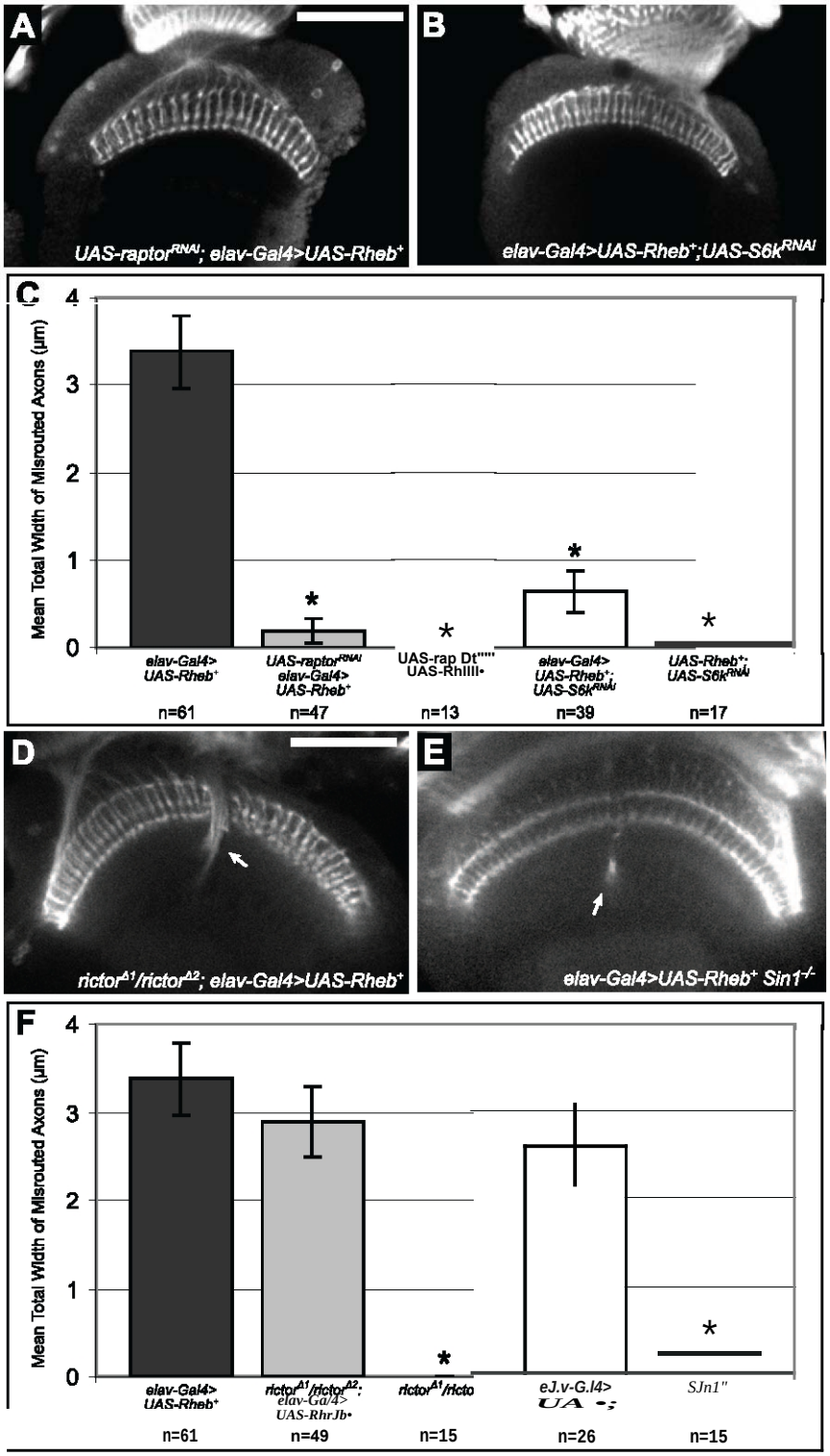

Figure 8. Rheb-mediated axon guidance defects are dependent on TorC1 downstream components, but not on TorC2. {A-C) *Rheb* was neuronally expressed in pupal brains along with *RNAi* constructs against either *raptor,* a principal component of Tor-complex 1, or *S6k,* an important downstream mediator of TorC1 activity. Genetic knockdown of either of these critical mediators of TorC1 signaling significantly rescued the axon misrouting defects normally observed in Rheb-overexpressing animals. {D–F) When *Rheb* was neuronally overexpressed in animals with null mutations in either of the critical TorC2 components *rictor* or *Sin1,* we saw no significant rescue of axon guidance defects (arrows). Although *Sin1* mutants did show a small degree of axon misrouting even in the absence of *Rheb* misexpression, this level of defect was not substantial enough to confound the interpretation of our primary results. Asterisks denote a two-tailed Student's t-test statistic of p<O.OS compared to *elav-Gai4>UAS-Rheb+* controls. Scale bars are 50 microns.

doi:1 0.1371/journa l.po ne.0030722.g008

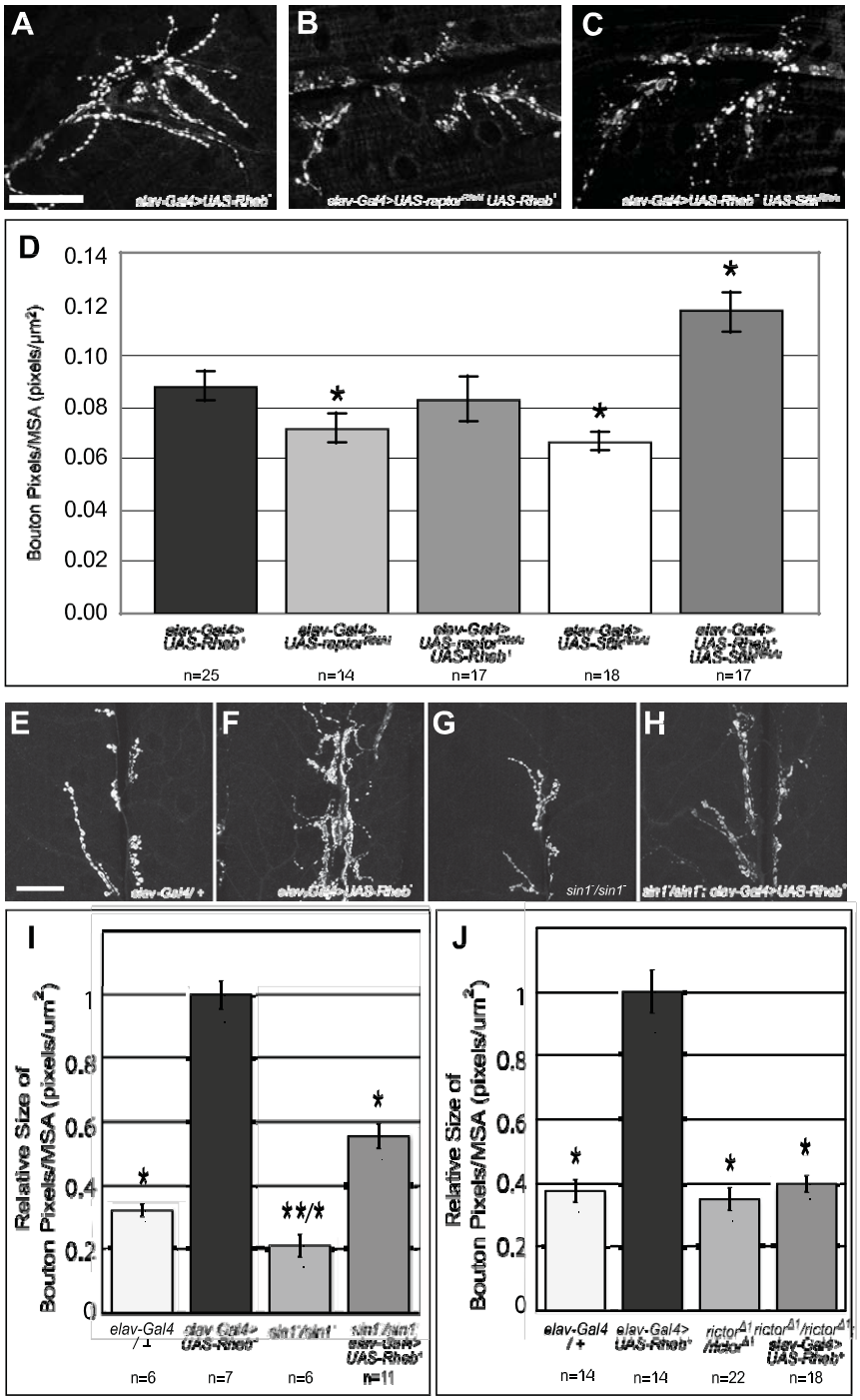

Figure 9. Rheb-mediated synapse overgrowth was not rescued by knockdown of TorC1 signaling, however it was rescued by loss of the TorC2 components sin1 and rictor. (A) Anti-CSP staining of third-instar larval NMJs shows considerable overgrowth of motoneuron boutons in Rheb-overexpressing animals. (B–D) RNAi knockdown of either the TorC1 component raptor or the TorC1 downstream mediator S6K failed to decrease the severity of synapse overgrowth defects when Rheb was overexpressed. Reducing S6K function actually worsened the severity of this phenotype. (E–J) In contrast, homozygous loss of the TorC2 components sin1 and rictor significantly rescued synaptic overgrowth in Rheb-overexpressing animals, indicating that this is a TorC2-dependent event. Asterisks denote a two-tailed Student's t-test statistic of $p > 0.05$ compared to elav-Gal4 > UAS-Rheb^{+}(*) or to elav-Gal4/+ (**) controls. Scale bars are 50 microns.
doi:10.1371/journal.pone.0030722.g009

effects. This is precisely the situation that exists in individuals with tuberous sclerosis since heterozygosity for TSC1 or TSC2 is causative for the disorder.

Expression of a constitutively activated AMPK in neurons also rescued Rheb-mediated misrouting of photoreceptor axons. This finding is consistent with current models where AMPK serves to

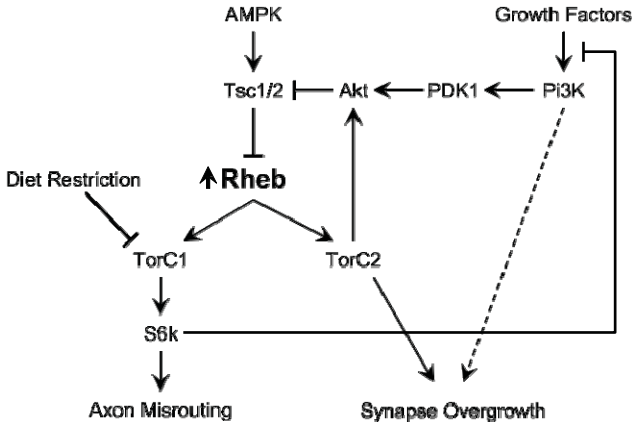

Figure 10. Axon guidance and synapse growth are controlled by separate branches of the Tor signaling pathway. A schematic diagram illustrating the effects of Tor-signaling elements on axon guidance and synapse growth. Rheb-mediated axon misrouting defects are dependent on signaling through TorC1 and S6k, and can be rescued by diet restriction or AMPK expression. Axon guidance is largely insensitive to changes in Pi3K. Synapse overgrowth mediated by Rheb overexpression is dependent on signaling through TorC2, is not rescued by caloric restriction or AMPK activation, and is exacerbated by knockdown of S6k, suggesting the removal of a feedback inhibition. Synapse overgrowth is also induced by Pi3K overexpression, similarly to Rheb.
doi:10.1371/journal.pone.0030722.g010

activate the Tsc1/Tsc2 complex, thus limiting Tor activation under conditions of energy depletion. However, neither diet restriction nor AMPK activation rescued synapse overgrowth. In fact, expression of a constitutively activated AMPK enhanced the Rheb-mediated synapse overgrowth phenotype. This finding emphasizes that axon misrouting and synapse growth are fundamentally different Tor-regulated processes. If AMPK primarily affects reduction of TorC1 activity, perhaps the downregulation of TorC1 influences a feedback loop that enhances other Tor-dependent events at the NMJ. In fact, we have evidence that Rheb-directed synapse overgrowth is largely a TorC2-mediated process and is relatively insensitive to TorC1 activity.

A similar rescue of some Tor-hyperactivation phenotypes but not others was recently reported for a mouse model of TS in which Tsc1 function had been eliminated in most neurons [7]. In this system, rapamycin treatment rescued abnormal cell body growth, myelination deficits, and neurofilament overenlargement, yet rapamycin had no effect on neuronal dysplasia and it only slightly rescued defects in dendritic spine density. These results illustrate a categorical difference between different outputs of TOR hyper-activation, and they demonstrate that various inputs to TOR signaling are specifically targeted to some functions of TOR and not others.

TorC1 and TorC2 control distinct processes in neural development

Rapamycin treatment and amino acid restriction act primarily on TorC1 rather than TorC2. The ability of diet and AMPK activity to affect axon misrouting and phototaxis deficits in Rheb-overexpressing animals suggested that these defects were largely TorC1-dependent events. This model was supported by our finding that Rheb-directed axon misrouting was rescued by knockdown of the TorC1 component raptor or the primary downstream component of TorC1 signaling, S6k. These results are on the face of it in contrast with previously published findings that reductions in S6K function or rapamycin treatment (a TORC1-inhibitor) were unable to ameliorate axon guidance abnormalities in genetic mosaics where photoreceptor neurons are homozygous mutant for Tsc1 [41]. It is important to point out the substantial difference in phenotype severity produced by loss of Tsc1 in the retina versus overexpression of Rheb described here, a much milder phenotype. We interpret these findings that modulation of TORC1 function (rapamycin) and output (S6K) is only effective in altering the severity of the axon guidance abnormality in the context of an intact Tsc-Rheb-Tor axis. It is also possible that TORC1 is only one TOR-containing signaling complex that affects axon guidance, and in the presence of very high levels of TOR activity, TORC1-modulation cannot suppress the most severe phenotypes. Axon guidance abnormalities produced by overxpression of Rheb were however, entirely insensitive to mutations in rictor, an essential TorC2-component. These findings show that disruptions of Tor pathway function that affect axon misrouting can be affected by TorC1-directed processes (Fig. 10) and we were unable to detect TORC2-modulation or regulation of axon routing processes in the visual system.

Unlike axon misrouting defects, synapse overgrowth was not rescued by dietary restriction or knockdown of TORC1 signaling. Rather, Rheb-mediated synapse overgrowth was rescued by knockout of either of two TORC2 components, rictor or sin1. Sin1 mutants also displayed a smaller synapse compare to controls, indicating that TORC2 serves a role in normal synapse growth. A recent study also discovered a role for TorC2 in the growth of sensory neuron dendritic arbors in Drosophila [9], thus TorC2 is clearly an important element in Tor regulation of neuron and synapse morphogenesis.

The inability of raptor or S6k RNAi to suppress Rheb-directed synapse overgrowth, together with the clear effects of rictor and sin1 on this phenotype, emphasizes that hyperactivation of the Tor pathway in neurons produces NMJ expansion at least in some measure via a TorC2-directed process. Paradoxically, however, knockdown of the downstream TorC1 effector S6k produced a significant increase in the severity of this Rheb-mediated synapse overgrowth phenotype. In situations where Tor signaling is elevated, such as occurs when Rheb is overexpressed, an inhibitory feedback mechanism exists between S6k and the insulin receptor substrate Chico that dampens the level of Tor pathway activation [45]. Knockdown of S6k in the context of Rheb overexpression decreases or eliminates this feedback and could result in even higher levels of Tor activation. It is possible that this loss of S6k feedback indirectly increases the level of TorC2 activation, resulting in the enhancement of synapse overgrowth we see in these animals.

Although it is widely accepted that TorC1 is directly activated by Rheb [20,34], the relationship between Rheb and TorC2 is not fully understood. Studies using cultured Drosophila S2 cells previously suggested an inhibitory effect of Rheb on TorC2 activity [16,46], yet this model doesn't fit with our observations in vivo. Overexpression of Rheb caused synapse overgrowth at the NMJ which could be rescued by knockout of TorC2 components rictor and sin1. Rather than an inhibitory relationship, this finding suggests a positive relationship between Rheb and TorC2 in this context. Whether Rheb can directly activate TorC2 or must activate it through some indirect process remains to be explored, but the basic relationship is clear. The observation that Tor pathway components can behave differently in various cellular contexts is not without precedent. In the mouse brain, for example, inactivation of PDK1, a critical mediator of PI3K

signaling, caused an increase in phosphorylated AKT at the TORC2-dependent site, but this effect was seen only in glial cells and not in neurons [47]. Likewise, AMPK mutations have been shown to cause cell-polarity defects in Drosophila epithelial tissues [21], yet in the retinal epithelium AMPK mutations caused a progressive neural degeneration phenotype and cell polarity was normal [48]. Even within cells of the same type there is evidence that Tor-signaling components interact with each other differently based on changes in the cellular environment. In the Drosophila wing disk, for example, under normal physiological conditions feedback inhibition of Akt phosphorylation is primarily mediated through an S6k-independent function of TorC1, yet under conditions of elevated Tor pathway activity, feedback inhibition becomes S6k-dependent [45]. Taken as a whole, these observations show that the relationships between different Tor-signaling components are cell-type specific and respond dynamically to different signaling states.

Recently autophagy has been shown to affect NMJ expansion via the regulation of Highwire (Hiw), a ubiquitin E3 ligase [49]. Activation of autophagy, either by reduction of TorC1 signaling or overexpression of atg1, produced a characteristic synapse expansion phenotype with long synaptic branches and many small diameter boutons. Loss of hiw, in addition to producing a larger NMJ, compromises the physiological function of the NMJ and results in markedly reduced EJP responses [50,51]. We consider this type of synapse expansion to be functionally distinct from what we have produced in our Drosophila model of TS, where hyperactivation of Tor signaling produces a large synapse with many large boutons and an enhanced EJP response to suprathreshold stimulation of the motoneuron. The involvement of TorC1-directed autophagy in regulating the levels of Hiw, a modulator of synapse growth, and the clear role of TorC2 in the synapse expansion we describe here, emphasizes the complexity of Tor function in synapse development.

Implications from a fly model of TS

Understanding the complex relationships between various inputs to Tor is important for designing interventions that could ameliorate the neurological and behavioral consequences of elevated TOR signaling, as occurs in humans with TS. In traditional metabolic disorders such as phenylketonuria, nervous system function is disrupted by a buildup of toxic intermediaries produced by deficits in particular metabolic pathways [52]. Disruptions of TOR signaling operate much differently, where it is the levels of common metabolic regulatory molecules that must be tightly controlled to ensure appropriate activation of the pathway. Our results using this relatively simple model system suggest that pharmaceutical interventions at different levels of TOR signaling may have very different effects with respect to neurological function. Neurological deficits of TS individuals might best be affected by Rheb-directed interventions, since that level of the pathway affects both axon guidance and synapse assembly. Targeting more distant inputs must be done carefully, since some of these may have unanticipated effects. For example, AMPK expression substantially diminished axon guidance and behavioral deficits, but it also caused a marked increase in the severity of synaptic overgrowth and hyperfunctionality. Similarly, although TORC1-specific drugs such as rapamycin can be used to treat the effects of TOR-hyperactivation in humans, these will likely not affect TORC2-mediated abnormalities which could contribute to some elements of the neurological or behavioral deficits. The possibility of ameliorating TOR-misregulation with diet suggests a viable alternative to pharmaceutical intervention. Diet restriction has long been used to effectively treat seizure disorders [24], but a better understanding of this pathway is needed to make optimal decisions about the dietary changes that would be most effective and clinically realistic. Clearly, the more we come to understand about this unique system that links metabolism and neural development, the better equipped we will be to address the various problems that arise when control of this pathway is lost.

Materials and Methods

Fly Stocks

w^*; P{UAS-Rheb.Pa}3 (UAS-Rheb$^+$), w^*; P[w^+;Gal4-elav.L]2/CyO (elav-Gal4), P{GawB}elav^{C155} (elav^{C155}), Oregon-R-C (Oregon-R), y^1 w^*; P{WT-Dp110}2 (UAS-Pi3K^{WT}), P{Dp110-CAAX}1 (UAS-Pi3K^{CAAX}), and w^{1118}; PBac{RB}Sin1^{e03756} (Sin1$^{2/2}$) were from the Bloomington Drosophila Stock Center. P{GD5138}v13112/CyO (UAS-raptor^{RNAi}) and w^{1118} P{GD6646}v18126 (UAS-S6K^{RNAi}) were from the Vienna Drosophila RNAi Center. Tor^{D6B} was a gift from T. Neufeld, UAS-AMPK^{TD} 4-1 was a gift from J. Chung [21], and both rictor^{D1} and rictor^{D2} were gifts from S. Cohen [13].

Food Preparation

Our standard fly food contains approximately 869 kcal/L from the cornmeal, sugar and yeast ingredients (Harvard Biolabs). The four diets were taken directly from a recipe previously described [36]. Per Liter of food, all diets contained 20 g of agar, 30 mL of a 100 g/L methyl 4-hydroxybenzoate (Sigma) solution, 3 mL of propionic acid, and varying amounts of brewer's yeast and sucrose depending on the diet. The rich, high-calorie (HC) diet contained 150 g/L of both yeast and sucrose resulting in an estimated total of 1203 kcal/L, the yeast-restricted (YR) diet contained 65 g/L of yeast and 150 g/L of sucrose for an estimated total of 861 kcal/L, the sugar-restricted (SR) diet contained 150 g/L of yeast and 65 g/L of sucrose for an estimated total of 863 kcal/L, and the calorie-restricted (CR) diet contained 65 g/L of both yeast and sucrose for an estimated total of 521 kcal/L.

Phototaxis analysis

Phototaxis analysis was performed using an 11-tube countercurrent distribution apparatus similar to one previously described [53] and based on the phototaxis sorting technique developed by S. Benzer [54]. Newly-eclosed Drosophila adults were sedated by carbon dioxide and counted into sample groups of 50–100 mixed male and female populations. After a 24-hour period of recovery, the flies were dark-adapted (placed in a dark room) for 30 minutes and then transferred into the first tube of the phototaxis apparatus. A 15-watt soft-white fluorescent lamp was placed 6 cm away, and the flies were allowed 60 seconds between each shift of the apparatus to move towards the lighted end of each tube. After ten trials, the number of flies in each tube was counted and the results were then analyzed using the phototaxis index equation, $PI = (1/N) \sum_i i \cdot n_i$ where i is the fraction number (tube number), n is the number of flies in the given fraction, and N is the total number of flies tested [31].

Immunohistochemistry

For visualization of photoreceptors, Drosophila were dissected 40-hours after pupal formation and stained according to established protocols [55]. Anti-Chaoptin (MAb 24B10, Developmental Studies Hybridoma Bank) was used at 1:25. The widths of misrouted axon bundles were measured using ImageJ data analysis software (NIH). For visualization of NMJ synapses, third instar larvae were filleted in PBS and fixed in 4% formaldehyde before staining with anti-Cysteine String Protein at 1:1000 (MAb 1G12,

Developmental Studies Hybridoma Bank). For determining ''bouton pixel number,'' a measure of synapse size, individual confocal optical sections were volume-rendered to show the entire depth of Anti-CSP staining for each synapse (between muscles 6 and 7 of the second abdominal (A2) hemisegment). Traditionally, synapse size at the NMJ has been assessed by counting boutons detected by anti-CSP or other presynaptic marker staining in a two dimensional projection of a serially-sectioned preparation. We found this method limiting in conditions where individual boutons are not distinct and it is difficult to obtain a reliable bouton count. We therefore measured synapse size by determining the number of anti-CSP stained pixels, setting a threshold for staining above background. Images were opened in Adobe Photoshop CS3 (Adobe Systems Inc., San Jose, CA) and a threshold value was set for each image to maximize the synapse while removing background fluorescence. Pixels below threshold were assigned an intensity value of 0 and all pixels above threshold intensity were assigned a value of 255. A histogram function was used to measure the total number of pixels within the synapse that were above threshold. This method of synapse size measurement provides for quantitation where the subjective assignment of whether fluorescence is coalesced into a defined bouton is not part of the process. This method was compared to the standard bouton-counting procedure, where individual boutons are scored, and similar relationships between experimental samples were obtained. For example, the bouton-counting method (normalized for muscle area) for elav-Gal4 - UAS-Rheb animals reared on different diets gave the following measures (HC = 0.00296 0.000188, YR = 0.00275 6 0.00018, SR = 0.00335 6 0.000164 and CR = 0.00283 6 0.00020 with n = 30, 25, 32 and 12 respectively). Note that the relationships between the different data sets are the same as when assessed using the pixel counting method (shown in Figure 6D), with one sample significantly different (larger) than the others (SR diet). In all cases, muscle surface areas were the combined measurements of muscles 6 and 7 as determined by ImageJ data analysis software (NIH,Bethesda, MD). Images were collected using a Nikon C1 upright laser confocal and Olympus FV1000 laser scanning confocal microscope with Nikon EZC1 imaging software and Imaris V7.3 (Bitplane Inc. Saint Paul, MN).

Electrophysiology

EJP recordings were taken from muscle six of the second abdominal hemisegment (A2) in third instar larvae. Dissections were performed in calcium-free saline and recordings were taken in modified HL3 medium with a calcium concentration of 1.2 mM [39]. Thin-walled glass recording electrodes with resistances of 10–30 mV were pulled on a Model P-87 needle puller (Sutter Instrument Company) and back-filled with 3 M KCl. Muscle six of A2 was impaled with the recording electrode, and a suction electrode was used to stimulate the motoneuron with a Grass stimulator delivering six 1 ms pulses at a frequency of 0.1 Hz and an intensity of approximately 1.5 times the minimum required to evoke a compound response. Recordings were acquired with an Axoclamp 2B amplifier and Clampex 9.2 software (Axon Instruments). EJP amplitudes were measured with MiniAnalysis software from Synaptosoft.

Food Consumption Analysis

Rates of ingestion and nutrient absorption were measured based on previously published techniques [38]. Flies were reared on four different diets from hatching to early third instar, at which point they were transferred to new vials containing the same food seeded with 10 mCi/mL of dCTP[a-32P] (MP Biomedicals). After six hours of free feeding, 10–15 larvae from each group were washed and placed in 10 mL of scintillation fluid. Accumulated levels of radioactivity were then measured using a Beckman Liquid Scintillation counter and the amount of ingested food was calculated.

Supporting Information

Figure S1 Diets that vary in nutritional content are consumed and absorbed equally by third instar larvae. Food ingestion was measured for elav-Gal4 - UAS-Rheb^{+} third instar larvae raised on four different diets. Despite having varying nutritional content, each of the foods we tested was consumed approximately equally during a six hour period of free feeding. Although there appeared to be a trend towards increased feeding on the SR diet, the difference was not statistically significant ($p \# 0.39$ in a two-tailed Student's t-test compared against HC food).
(EPS)

Acknowledgments

We would like to acknowledge materials provided by the Developmental Studies Hybridoma Bank.

Author Contributions

Conceived and designed the experiments: BDD KH AW HGL NZ BC SBS. Performed the experiments: BDD KH AW HGL NZ BC. Analyzed the data: BDD KH AW HGL NZ BC. Contributed reagents/materials/analysis tools: MBO TPN SBS. Wrote the paper: BDD HGL SBS.

References

1. Zhang H, Stallock J, Ng J, Reinhard C, Neufeld T (2000) Regulation of cellular growth by the Drosophila target of rapamycin dTOR. Genes Dev 14: 2712–2724.
2. Swiech L, Perycz M, Malik A, Jaworski J (2008) Role of mTOR in physiology and pathology of the nervous system. Biochim Biophys Acta 1784: 116–132.
3. Tavazoie S, Alvarez V, Ridenour D, Kwiatkowski D, Sabatini B (2005) Regulation of neuronal morphology and function by the tumor suppressors Tsc1 and Tsc2. Nat Neurosci 8: 1727–1734.
4. Inoki K, Corradetti M, Guan K (2005) Dysregulation of the TSC-mTOR pathway in human disease. Nat Genet 37: 19–24.
5. Curatolo P, Bombardieri R, Jozwiak S (2008) Tuberous sclerosis. Lancet 372: 657–668.
6. Neufeld T (2004) Genetic analysis of TOR signaling in Drosophila. Curr Top Microbiol Immunol 279: 139–152.
7. Meikle L, Pollizzi K, Egnor A, Kramvis I, Lane H, et al. (2008) Response of a neuronal model of tuberous sclerosis to mammalian target of rapamycin (mTOR) inhibitors: effects on mTORC1 and Akt signaling lead to improved survival and function. J Neurosci 28: 5422–5432.
8. Kwon C, Luikart B, Powell C, Zhou J, Matheny S, et al. (2006) Pten regulates neuronal arborization and social interaction in mice. Neuron 50: 377–388.
9. Koike-Kumagai M, Yasunaga K, Morikawa R, Kanamori T, Emoto K (2009) The target of rapamycin complex 2 controls dendritic tiling of Drosophila sensory neurons through the Tricornered kinase signalling pathway. EMBO J 28: 3879–3892.
10. Wullschleger S, Loewith R, Hall M (2006) TOR signaling in growth and metabolism. Cell 124: 471–484.
11. Jacinto E, Loewith R, Schmidt A, Lin S, Rü egg M, et al. (2004) Mammalian TOR complex 2 controls the actin cytoskeleton and is rapamycin insensitive. Nat Cell Biol 6: 1122–1128.
12. Sarbassov D, Guertin D, Ali S, Sabatini D (2005) Phosphorylation and regulation of Akt/PKB by the rictor-mTOR complex. Science 307: 1098–1101.
13. Hietakangas V, Cohen S (2007) Re-evaluating AKT regulation: role of TOR complex 2 in tissue growth. Genes Dev 21: 632–637.
14. Scanga S, Ruel L, Binari R, Snow B, Stambolic V, et al. (2000) The conserved PI3'K/PTEN/Akt signaling pathway regulates both cell size and survival in Drosophila. Oncogene 19: 3971–3977.

15. Manning B, Cantley L (2007) AKT/PKB signaling: navigating downstream. Cell 129: 1261–1274.
16. Yang Q, Guan K (2007) Expanding mTOR signaling. Cell Res 17: 666–681.
17. Kim E, Goraksha-Hicks P, Li L, Neufeld T, Guan K (2008) Regulation of TORC1 by Rag GTPases in nutrient response. Nat Cell Biol 10: 935–945.
18. Sancak Y, Peterson T, Shaul Y, Lindquist R, Thoreen C, et al. (2008) The Rag GTPases bind raptor and mediate amino acid signaling to mTORC1. Science 320: 1496–1501.
19. Binda M, Péli-Gulli M, Bonfils G, Panchaud N, Urban J, et al. (2009) The Vam6 GEF controls TORC1 by activating the EGO complex. Mol Cell 35: 563–573.
20. Avruch J, Long X, Lin Y, Ortiz-Vega S, Rapley J, et al. (2009) Activation of mTORC1 in two steps: Rheb-GTP activation of catalytic function and increased binding of substrates to raptor. Biochem Soc Trans 37: 223–226.
21. Lee J, Koh H, Kim M, Kim Y, Lee S, et al. (2007) Energy-dependent regulation of cell structure by AMP-activated protein kinase. Nature 447: 1017–1020.
22. Richardson C, Schalm S, Blenis J (2004) PI3-kinase and TOR: PIKTORing cell growth. Semin Cell Dev Biol 15: 147–159.
23. Cummings A, Kavlock R (2004) Gene-environment interactions: a review of effects on reproduction and development. Crit Rev Toxicol 34: 461–485.
24. Hartman A, Vining E (2007) Clinical aspects of the ketogenic diet. Epilepsia 48: 31–42.
25. Potter C, Huang H, Xu T (2001) Drosophila Tsc1 functions with Tsc2 to antagonize insulin signaling in regulating cell growth, cell proliferation, and organ size. Cell 105: 357–368.
26. Tapon N, Ito N, Dickson B, Treisman J, Hariharan I (2001) The Drosophila tuberous sclerosis complex gene homologs restrict cell growth and cell proliferation. Cell 105: 345–355.
27. Knox S, Ge H, Dimitroff B, Ren Y, Howe K, et al. (2007) Mechanisms of TSC-mediated control of synapse assembly and axon guidance. PLoS One 2: e375.
28. Avruch J, Long X, Ortiz-Vega S, Rapley J, Papageorgiou A, et al. (2009) Amino acid regulation of TOR complex 1. Am J Physiol Endocrinol Metab 296: E592–602.
29. McGuire S, Roman G, Davis R (2004) Gene expression systems in Drosophila: a synthesis of time and space. Trends Genet 20: 384–391.
30. Choe K, Clandinin T (2005) Thinking about visual behavior; learning about photoreceptor function. Curr Top Dev Biol 69: 187–213.
31. Fayyazuddin A, Zaheer M, Hiesinger P, Bellen H (2006) The nicotinic acetylcholine receptor Dalpha7 is required for an escape behavior in Drosophila. PLoS Biol 4: e63.
32. Newsome T, Asling B, Dickson B (2000) Analysis of Drosophila photoreceptor axon guidance in eye-specific mosaics. Development 127: 851–860.
33. Li H, Peng X, Cooper R (2002) Development of Drosophila larval neuromuscular junctions: maintaining synaptic strength. Neuroscience 115: 505–513.
34. Long X, Lin Y, Ortiz-Vega S, Yonezawa K, Avruch J (2005) Rheb binds and regulates the mTOR kinase. Curr Biol 15: 702–713.
35. Leevers S, Weinkove D, MacDougall L, Hafen E, Waterfield M (1996) The Drosophila phosphoinositide 3-kinase Dp110 promotes cell growth. EMBO J 15: 6584–6594.
36. Mair W, Piper M, Partridge L (2005) Calories do not explain extension of life span by dietary restriction in Drosophila. PLoS Biol 3: e223.
37. Parsons P (1975) Phototactic responses along a gradient of light intensities for the sibling species Drosophila melanogaster and Drosophila simulans. Behav Genet 5: 17–25.
38. Carvalho G, Kapahi P, Benzer S (2005) Compensatory ingestion upon dietary restriction in Drosophila melanogaster. Nat Methods 2: 813–815.
39. Stewart B, Atwood H, Renger J, Wang J, Wu C (1994) Improved stability of Drosophila larval neuromuscular preparations in haemolymph-like physiological solutions. J Comp Physiol A 175: 179–191.
40. Kim D, Sarbassov D, Ali S, King J, Latek R, et al. (2002) mTOR interacts with raptor to form a nutrient-sensitive complex that signals to the cell growth machinery. Cell 110: 163–175.
41. Knox S, Ge H, Dimitroff BD, Ren Y, Howe KA, et al. (2007) Mechanisms of TSC-mediated control of synapse assembly and axon guidance. PLoS One 2: e375.
42. von der Brelie C, Waltereit R, Zhang L, Beck H, Kirschstein T (2006) Impaired synaptic plasticity in a rat model of tuberous sclerosis. Eur J Neurosci 23: 686–692.
43. Meikle L, Talos D, Onda H, Pollizzi K, Rotenberg A, et al. (2007) A mouse model of tuberous sclerosis: neuronal loss of Tsc1 causes dysplastic and ectopic neurons, reduced myelination, seizure activity, and limited survival. J Neurosci 27: 5546–5558.
44. Choi Y, Di Nardo A, Kramvis I, Meikle L, Kwiatkowski D, et al. (2008) Tuberous sclerosis complex proteins control axon formation. Genes Dev 22: 2485–2495.
45. Kockel L, Kerr K, Melnick M, Brückner K, Hebrok M, et al. (2010) Dynamic switch of negative feedback regulation in Drosophila Akt-TOR signaling. PLoS Genet 6: e1000990.
46. Yang Q, Inoki K, Kim E, Guan K (2006) TSC1/TSC2 and Rheb have different effects on TORC1 and TORC2 activity. Proc Natl Acad Sci U S A 103: 6811–6816.
47. Chalhoub N, Zhu G, Zhu X, Baker S (2009) Cell type specificity of PI3K signaling in Pdk1- and Pten-deficient brains. Genes Dev 23: 1619–1624.
48. Spasić M, Callaerts P, Norga K (2008) Drosophila alicorn is a neuronal maintenance factor protecting against activity-induced retinal degeneration. J Neurosci 28: 6419–6429.
49. Shen W, Ganetzky B (2009) Autophagy promotes synapse development in Drosophila. J Cell Biol 187: 71–79.
50. Wan H, DiAntonio A, Fetter R, Bergstrom K, Strauss R, et al. (2000) Highwire regulates synaptic growth in Drosophila. Neuron 26: 313–329.
51. DiAntonio A, Haghighi A, Portman S, Lee J, Amaranto A, et al. (2001) Ubiquitination-dependent mechanisms regulate synaptic growth and function. Nature 412: 449–452.
52. van Spronsen F (2010) Phenylketonuria: a 21st century perspective. Nat Rev Endocrinol 6: 509–514.
53. Gibbs S, Becker A, Hardy R, Truman J (2001) Soluble guanylate cyclase is required during development for visual system function in Drosophila. J Neurosci 21: 7705–7714.
54. Benzer S (1967) BEHAVIORAL MUTANTS OF Drosophila ISOLATED BY COUNTERCURRENT DISTRIBUTION. Proc Natl Acad Sci U S A 58: 1112–1119.
55. Blair SS (2000) Imaginal Discs. In: Sullivan W, Ashburner M, Hawley R, eds. Drosophila Protocols. Cold Spring HarborNew York: Cold Spring Harbor Laboratory Press. pp 159–173.

Akt Regulates Glutamate Receptor Trafficking and Postsynaptic Membrane Elaboration at the Drosophila Neuromuscular Junction

Hyun-Gwan Lee,[1]* Na Zhao,[1]* Bridget K. Campion,[2] Michelle M. Nguyen,[1] Scott B. Selleck[1]

[1] Department of Biochemistry and Molecular Biology, The Pennsylvania State University, University Park, Pennsylvania 16802

[2] Graduate Program in Neuroscience, The University of Minnesota, Minneapolis, Minnesota 55455

Received 29 October 2012; revised 16 March 2013; accepted 12 April 2013

ABSTRACT: The Akt family of serine-threonine kinases integrates a myriad of signals governing cell proliferation, apoptosis, glucose metabolism, and cytoskeletal organization. Akt affects neuronal morphology and function, influencing dendrite growth and the expression of ion channels. Akt is also an integral element of PI3Kinase-target of rapamycin (TOR)-Rheb signaling, a pathway that affects synapse assembly in both vertebrates and Drosophila. Our recent findings demonstrated that disruption of this pathway in Drosophila is responsible for a number of neurodevelopmental deficits that may also affect phenotypes associated with tuberous sclerosis complex, a disorder resulting from mutations compromising the TSC1/TSC2 complex, an inhibitor of TOR (Dimitroff et al., 2012). Therefore, we examined the role of Akt in the assembly and physiological function of the Drosophila neuromuscular junction (NMJ), a glutamatergic synapse that displays developmental and activity-dependent plasticity. The single Drosophila Akt family member, Akt1 selectively altered the postsynaptic targeting of one glutamate receptor subunit, GluRIIA, and was required for the expansion of a specialized postsynaptic membrane compartment, the subsynaptic reticulum (SSR). Several lines of evidence indicated that Akt1 influences SSR assembly by regulation of Gtaxin, a Drosophila t-SNARE protein (Gorczyca et al., 2007) in a manner independent of the mislocalization of GluRIIA. Our findings show that Akt1 governs two critical elements of synapse development, neurotransmitter receptor localization, and postsynaptic membrane elaboration. © 2013 Wiley Periodicals, Inc. Develop Neurobiol 73: 723–743, 2013

Keywords: Akt1; glutamate receptor; Gtaxin; subsynaptic reticulum; membrane trafficking

Additional Supporting Information may be found in the online version of this article.

*H.-G.L. and N.Z. contributed equally to this work.

Correspondence to: S.B. Selleck (sbs24@psu.edu).

Contract grant sponsors: United States Department of Defense; contract grant number: W81XWH-07-1-0368.

Published online 17 April 2013 in Wiley Online Library (wileyonlinelibrary.com).
DOI 10.1002/dneu.2208

INTRODUCTION

Synaptic plasticity requires molecular and morphological changes that allow previous activity to shape the physiological properties of synaptic communication. Secreted protein growth factors such as brain-derived neurotrophic factor play essential roles in synaptic plasticity, directing developmental and activity-dependent changes at these specialized cell junctions (Lauterborn et al., 2007). While an expanding set of growth factors are being identified as important determinants of synaptic plasticity, the molecular outputs of these signaling systems are less well understood (Rawson et al., 2003; Salinas, 2003). One signaling molecule of central importance for the integration of many growth factor inputs is the serine-threonine kinase Akt (Franke, 2008). In mammalian systems, three Akt isoforms govern a range of cellular and physiological processes from cell growth to membrane trafficking (Zhang et al., 2002; Manning and Cantley, 2007). Akt1 plays critical roles in cell growth and cell survival (Chen et al., 2001). Akt phosphorylation of AS160 influences exocytosis of glucose transporter-containing vesicles, providing an increased capacity for glucose transport across the plasma membrane (Gonzalez and McGraw, 2006; Watson and Pessin, 2006; Grillo et al., 2009). Consistent with a role of Akt in glucose uptake and homeostasis, mice null for Akt2, expressed ubiquitously in all cell types, show defects in insulin-stimulated glucose uptake (Nakatani et al., 1999; Cho et al., 2001; Bae et al., 2003; Easton et al., 2005; McCurdy and Cartee, 2005). Akt3, the isoform expressed most abundantly in the central nervous system, is essential for normal brain growth affecting both the number and size of neurons (Tschopp et al., 2005). Akt signaling is also known to govern neuronal morphology and synapse development directly (Dudek et al., 1997; Grider et al., 2009; Lee et al., 2011). Phosphorylation of the type A GABA receptor by Akt increases its localization to the synapse (Serantes et al., 2006). Akt regulates dendrite formation in Drosophila peripheral sensory neurons, demonstrating the capacity of this kinase to govern membrane processes that influence synaptic function (Parrish et al., 2009). The central role of Akt in signal integration prompted us to explore its function in the development of the Drosophila neuromuscular junction.

The Drosophila neuromuscular junction is a powerful model for molecular analysis of synapse development and plasticity. Each muscle of the larval body wall is innervated by identifiable motoneurons, and these peripheral synapses are well described at the molecular, morphological, and physiological levels (Jan and Jan, 1976; Gramates and Budnik, 1999; Ruiz-Canada and Budnik, 2006; Schuster, 2006). The Drosophila NMJ is a synapse that expands greatly during larval growth, and the dynamic matching of pre- and postsynaptic elements is critical for its assembly. The growth of the NMJ is accompanied by the expansion of a specialized postsynaptic membrane, the subsynaptic reticulum (SSR), as well as the regulated expression of specific glutamate receptor subunits. GluRIIA is critical for the functional strengthening and morphological growth of the synapse that accompanies muscle expansion during development (Petersen et al., 1997; Sigrist et al., 2002).

We have explored the function of the single Akt gene in Drosophila, Akt1, in synapse assembly and function using the NMJ as a model. We demonstrate that Akt1 is required for the developmentally regulated expansion of the SSR, in addition to regulating glutamate receptor composition. These findings demonstrate that Akt1 serves a critical role in two fundamental elements of synapse development.

MATERIALS AND METHODS

Fly Stocks

All fly strains were raised in standard cornmeal food at 25°C during embryogenesis and 30°C during larval development under a 12-h/12-h day/night cycle, unless otherwise stated. Oregon-R strain served as the wild type stock. $Akt1^{1}$/TM3 and $Akt1^{04226}$/TM3 were obtained from the Bloomington Drosophila Stock Center (BDSC). $Akt1^{04226}$ is a P-element insertion and hypomorphic allele. The null allele $Akt1^{1}$ is embryonic lethal, but $Akt1^{1}/Akt1^{04226}$ transheterozygotes are semi-viable and some survive to the adult stage. G14-GAL4, 24B-GAL4, Mef2-GAL4, and elav-GAL4 transposon-containing stocks (BDSC) were used for muscle and neuronal-specific expression of UAS-$Akt1^{RNAi}$ (Vienna Drosophila RNAi Center (VDRC) #103703), UAS-Gtx^{RNAi} (VDRC #105113), UAS-Gtaxin (from V. Budnick, University of Massachusetts (Gorczyca et al., 2007)), UAS-GluRIIA-mRFP (Kittel et al., 2006), and UAS-mCD8-GFP (BDSC #5137) constructs, respectively. Protein trap line Bsg-GFP (Flytrap #G00311) directs the expression of GFP-tagged Basigin under the control of its endogenous promoter. UAS-DicerII was used together with elav-GAL4 to increase the effectiveness of RNA interference in neurons (Dietzl et al., 2007). The temperature-sensitive GAL80 repressor, $GAL80^{ts}$ under tubulin promoter (Tubp-$GAL80^{ts}$, from BDSC), was combined with Mef2-GAL4 line for temporal control of UAS-$Akt1^{RNAi}$ expression in the muscle (Zeidler et al., 2004). $GAL80^{ts}$ suppressed GAL4 function at the permissive temperature (18°C). At the restrictive temperature (30°C), $GAL80^{ts}$ released GAL4, allowing its

binding to the UAS, and inducing the expression of $Akt1^{RNAi}$. To inhibit the expression of Akt1 at the early developmental stage, embryos were kept at 30°C for 2 days and then raised at 18°C until they reached third instar larval stage. In contrast, animals, which Akt1 was suppressed at the late stage, were raised at 18°C until second instar stage and then shifted to 30°C for 2 days before immunohistochemistry. The constitutively active forms of Akt1 ($Akt1^{CA}$) and GFP tagged $Akt1^{CA}$ ($Akt1^{CA}$-GFP) were generated using QuikChange II Site-Directed Mutagenesis Kit (Agilent Technologies, Santa Clara, CA), resulting in the replacement of amino acids Threonine 342 (ACC) and Serine 505 (AGC) with Aspartic Acid (GAC). The $Akt1^{CA}$ and $Akt1^{CA}$-GFP constructs were cloned into pUAST-attB vector and then integrated into the third chromosome (99F8) by site-specific P-element mediated germline transformation (Rainbow Transgenic, CA).

Immunohistochemistry and Confocal Microscopy

The third instar larval muscles were dissected in ice-cold Ca^{21} free HL-3 media and fixed with either 4% paraformaldehyde for 30 min or Bouin's fixative solution for 5 min (for glutamate receptor subunits antibody immunostaining) or 15 min (for Gtaxin antibody immunostaining). All subsequent washes were performed in PBST (0.5% triton X-100 in phosphate buffered saline (PBS)). A total of 5% normal goat serum in PBST was used for sample blocking and antibody incubations. Primary antibodies mouse anti-glutamate receptor IIA antibody (1:50, 8B4D2, Developmental Studies Hybridoma Bank (DSHB), University of Iowa, Iowa City, IA), rabbit anti-glutamate receptor IIB and IIC antibodies (1:2000 from D. Featherstone, University of Illinois at Chicago), mouse anti-DsRed (1:500, Santa Cruz Biotechnology), rat anti-Syndapin (1:100, from M. Ramaswami, University of Arizona), rat anti-Gtaxin (1:200, from V. Budnick, University of Massachusetts), rabbit anti-Dorsal and Cactus antibodies (1:1000, from S. Wasserman, University of California, San Diego), mouse anti-Discs large (1:500, 4F3, DSHB), mouse anti-Cysteine string protein (1:1000, 6D6, DSHB), mouse anti-a-Spectrin (1:1000, 3A9, DSHB), and mouse anti-Bruchpilot (1:1000, nc82, DSHB) were incubated with sample for at least 12 h at 4°C. Alexa-fluorescence conjugated secondary antibodies were obtained from Life Technologies (Grand Island, NY).

Images were acquired using an Olympus Fluoview FV1000 laser scanning confocal microscope (Olympus America, Lake Success, NY). Quantification of protein levels were performed using Imaris 7.3 (Bitplane, Saint Paul, MN) and ImageJ1.42q (NIH) software for image processing and analysis. Serial images taken by confocal microscopy were reconstructed into 3D images using Imaris without any other processing. Immunoreactivity-positive voxels were then assayed by counting the total number of voxels (Abundance) and by measuring their average fluorescent intensity. Both of the values were further normalized by muscle size for each preparation.

Western Blotting Analysis

Total protein was prepared from dissected third instar larval muscle tissues in SDS-loading buffer and ran on 9% sodium dodecyl sulfate polyacrylamide gel (SDS-PAGE), polyvinylidene difluoride (PVDF) membrane was incubated overnight with anti-phosphorylated Akt1 or anti-b-Actin antibodies (Cell Signaling Technology, MA) in blocking solution (5% w/v nonfat dry milk in 0.5% Tween-20 in Tris-buffer saline) at 4°C. Signals were amplified using horseradish peroxidase (HRP) conjugated secondary antibody and detected using Supersignal West Femto Maximum Sensitivity Substrate (Thermo Scientific, IL).

Transmission Electron Microscopy

The third instar larval muscles were dissected in ice-cold Ca^{21} free HL-3 media and fixed in buffer (1.5% glutaraldehyde, 2.5% paraformaldehyde, 1.8 mM Ca^{21} in 0.1M Na-cacodylate, pH 7.4) at 4°C overnight. Postfixation was done in 1% osmium tetroxide, and en bloc staining was performed with 2% uranyl acetate in dark condition. The samples were rinsed in 0.1M sodium cacodylate buffer (pH 7.4), dehydrated and infiltrated, embedded in Spurr's resin, and sectioned to 70 nm slices. The images were taken with a transmission electron microscope (JEOL1200, Tokyo, Japan) and analyzed by ImageJ1.42q (NIH).

Electrophysiology

Excitatory junction potentials (EJPs) and miniature excitatory junction potentials (mEJPs) were recorded at room temperature from muscle 6 of abdominal hemi-segment A3 in third instar larvae (Rawson et al., 2003). The third instar larvae were dissected in ice-cold Ca^{21} free HL-3 media and recordings were performed with larvae in HL-3 media containing 1.2 mM Ca^{21}. Muscle 6 of A3 was impaled with the recording electrode and before stimulation, recordings were taken for 1 min to measure spontaneous activities (mEJPs) (Stewart et al., 1994). Following the recording of mEJPs, evoked EJPs were elicited in the same muscle with 1 Hz pulses. A total of 1 nA of current was injected for 200 ms to record plasma membrane resistance and capacitance. Recordings were acquired with Axoclamp 2B amplifier and Clampex 9.2 software (Axon Instruments, CA). Only the recordings with resting membrane potentials lower than 260 mV were included in this analysis. EJP and mEJP amplitudes and kinetics were analyzed with MiniAnalysis (Synaptosoft, Fort Lee, NJ).

Statistical Analysis

Statistical analyses for quantitative data were performed in Minitab Release 16 (Minitab, State College, PA). All data points were presented as mean 6 SEM and analyzed using Student's t-tests for normally distributed data or post hoc Tukey–Kramer for pairwise comparisons of data with non-normal distributions.

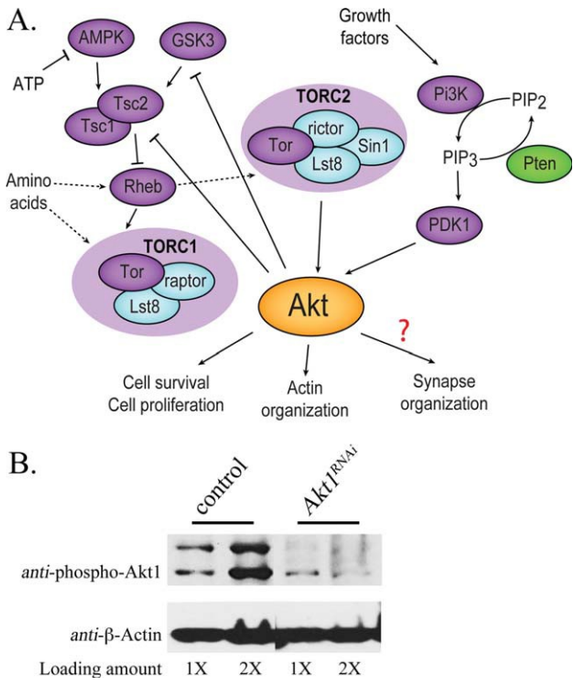

Figure 1 The Akt signaling system and level of Akt1 knockdown using RNA interference in Drosophila. A: In this summary, kinases Rheb, and Tsc1/2 are purple symbols, phosphatases are green, and other components of TOR1 and TOR2 complex are blue. Akt1 is activated by growth factors via Pi3K and PDK1 and by nutritional sensing through Tsc1/2 and TOR complexes. Relationships that are not fully understood or have several possible intermediary steps are shown as dashed arrows or a question mark (adapted from Dimitroff et al., 2012). B: Akt1 function was compromised by muscle-specific expression of an Akt1^{RNAi} construct using the GAL4-UAS system. The level of phosphorylated Akt1 was measured by Western blot. Total muscle proteins were prepared from third instar larval muscles of control animals (UAS-Akt1^{RNAi} transgene only; UAS-Akt1^{RNAi}/1) or Akt1^{RNAi} animals with muscle specific knockdown of Akt1 using 24B-GAL4 driver (24B-GAL4>UAS-Akt1^{RNAi}). Akt1 was dramatically decreased in muscle tissue expressing Akt1^{RNAi} as compared with controls. Measures of b-Actin were used as a protein loading controls. Total proteins extracted from either one (1) or two larvae (2) were loaded.

RESULTS

Akt1 plays a central role in a number of signaling processes, acting both downstream and upstream of growth factor and target of rapamycin-directed events. The Akt1 kinase governs a number of cellular activities including cell proliferation, cell survival, and cytoskeleton organization [Fig. 1(A)]. Given these diverse and critical functions, we explored the role of Akt1 in synapse assembly. In addition to the well-described Akt1 mutant alleles (Staveley et al., 1998; Mozden and Rubin, 1999; Guo and Zhong, 2006), we used an Akt1^{RNAi} transgene (Dietzl et al., 2007) to inhibit Akt1 function selectively in either motoneurons or muscle cells. To assess the level of inhibition achieved by the Akt1^{RNAi} construct, we measured the level of phosphorylated Akt1 (active form of Akt1) by western blot. Using a muscle-directed GAL4 to drive the expression of UAS-Akt1^{RNAi}, phosphorylated Akt1 protein was reduced to 24.2% of wild-type level in third instar larval muscle tissue [Fig. 1(B)].

We began assessing the role of Akt1 in NMJ assembly by examining the distribution and level of glutamate receptor IIA (GluRIIA), one of the neurotransmitter receptor subunits at this glutaminergic synapse. Glutamate is the major excitatory neurotransmitter at the type I bouton of the Drosophila larval NMJ (Brunner and Okane, 1997; Collins and DiAntonio, 2007). The NMJ glutamate receptor (GluR) is a heterotetramer comprised of three invariant subunits: GluRIIC, D, and E. The fourth subunit, either GluRIIA or B, determines the type and the electrophysiological properties of the receptor

(DiAntonio et al., 1999; Featherstone et al., 2005; Qin et al., 2005a; DiAntonio, 2006). Subunit GluRIIA and B competitively bind to GluRIIC; hence, the preferential expression of these two subunits constitutes one element of developmental plasticity exhibited by this synapse (Marrus et al., 2004). We examined the levels and distributions of GluRIIA using a well-characterized monoclonal antibody, anti-GluRIIA (Featherstone et al., 2002; Qin et al., 2005a; Karr et al., 2009). The specificity of this antibody has been well documented by showing that immunoreactive signal is lost in GluRIIA null mutant (Marrus et al., 2004). Partial loss of Akt1 function, achieved with the heteroallelic combination $Akt1^{1}$/$Akt1^{04226}$, altered GluRIIA distributions and levels, with a reduction at postsynaptic structures and the appearance of GluRIIA immunoreactivity within repeated bands throughout the muscle cells [Fig. 2 compare (A), (B) to (C), (D)]. This latter phenotype was more prominent in muscles 15 and 16 and was observed to a lesser extent in muscles 6 and 7, the postsynaptic cells typically used for electrophysiological analysis [arrowheads in Fig. 2(C,D)].

Directed expression of an $Akt1^{RNAi}$ in either muscle or neuron using the GAL4-UAS binary system (Brand and Perrimon, 1993) provided the means of assessing the cell-type specific requirements for Akt1. We used multiple muscle-specific GAL4 driver lines, G14, 24B, and Mef2 to confirm that the associated phenotypes were due to muscle-directed RNAi expression, but not expression in some alternative cell types. These GAL4 drivers showed some differences in the level of transcriptional activity, but all induced similar Akt1 knockdown phenotypes for GluRIIA localization and SSR expansion. Muscle-specific expression of $Akt1^{RNAi}$ produced a dramatic loss of GluRIIA at the synapse and its redistribution into intracellular bands in the muscle cell, confirming the phenotype observed in $Akt1^{1}$/$Akt1^{04226}$ mutants [Fig. 2 compare controls shown in (E–H) to muscle cell-directed $Akt1^{RNAi}$ animals in (I–L)]. Knockdown of Akt1 in the motoneuron had no effect on GluRIIA distribution (data not shown). GAL4-directed transcriptional activation is temperature-dependent, allowing for different levels of $Akt1^{RNAi}$ expression and consequently loss of Akt1 function, by simply rearing the animals at different temperatures. At 18°C, GluRIIA distributions were normal, but with decreasing levels of Akt1 function produced at 25°C and 30°C, GluRIIA was progressively lost from the postsynaptic site and increasingly localized within intracellular bands [Fig. 2 compare control animals, panels (E–H), to muscle-specific $Akt1^{RNAi}$, panels (I–L); in enlarged images (H) and (L), arrows indicate synaptic boutons; arrowheads indicate GluRIIA in bands]. Although GluRIIA failed to localize to the postsynaptic specialization upon inhibition of Akt1 function, we did note a net and significantly increased level of GluRIIA within intracellular structures [Supporting Information Fig. 1(A), animals reared at 30°C]. These findings established that localization of GluRIIA was affected by reductions of Akt1 function mediated by $Akt1^{RNAi}$ transgene expression in the postsynaptic cell.

To further explore the mechanism of the dramatic redistribution of GluRIIA achieved by knockdown of Akt1, we examined the expression pattern of an mRFP-tagged GluRIIA derived from a UAS-transgene. This provided the opportunity to visualize the transgenic GluRIIA-mRFP by both fluorescence of the mRFP protein, and immunodetection of the polypeptide with an anti-RFP antibody, anti-DsRed. Consistent with our earlier results looking at endogenous GluRIIA, compromising Akt1 function produced loss of GluRIIA-mRFP at the synapse, detected by either mRFP fluorescence or anti-RFP antibody [Fig. 3 compare (B), (C) to (F), (G)]. Interestingly, the redistribution of GluRIIA-mRFP to intracellular bands was only detected with the anti-RFP antibody, but not by monitoring the fluorescence of the mRFP-tagged receptor subunit [Fig. 3(F,G)]. In control animals, the RFP-fluorescence pattern precisely overlaps the anti-RFP signal [Fig. 3(B,C)]. This result suggests that reduction of Akt1 function may disrupt the structural integrity of GluRIIA-mRFP, resulting in loss of its native fluorescence, whereas the RFP-epitope is found redistributed to intracellular membrane structures.

We have also examined the developmental window during which Akt1 is essential for GluRIIA localization by using the temperature-sensitive $GAL80^{ts}$ system (Zeidler et al., 2004). When a $GAL80^{ts}$ transgene is present with GAL4-UAS components, the GAL80 suppresses the activity of the transcriptional activator GAL4, preventing expression of the UAS-transgene, in this case, UAS-$Akt1^{RNAi}$. Raising the temperature to restrictive level inactivates $GAL80^{ts}$ and permits expression of the $Akt1^{RNAi}$. We used this system to inactivate Akt1 during different developmental stages. Reduction of Akt1 function during a 2-day window early in development (embryo-first instar larva) produced some redistribution of GluRIIA into intracellular stripes, whereas a later 2-day inactivation window in third instar larval stage merely reduced the levels of GluRIIA at the synapse [Fig. 3(I–P)]. These data suggest that the redistribution of GluRIIA observed with reduction of Akt1 throughout development is not merely the result of a failure of synaptic stabilization

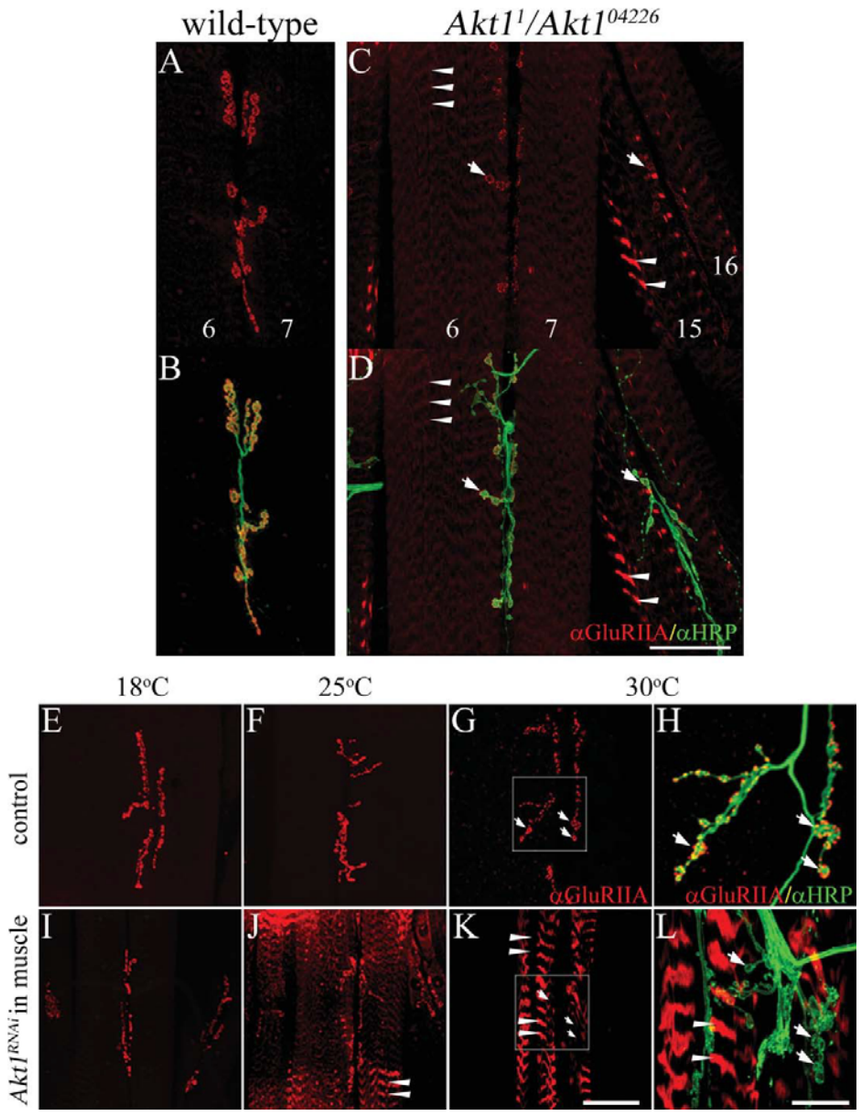

Figure 2 GluRIIA localization was modified in Akt1 mutants and animals with muscle-specific inhibition of Akt1. GluRIIA localization was examined in muscles 6 and 7 using monoclonal anti-GluRIIA antibody (red). Anti-HRP antibody detected neuronal projections (green). A and B: In wild-type animals, GluRIIA was located in the postsynaptic specialization that surrounds the motoneuron boutons. C and D: $Akt1^{1}/Akt1^{04226}$ mutants showed reduction of GluRIIA at synaptic boutons (see arrows) and redirection to intracellular bands (faint staining in muscles 6 and 7, and more prominent in muscles 15 and 16; see arrowheads). E–L: Akt1 function was compromised by muscle-specific expression of an $Akt1^{RNAi}$ construct using the GAL4-UAS system. UAS-$Akt1^{RNAi}$/**1** animals served as controls. GAL4 transcriptional activation shows temperature dependence, permitting a graded level of Akt1 blockade from 18°C (low level of inhibition) to 30°C (high level of inhibition). E–H: In control larvae, GluRIIA immunoreactivity was concentrated in the postsynaptic region surrounding boutons at all temperatures. H: Enlarged view of white box area in (G), arrows show the motoneuron boutons surrounded by GluRIIA. I–L: In $Akt1^{RNAi}$ expressing larval muscle (24B-GAL4>UAS-$Akt1^{RNAi}$), GluRIIA mislocalization (arrowheads) was more severe with greater inhibition of Akt1 function at increasing temperature (larvae reared at 18°C (I), 25°C (J), or 30°C (K and L)). L Enlarged view of white box area in (K), arrows show synaptic boutons lacking GluRIIA immunoreactivity; arrowheads mark ectopic GluRIIA within intracellular bands. Scale bar in (A–G) and (I–K), 50 mm, in (H) and (L), 5 mm.

because the levels of GluRIIA would likely recover quickly from new synthesis (Rasse et al., 2005) but is affecting a process occurring in early development that alters GluRIIA production and delivery to the synaptic specialization.

We also examined the effect of Akt1 on two potential downstream targets, Dorsal and Cactus (Drosophila homologs of NF-**j**B and I**j**-B, respectively). These two proteins have recently been shown to localize to postsynaptic specializations and regulate glutamate receptor levels at the NMJ (Heckscher et al., 2007). While Dorsal and Cactus have been well characterized as transcriptional activator proteins, their activity at the NMJ is posttranscriptional, affecting the localization or stabilization of glutamate receptors in the SSR (Heckscher et al., 2007). To determine whether Akt1's effects on GluRIIA localization could be mediated at least in part by an influence on Dorsal or Cactus, the levels and distributions of these two proteins at the NMJ were evaluated. As previously described, Dorsal and Cactus were concentrated in postsynaptic specializations at type Ib boutons in control animals [Fig. 4(A,B,E,F)]. Upon RNAi knockdown of Akt1, both Dorsal and Cactus levels significantly decreased at the NMJ [Fig. 4(C,D,G,H)] [Supporting Information Fig. 1(B)]. In addition to the reduction of Dorsal levels at the NMJ, Dorsal was mislocalized in a number of animals (23.8% penetrance) and partially colocalized with GluRIIA into intracellular bands in the muscle cell [Fig. 4(L–N); arrowheads indicate the bands of GluRIIA and Dorsal, arrows indicate synaptic boutons]. Although the penetrance of this phenotype was modest, it was reproducible across three different sets of experiments. These findings showed that Akt1 affects the levels of two potential Akt1 downstream targets known to regulate GluRIIA levels, and suggest the possibility that Akt1 regulates GluRIIA at least in part via the control of Dorsal and Cactus.

The ability of Akt1 to affect the trafficking of one glutamate receptor subunit to the postsynaptic specialization suggested the possibility that this mechanism could regulate GluR subunit composition. The distributions of glutamate receptor subunits IIB and IIC were therefore examined in animals with knockdown of Akt1 in the muscle. In the animals with reduced Akt1 function, GluRIIB, the functional alternative to IIA, remained at the synapse under conditions where GluRIIA was localized almost exclusively within intracellular bands [Supporting Information Fig. 2(H–K)]. The correct delivery of GluRIIB to the postsynaptic specialization when Akt1 function was compromised with $Akt1^{RNAi}$ was confirmed by showing its spatial colocalization with Bruchpilot, a presynaptic protein required for active zone function [Supporting Information Fig. 2(E–G) for control and (L–N) for Akt1 knockdown] (Wagh et al., 2006). The correct delivery of GluRIIB is consistent with the observation that these larvae were motile, and that a functional receptor must contain either GluRIIA or GluRIIB. Likewise, the essential subunit GluRIIC was appropriately localized to the postsynaptic specialization in the face of reduced Akt1 function (data not shown). Akt1 is therefore selectively regulating the delivery of GluRIIA to the synapse, and reductions in Akt1 result in mislocalization of IIA to an intracellular compartment.

The selective requirement for Akt1 function to correctly localize GluRIIA but not the other receptor subunits begs the question as to whether other proteins require Akt1 for correct targeting to the postsynaptic specialization. Therefore, we have examined three other synaptic components: Discs-Large (DLG), the homolog of mammalian PSD-95; Syndapin, an F-BAR domain-containing protein; and Basigin, a transmembrane protein located principally in the SSR. Both DLG and Syndapin promote SSR expansion (Lahey et al., 1994; Budnik et al., 1996; Guan et al., 1996; Kumar et al., 2009) and associate with SSR membrane following their translation in the cytoplasm (Thomas et al., 2000). Basigin is a synaptic transmembrane protein located principally in the postsynaptic SSR and is required for synaptic function (Besse et al., 2006, 2007). Reduction of Akt1 function in the muscle to a degree that completely disrupted GluRIIA localization did not alter the selective targeting of Basigin to the synapse [Supporting Information Fig. 3, compare (A) to (B)]. DLG and Syndapin, the two cytoplasmically synthesized and SSR-associated proteins, showed normal localization to the postsynaptic specialization of the NMJ [Supporting Information Fig. 3 compare controls without GAL4 driver, (C–E) to muscle-specific 24B-GAL4>UAS-$Akt1^{RNAi}$ animals in (F–H)]. Quantitation of the immunofluorescence signal for these proteins did show significantly reduced levels of Basigin and Syndapin, whereas DLG signal was lower but did not achieve statistical significance (Supporting Information Fig. 4). Taken together these findings demonstrated that the mislocalization of GluRIIA upon reduction of Akt1 is specific, and does not affect the localization of other transmembrane (Basigin, GluRIIB) or cytoplasmically synthesized (Dlg, Syndapin) postsynaptic proteins.

The SSR is a complex postsynaptic membrane specialization that requires the activity of a number of proteins for its growth and maintenance, including DLG, Syndapin, and the Drosophila t-SNARE

Gtaxin (Lahey et al., 1994; Budnik et al., 1996; Gorczyca et al., 2007; Kumar et al., 2009). Given that reductions in *Aktl* function affected the levels of synaptic proteins Syndapin and Basigin, it was of interest to determine if *Aktl* affected the elaboration of the SSR. The ultrastructure of the SSR was evaluated in animals with reduced *Aktl* function using transmission electron microscopy (TEM) of NMJ synaptic

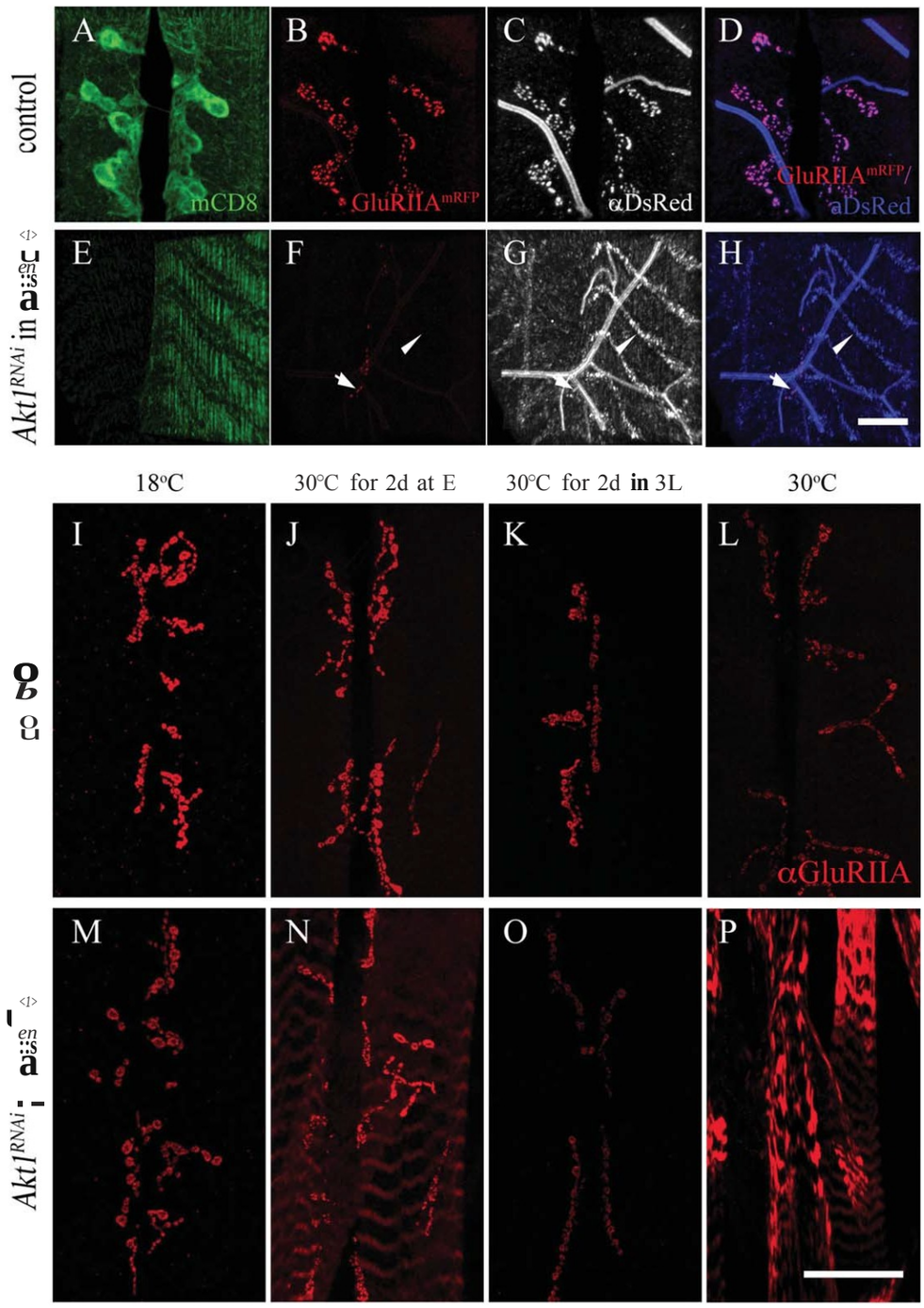

Figure3

boutons. At the Drosophila NMJ, the motoneuron boutons are "embedded" in the surface of the muscle cell (Jia et al., 1993). The tubulo-membranous SSR is seen as a complex set of multilayered membranes within the muscle cell and surrounding the nerve terminal [Fig. 5(A)]. The dimensions and complexity of the SSR were reduced in larvae expressing $Akt1^{RNAi}$ in the muscle cell without affecting the length of the presynaptic active zones [Fig. 5(A–C)]. These experiments demonstrated that Akt1 was required for the proper expansion of the SSR.

Gtaxin mutant shows reduced SSR elaboration as well as changes in the complex membrane architecture of the muscle cell (Gorczyca et al., 2007). This architecture was revealed by labeling all muscle membranes with a mouse transmembrane protein, mCD8-GFP, and performing 3D reconstruction of optically sectioned cells. The mCD8-GFP integral membrane protein tag uncovered a cortical membrane compartment above the muscle nuclei, and a subcortical membrane network below the nuclei intermingled with the contractile apparatus. The cortical membrane compartment was at the same level as the SSR and was greatly reduced in Gtaxin mutant (Gorczyca et al., 2007). There is evidence that DLG traffics through the cortical membrane compartment on its way to the SSR (Thomas et al., 2000; Gorczyca et al., 2007). Given that reductions of both Gtaxin and Akt1 affected SSR, we examined whether Akt1 also influenced the organization of intracellular membrane compartments, as documented for Gtaxin mutant. As previously reported, mCD8-GFP expression in the muscle cell revealed a complex set of membranous structures including a cortical domain (c), the nuclear envelope (n), and a subcortical network (sc) [Fig. 5(D,H)]. The SSR was also prominently labeled by mCD8-GFP in the muscle, as evidenced by colocalization with DLG [Fig. 5(E–G)]. Reduction of Akt1 function affected muscle cell membrane organization in a manner similar to that observed in Gtaxin mutant (Gorczyca et al., 2007). Namely, the cortical domain was nearly abolished and the subcortical domain was compressed, consistent with the much reduced muscle thickness in these animals [Fig. 5(H)]. The mCD8-GFP labeling of the SSR was also dramatically decreased, supporting the TEM findings of reduced SSR elaboration in animals with muscle-directed Akt^{RNAi} expression [Fig. 5(I–K)].

Based on the similar ultrastructural changes in the SSR and muscle membrane organization resulting from reductions in Gtaxin and Akt1 function, Gtaxin was a logical candidate as a downstream target of Akt1 activity. To explore this possibility, we examined Gtaxin levels and distribution in animals with muscle-specific expression of $Akt1^{RNAi}$ (Mef2-GAL4>UAS-$Akt1^{RNAi}$) or a constitutively active form

Figure 3 Akt1 affects GluRIIA trafficking to NMJ and is crucial in the early developmental stage. Two experiments are shown here. The first (panels A–H) shows the results from a study where the distribution of an engineered GluRIIA-RFP when Akt1 function was compromised with RNA interference. The GluRIIA-RFP was detected with either endogenous fluorescence from the mRFP or an anti-mRFP antibody (anti-DsRed). The second experiment (panels I–P) was designed to determine the developmental window when Akt1 activity was critical for GluRIIA localization. Time-limited inhibition of Akt1 function was achieved using $Akt1^{RNAi}$ and a temperature-sensitive GAL80 (see "Materials and Methods"). A–D: GluRIIA-mRFP (red) was colocalized with anti-DsRed signals (gray) at the NMJ in control animals (G14-GAL4, UAS-mCD8-GFP; UAS-GluRIIA-mRFP/**1**). E–H: GluRIIA-mRFP fluorescence was reduced significantly at the postsynaptic density (arrows) upon inhibition of Akt1 function. The redistribution of GluRIIA-mRFP protein into an intracellular compartment was detected only with anti-DsRed immunostaining in Akt1 compromised animals (G14-GAL4, UAS-mCD8-GFP; UAS-GluRIIA-mRFP>UAS-$Akt1^{RNAi}$) (arrowheads). I–P: To investigate the critical periods when Akt1 is required for GluRIIA localization at the NMJ during development, the temperature-sensitive GAL80 repressor under tubulin promoter, Tubp-$GAL80^{ts}$, was used along with the GAL4-UAS binary system to allow temporal spatial regulation of $Akt1^{RNAi}$ expression (Tubp-$GAL80^{ts}$, Mef2-GAL4>UAS-$Akt1^{RNAi}$). I–L: At all temperatures, control (Tubp-$GAL80^{ts}$, Mef2-GAL4/**1**) animals showed normal GluRIIA distribution at the NMJ. M: In Tubp-$GAL80^{ts}$, Mef2-GAL4/UAS-$Akt1^{RNAi}$ animals at the permissive temperature (18°C), when expression of $Akt1^{RNAi}$ is minimal on account of $GAL80^{ts}$ blockade of transcription, the animals displayed a normal GluRIIA distribution. N: Incubation at the restrictive temperature (30°C) for 2 days right after egg laying induced modest GluRIIA mislocalization in muscles while much of the GluRIIA remained at the NMJ. O: Temperature shift from 18°C to 30°C for 2 days at the third instar larval stage produced reduced levels of GluRIIA immunoreactivity at the NMJ but no abnormal localization. P: Animals reared at 30°C throughout the entire developmental stages displayed severe GluRIIA mislocalization. Scale bar in (A–H), 10 μm, in (I–P), 50 μm.

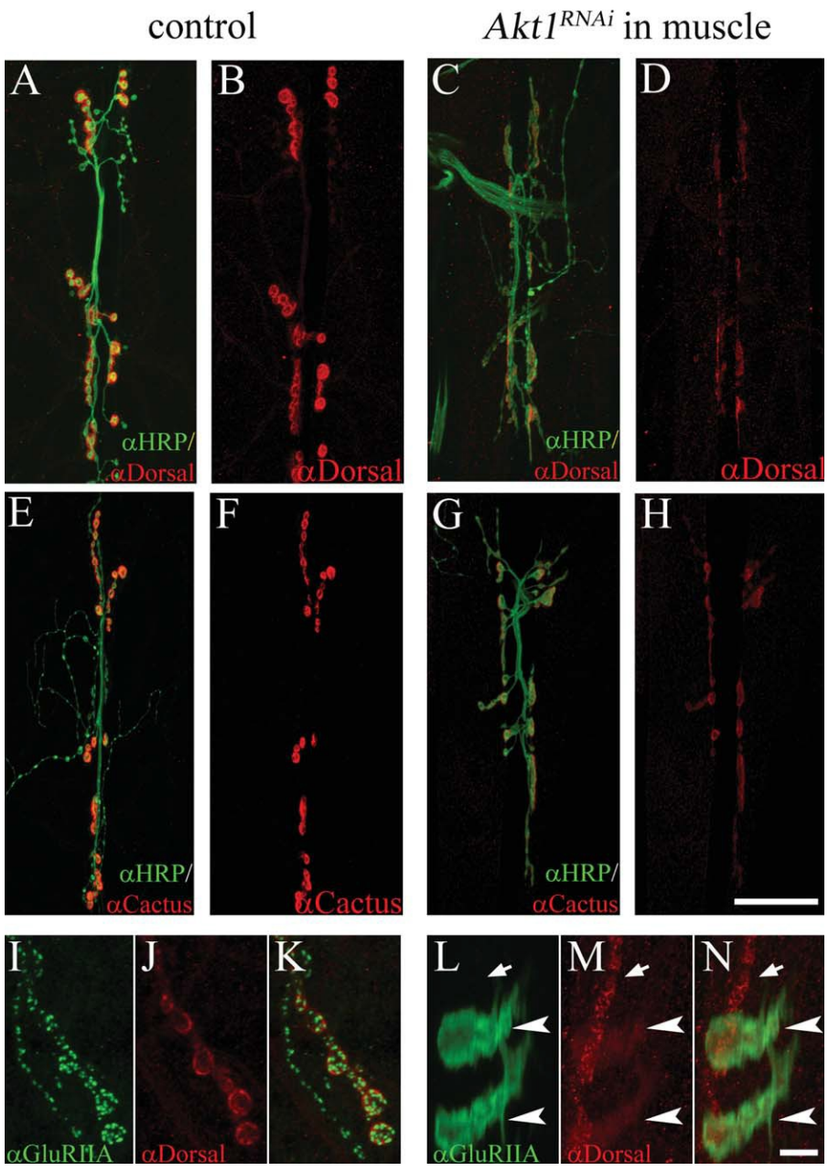

Figure 4 Influence of Akt1 on Dorsal and Cactus levels and distribution at the NMJ. A and B: In control animals (UAS-Akt1^{RNAi}/**1**), Dorsal (detected by anti-Dorsal antibody; red) is localized to the postsynaptic specialization. Neuronal projections were labeled by anti-HRP staining (green). C and D: Akt1 function was compromised by expressing UAS-Akt1^{RNAi} under the muscle-specific 24B-GAL4. Dorsal levels at the NMJ were significantly reduced. E and F: Cactus (red) was concentrated at the NMJ in control animals. G and H: Inhibition of Akt1 function in the muscle (24B-GAL4/UAS-Akt1^{RNAi}) resulted in reduced levels of Cactus at the NMJ. I–K: In control animals, Dorsal immunoreactivity (red) colocalized with GluRIIA (green) immunoreactivity at the postsynaptic specialization. L–N: In muscles where Akt1 expression was inhibited, both Dorsal and GluRIIA redistributed into intracellular bands, although the effect on Dorsal was less and incompletely penetrant. Mislocalized Dorsal partially overlapped with GluRIIA (arrowheads indicate bands of Dorsal and GluRIIA; arrows indicate synaptic boutons). Scale bar in (A–H), 50 mm, in (I–N), 5 mm.

of Akt1 (Mef2-GAL4>UAS-Akt1^{CA}). In wild-type animals, Gtaxin immunoreactivity is concentrated at the SSR [Fig. 6(B,C)], and muscle-directed RNAi of Akt1 greatly reduced Gtaxin levels at this postsynaptic specialization [Fig. 6(F,G)]. Gtaxin has been implicated in SSR formation not only on account of the reduction of SSR complexity in Gtaxin mutant but also from the production of ectopic, mCD8-GFP labeled membranous structures in animals overexpressing wild-type Gtaxin (Gorczyca et al., 2007). Muscle-directed expression of Akt1^{CA} produced membranous structures with the same visible features. In these animals, Gtaxin was present at increased levels and localized to patches throughout the muscle [Fig. 6(I–K)]. These ectopic membrane elaborations were confirmed at the TEM level and are structurally similar to those documented in animals overexpressing Gtaxin in the muscle [Fig. 6(M–O)].

The formation of mCD8-GFP-labelled membrane patches mediated by Akt1^{CA} was also found to be dependent on Gtaxin. The ectopic membranous patches induced by Akt1^{CA} expression in the muscle were visualized by mCD8-mRFP and showed some features of SSR, namely concentration of a-Spectrin and DLG (Pielage et al., 2006) [Fig. 7]. Reduction of Gtaxin by RNA interference blocked the Akt1^{CA}-mediated formation of these "ectopic" SSR structures [Fig. 7(B,D)]. The ectopic membrane patches induced by Akt1^{CA} overexpression were not reduced by expression of a control UAS-transgene, excluding the possibility that suppression of Akt1^{CA} function was due to titration of GAL4 proteins in Gtaxin^{RNAi} expressed animals (data not shown). Inhibition of Gtaxin by Gtaxin^{RNAi} expression in muscle induced loss of mCD8 at the SSR but DLG remained at the postsynaptic specialization [Fig. 7(F,H)]. In addition, GluRIIA localization was not disrupted by Gtaxin^{RNAi}, indicating that Gtaxin does not play a role in this aspect of Akt1 function and is consistent with published findings (Gorczyca et al., 2007) [Fig. 7(J)]. These results demonstrated that Gtaxin is required for Akt1^{CA}-mediated formation of ectopic membranous structures. It is of interest that Gtaxin bears a consensus sequence (RXRXXS/T) for Akt1 phosphorylation, indicating a potential phosphorylation site at Serine 255, suggesting that Gtaxin could be a direct target of Akt1 activity (Datta et al., 1999; Zhang et al., 2002).

The experiments described above establish that Akt1 is required for correct delivery of the GluRIIA subunit to the postsynaptic membrane and elaboration of the SSR. To assess the effects of Akt1 on NMJ physiology, we conducted single cell recordings on the muscles of both Akt1 mutants and animals with muscle-specific knockdown of Akt1 using RNA interference. In animals with Akt1^{RNAi} directed to the muscle, amplitudes of miniature excitatory junctional potentials (mEJPs) were dramatically reduced, consistent with earlier reports that this measure of muscle response to spontaneous neurotransmitter release is greatly reduced [Fig. 8(A)] (Petersen et al., 1997). In larvae bearing a combination of mutant alleles (Akt1^{1}/Akt1^{04226}), mEJPs amplitudes were reduced but not to a statistically significant level [Fig. 8(A,B)]. However, Akt1^{1}/Akt1^{04226} transheterozygotes showed significantly reduced EJP amplitudes, the response of the muscle to a single suprathreshold stimulus of the motoneuron [Fig. 8(C,D)]. The shape of the EJP was also altered in Akt1^{1}/Akt1^{04226} animals, with measures of the EJP decay indicating a significantly decreased time to restore the membrane voltage to resting levels [Fig. 8(E)]. We noted these same changes in EJP properties in animals with Akt1 function compromised in the muscle with targeted expression of Akt1^{RNAi}. The temperature sensitivity of the GAL4-UAS system allowed the graded reduction of Akt1 function in the muscle. At elevated temperatures, Akt1^{RNAi} expression was higher and thus the reduction in Akt1 function was more pronounced. At 24°C, expression of Akt1^{RNAi} in the muscle produced a significant reduction in the EJP amplitude, as observed in Akt1^{1}/Akt1^{04226} animals [Fig. 8(F,G)]. The EJP amplitudes were not significantly altered in animals reared at 18°C where Akt1 function was compromised modestly [Fig. 8(F,G)]. However, at both temperatures, significant differences in the decay times of the EJPs in Akt1^{RNAi} expressing animals were observed [Fig. 8(H)].

A number of factors can influence the dynamics of the EJP, including membrane capacitance and resistance, as well as changes in voltage-gated channels in the membrane. To determine if the muscle membrane showed any changes in baseline resistance or capacitance, muscle cell responses to small current injections (1nA) were examined. Akt1^{RNAi} expressing animals did not show any significant changes to these small current applications (data not shown), suggesting that nonvoltage-dependent membrane properties could not account for the changes we observed in the EJPs of animals with decreased Akt1 function.

It is important to note that electrophysiological changes observed in Akt1 mutant and muscle-specific Akt1 RNAi animals match the morphological and molecular alterations at the NMJ. In Akt1^{RNAi} expressing animals at 24°C, mEJP amplitudes were decreased to a nearly undetectable level [Fig. 8(A)], consistent with the previous characterization of

GluRIIA null mutant (DiAntonio et al., 1999). Furthermore, the decreased EJP decay times recorded in $Akt1^{1}/Akt1^{04226}$ and muscle-directed $Akt1^{RNAi}$ animals also mimicked a prominent phenotype of Gtaxin mutant animals (Gorczyca et al., 2007), supporting the hypothesis that changes in SSR and muscle membranous system were the reason for these physiological changes.

DISCUSSION

We explored Akt function in synapse development and function using a well-characterized model system, the Drosophila neuromuscular junction. There is a single Akt homolog in Drosophila, Akt1, facilitating the genetic and cellular studies of Akt function in synapse assembly. Our findings are summarized in

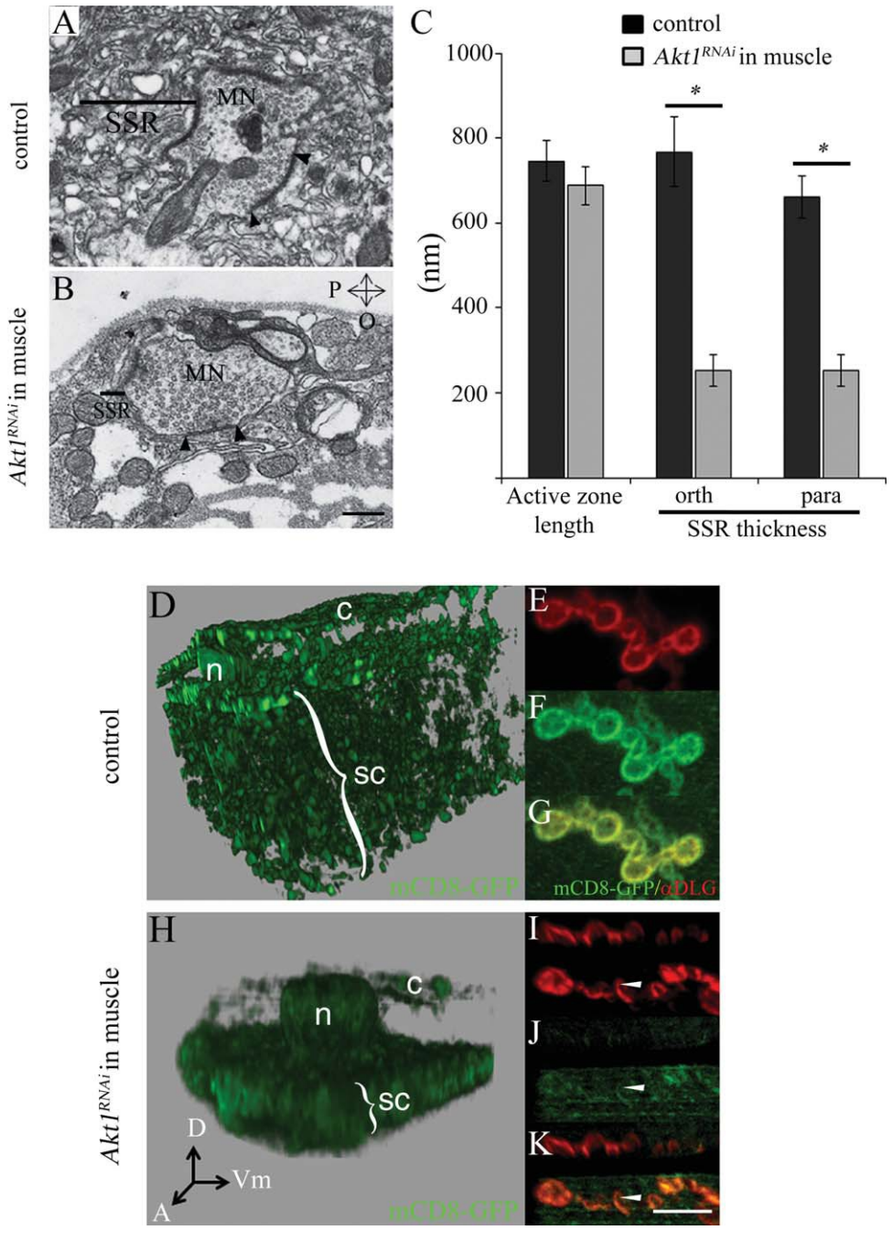

Figure 5

Figure 9. We found that Akt1 was specifically required for the correct assembly of A-type glutamate receptors. Reductions of Akt1 function either by mutation or RNA interference resulted in a loss of GluRIIA at the synapse paired with accumulation into intracellular structures. Reduction of Akt1 influenced the levels and localization of proteins shown to affect GluRIIA, Dorsal, and Cactus. Therefore, Akt1 could affect GluRIIA at least in part via control of these proteins. Akt1 was also required for the normal expansion of a specialized postsynaptic membrane compartment, the SSR. We provide evidence that Akt1 mediates its effects on SSR via control of the t-SNARE Gtaxin. RNA interference of Gtaxin did not affect GluRIIA localization, showing that the control of SSR expansion and glutamate receptor composi- tion mediated by Akt1 occurs via different molecular mechanisms.

The analysis of Akt1 reported here examined physiological, morphological, and cellular phenotypes, using both traditional Akt1 mutant alleles and cell-type directed knockdown achieved with either of two different UAS-Akt1^{RNAi} lines. The results from these different genetic tools were consistent and showed that Akt1 function is critical for both GluRIIA localization and SSR expansion. In particular, combinations of Akt1 alleles resulted in the redistribution of GluRIIA into intracellular bands, a phenotype found to be even more pronounced in muscle-directed RNAi of Akt1. This remarkable phenotype was also observed in larvae expressing both Akt1^{RNAi} and a UAS-transgene-derived GluRIIA-RFP in the muscle, the latter detected by either endogenous fluorescence or anti-RFP antibody. It was of note that fluorescent signal from the GluRIIA-RFP was reduced at the synapse but receptor mislocalization to intracellular compartments was detected only with anti-RFP antibody. Akt1-dependent events were clearly required for the proper formation of the folded RFP domain of the recombinant GluRIIA protein while the polypeptide, detected with the anti-RFP antibody was present and redirected to an alternative cellular location, as we observed for the endogenous GluRIIA. These data implicate Akt1 in processes of folding, stabilization, or assembly of GluRIIA.

A number of experiments were conducted to evaluate if Akt1 was required for the localization of specific postsynaptic proteins, or rather served a more generalized role in directing a variety of proteins to this membrane specialization. The correct localization of GluRIIB, GluRIIC, Basigin, Discs large, and Syndapin in animals with Akt1 knockdown in the

Figure 5 Muscle-specific inhibition of Akt1 affects the elaboration of the subsynaptic reticulum (SSR), and Akt1 is required for the integrity of the endomembrane system. A: Transmission electron microscopy shows SSR surrounding the motoneuron terminal in a control animal (UAS-Akt1^{RNAi}/**1**). Bar indicates approximate dimension of SSR. For both (A) and (B), the size of the SSR was determined by measuring its thickness in two-dimensions: parallel and orthogonal to the muscle surface. B: The dimensions and complexity of the SSR were dramatically reduced in Akt1-compromised larvae (24B-GAL4>UAS-Akt1^{RNAi}) without affecting the length of the presynaptic active zones (electron dense region, between two black arrowheads), where synaptic vesicles are released. C: Quantification of the length of presynaptic active zones, parallel and orthogonal SSR thicknesses. When compared with control animals, SSR thicknesses significant decreased in all dimensions with Akt1compromised (24B-GAL4>UAS-Akt1^{RNAi}). "*" denotes $p < 0.0005$, $n \geq 15$ each. P, parallel; O, orthogonal to the axis of muscle surface. D–K: To evaluate the organization of muscle membranes, mCD8-GFP, a transmembrane protein that tags cellular membranes, was used. mCD8-GFP expressed in the muscle (G14-GAL4>UAS-mCD8-GFP) localizes to membrane compartments, including plasma membrane, t-tubules, nuclear envelope, and the endoplasmic reticulum. The panels (D) (Control; G14-GAL4,UAS-mCD8-GFP/**1**) and (H) (muscle-specific Akt1 knockdown: G14-GAL4, UAS-mCD8-GFP>UAS-Akt1^{RNAi}) show 3D rendered images of serial confocal sections, representing the entire muscle cell thickness in a region where there are no synaptic boutons. The nuclear layer is located at the top of the image separating cortical (c) and subcortical (sc) membrane domains. Muscle-specific knockdown of Akt1 produced a decrease in overall muscle cell thickness and reduced the complexity of membrane compartments (H). Akt1^{RNAi} results in a more compact subcortical membrane domain and notable reduction in the cortical membrane domain compared to control animals (D). c, the cortical membrane domain; sc, the subcortical membrane domain; n, nucleus; A, anterior; D, dorsal; and Vm, ventral midline. E–G: Visualization of the SSR by mCD8-GFP, and of the postsynaptic specialization with anti-DLG antibody (red). I–K: The extent of mCD8-GFP tagged SSR was dramatically reduced (arrowheads) by loss of Akt1 function. DLG was correctly localized and modestly reduced in comparison with mCD8-GFP in these animals. Scale bar in (A and B), 0.5 mm, in (E–G) and (I–K), 5 mm.

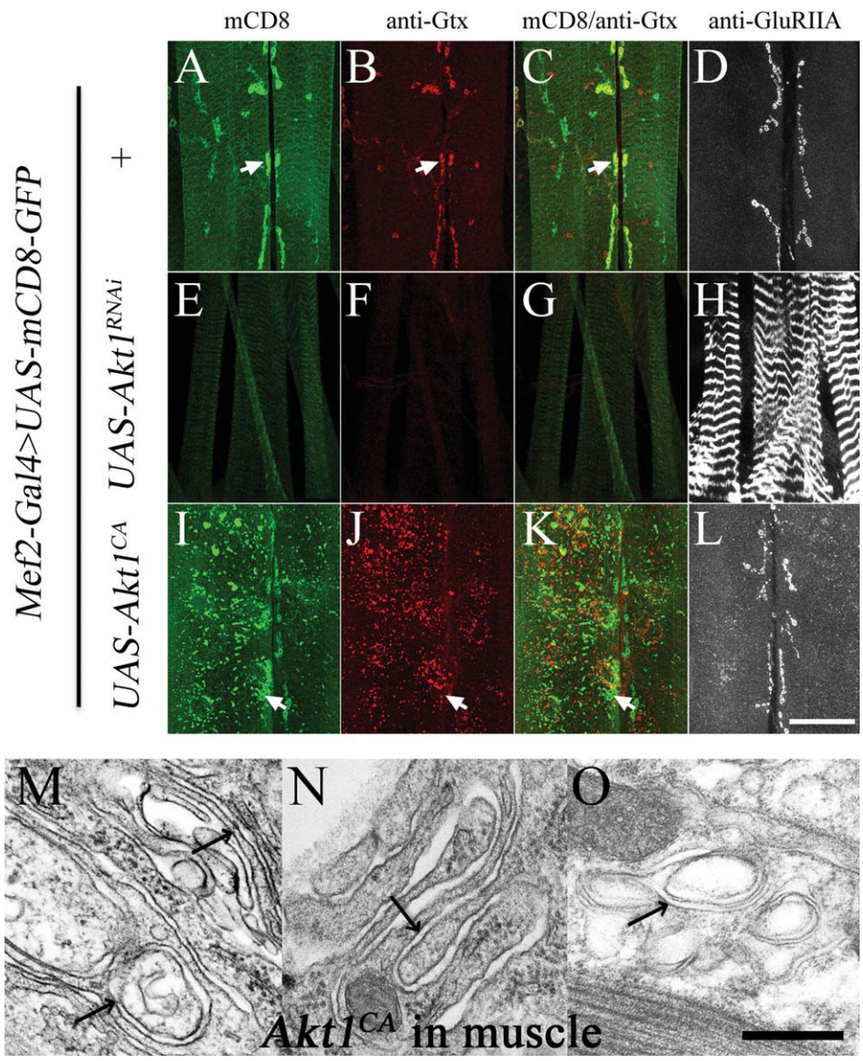

Figure 6 The localization and levels of Gtaxin at the postsynaptic specialization are Akt1-dependent, and overexpression of a constitutively active form of Akt1 creates ectopic membranes distant from the synaptic region. Gtaxin localization and levels were examined in animals with reduced Akt1 function or muscle directed expression of a constitutively active form of Akt1, $Akt1^{CA}$. All animals in this experiment also carried the muscle-specific driver Mef2-GAL4 and UAS-mCD8-GFP transgenes. Gtaxin and GluRIIA were detected with anti-Gtx (red) and anti-GluRIIA (grayscale) antibodies. Panels (A–C), (E–G), and (I–K) are each from a single animal. Panels (D), (H), and (L) are anti-GluRIIA staining each from a single larva. A–D: Control animals had no Akt1-bearing transgene either $Akt1^{RNAi}$ or $Akt1^{CA}$ (labeled as **1**). Gtaxin is concentrated at the SSR, colocalizing with mCD8-GFP (arrows). GluRIIA is also highly concentrated at the NMJ specialization. E–H: Animals expressing UAS-$Akt1^{RNAi}$ showed dramatic reductions in the levels of mCD8-GFP at the SSR (E) and loss of Gtaxin at the synapse (F), as well as mislocalization of GluRIIA (H). I–L: Overexpression of $Akt1^{CA}$ caused ectopic mCD8 patches throughout the muscle (I), as well as increased levels of Gtaxin (J). The normal distribution of Gtaxin at the SSR was lost, with mislocalized Gtaxin patches evident throughout the muscle cell (J). Correct GluRIIA localization was maintained in these animals (L). M–O: Transmission electron microscope photomicrographs show ectopic membranous structures in muscles overexpressing the constitutively active form of Akt1 (Mef2-GAL4>UAS-Akt1CA). Arrows point to infoldings of multilayered membranes in the cytosol or underneath the plasma membrane. Scale bar in (A–L), 50 mm, in (M–O), 0.1 mm.

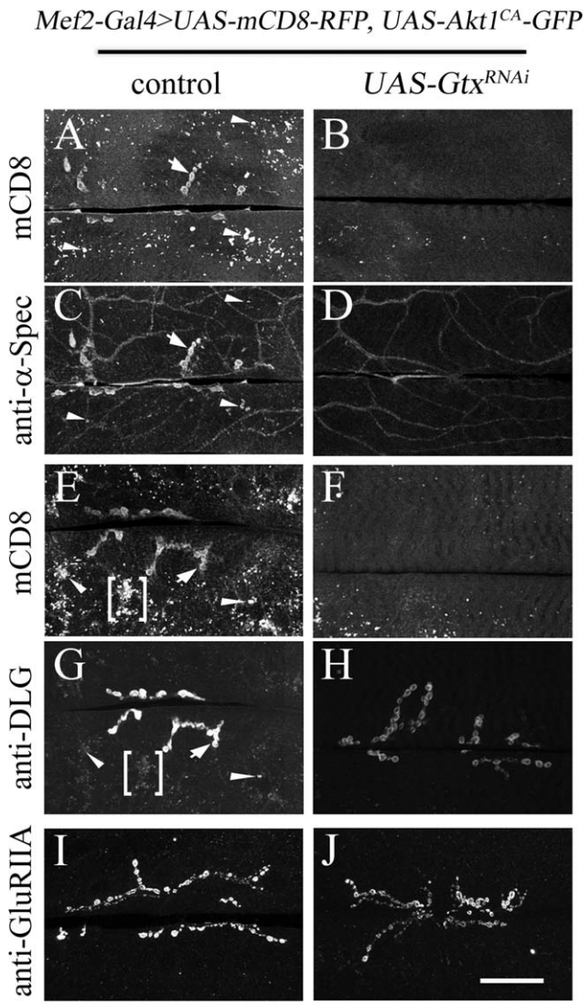

Figure 7 Gtaxin is required for ectopic membranous patches produced by expression of a constitutively activated form of Akt1. Synapse organization was assessed with mCD8-RFP and anti-a-Spectrin or anti-DLG antibody staining. All animals carried Mef2-GAL4, UAS-mCD8-RFP, UAS-Akt1^{CA}-GFP, and over either OreR as a control or UAS-Gtx^{RNAi}. Either anti-a-Spectrin or anti-DLG with mCD8-RFP images for each genotype were from the same animal, with a second preparation providing the anti-GluRIIA data. A and C: In animals with muscle-directed expression of Akt1^{CA}-GFP, ectopic patches of mCD8 were observed throughout the muscle (panel A, arrows), while leaving the SSR structure intact (on set of postsynaptic specializations shown with small arrow). Some of the ectopic mCD8 membrane patches also showed anti-a-Spectrin antibody staining (arrowheads in C). Inhibition of Gtx with RNAi abolished the mCD8 patches and greatly reduced the anti-a-Spectrin staining (panels B and D). Using anti-DLG to examine SSR structure in animals with muscle-directed expression of Akt1^{CA} also revealed that the membranous patches show some SSR-properties as evidenced by anti-DLG colocalization (arrowheads and a bracket in panels E and G). Inhibition of Gtx produced loss of mCD8-concentrated SSR membrane but not DLG localization to the postsynaptic specialization (panels F and H). As reported earlier and confirmed here, loss of Gtx did not compromise GluRIIA localization (panels I and J). Scale bar for A–J, 50 mm.

muscle demonstrated that Akt1 has specific targeting functions for GluRIIA and is not a general factor for delivery of all postsynaptic proteins. Levels of these postsynaptic proteins were reduced in Akt1^{RNAi} bearing animals, not surprisingly given the substantial size reduction in the SSR.

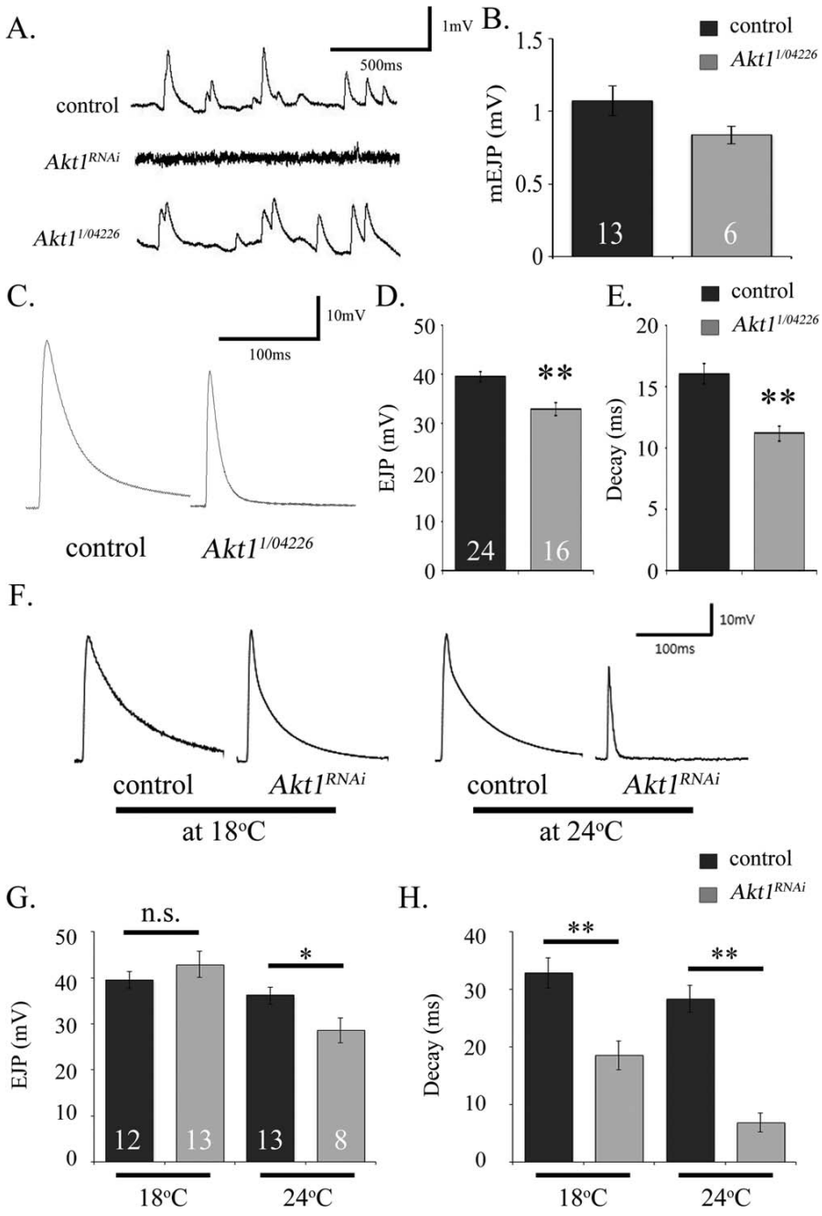

Figure 8 Akt1 is required for normal electrophysiological response at neuromuscular synapses. A: Representative traces of miniature excitatory junction potentials (mEJPs) for OreR strain (as control), Akt1 knockdown in the muscle, and $Akt1^{1}/Akt1^{04226}$ transheterozygous mutant animals. The $Akt1^{RNAi}$ expressing animals showed no readily detectable mEJP. B: $Akt1^{1}/Akt1^{04226}$ mutants, a mild hypomorphic combination of alleles, displayed somewhat reduced but not statistically significant different mEJP amplitude compared with controls ($p \backsimeq 0.08$). C: EJP responses, detected in the muscle following motoneuron stimulation for control and $Akt1^{1}/Akt1^{04226}$ mutant. D and E: $Akt1^{1}/Akt1^{04226}$ mutant larvae exhibited significantly decreased EJP amplitudes and decay time compared to control ($^{**}p < 0.005$, $n \backsimeq 24/16$). F: Traces of EJP in control (Mef2-GAL4>UAS-mCD8-GFP) and $Akt1^{RNAi}$ expressing larvae (Mef2-GAL4>UAS-$Akt1^{RNAi}$) reared at two different temperatures. G: EJP amplitude showed no difference at 18°C (low level of inhibition, n.s., no significant, $n \backsimeq 12/13$), but was significantly decreased at 24°C (greater degree if Akt1 inhibition, $^{*}p < 0.05$, $n \backsimeq 13/8$). H: Similar to the electrophysiological changes observed in the $Akt1^{1}/Akt1^{04226}$ mutant animals, EJP decay time was abbreviated in $Akt1^{RNAi}$ expressing larvae, both at 18°C or 24°C ($^{**}p < 0.005$).

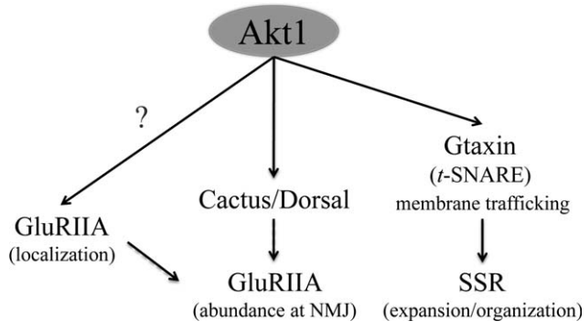

Figure 9 Model for Akt1's regulatory role at the NMJ. Akt1 selectively affects A-type glutamate receptor abundance at the NMJ. Compromising Akt1 function reduced the levels of Dorsal and Cactus at the NMJ, two potential Akt1 targets that regulate GluRIIA levels. Loss of Akt1 also results in GluRIIA mislocalization to intracellular membrane compartments, suggesting that other Akt1 targets are involved as well. Akt1-dependent subsynaptic membrane expansion is mediated through a separate pathway where the Drosophila t-SNARE protein Gtaxin acts downstream of Akt1 function.

At the Drosophila NMJ, two types of glutamate receptors have been defined by their distinct compositions and physiological properties (DiAntonio et al., 1999; DiAntonio, 2006). The shifting between A- and B-type receptors provides a mechanism for modulating postsynaptic responses to variable presynaptic inputs during development (Sigrist et al., 2002). There is considerable evidence that modulation of GluRIIA and B representation at the NMJ is governed by different signaling systems. Coracle, a homolog of protein 4.1 in Drosophila, has been shown to specifically influence the targeting of GluRIIA but not IIB (Chen et al., 2005). A physical interaction between Coracle and GluRIIA was essential for actin-dependent trafficking of GluRIIA-containing vesicles to the plasma membrane. Conversely, DLG has been shown to be required for GluRIIB but not GluRIIA localization at the NMJ (Chen and Featherstone, 2005). Our finding supports the conclusion that A and B receptor subunits are differentially regulated and show that Akt1 serves a role in A but not B subunit control.

There is evidence that the assembly and localization of GluRIIA into the postsynaptic density at the NMJ is accomplished following delivery to the plasma membrane (Broadie and Bate, 1993; Rasse et al., 2005). This conclusion is based upon the observation that fluorescence photobleaching of the entire muscle delays accumulation of new GluRIIA to synaptic sites more so than local bleaching at the NMJ (Rasse et al., 2005). The effects of Akt1 on GluRIIA localization could therefore be mediated by either regulated delivery of GluRIIA-containing vesicles to the plasma membrane, or by affecting the localization to the postsynaptic density following insertion into the plasma membrane. The accumulation of GluRIIA into an intracellular membrane compartments argues for a trafficking-based mechanism. This model is further supported by the results from the developmental timing experiments, where Akt1 function was removed during different stages in synapse assembly. Loss of Akt1 in a 2 day window early in development produced the phenotypes observed with continuous loss of Akt1, whereas a 2 day loss in third instar did not. If Akt1 simply served to retain GluRIIA at the synapse, there should have been time for new synthesis to repopulate the NMJ. Therefore, we favor a model where Akt1 affects developmental processes required for the selective delivery of GluRIIA from the endoplasmic reticulum into functional receptor units that arrive at the plasma membrane. It is notable that in mammalian systems, Akt is critical for the insulin-stimulated exocytosis of glucose transporter containing vesicles to the plasma membrane (Gonzalez and McGraw, 2006; Grillo et al., 2009). Perhaps Akt1 governs similar exocytic processes at synapses. Akt1 signaling has also shown to be essential for AMPA receptor trafficking in hippocampal neurons, further supporting a role for Akt1 in trafficking of synaptic proteins (Qin et al., 2005b; Hou et al., 2008; Pratt et al., 2011).

A striking phenotype of animals with reduced Akt1 function in muscles was a severe reduction in the SSR and disruption of intracellular membrane organization. These phenotypes were similar to those found in a Gtaxin mutant and suggested the possibility that Akt1 and Gtaxin are involved in the same cellular process (Gorczyca et al., 2007). A number of

observations reported here indicate Akt1 activity is mediated at least in part by control of Gtaxin. First, Gtaxin levels at the SSR are greatly reduced in animals with reduced Akt1 function in the muscle cells. Second, muscle-directed overexpression of a constitutively active form of Akt1 ($Akt1^{CA}$) produced ectopic membranous structures; a phenotype also observed with Gtaxin overexpression and elevated levels of Gtaxin. Third, inhibition of Gtaxin blocks the effects of the constitutively active Akt1 in the muscle cell. Gtaxin does contain a consensus site for Akt1 phosphorylation and could therefore be a direct target of Akt1 kinase activity in regulating SNARE complex assembly.

The regulatory roles of Akt1 in glutamate receptor composition and postsynaptic membrane expansion could be accomplished through separate or identical downstream effectors. The fact that Gtaxin mutants did not disrupt GluRIIA distribution suggests different downstream effectors regulated by Akt1. The regulation of GluRIIA localization by Akt1 does not involve Gtaxin but could be mediated via Dorsal and Cactus. Dorsal and Cactus influence glutamate receptor delivery and are known effectors of Akt activity in mammalian cells (Heckscher et al., 2007; Dan et al., 2008). The levels of both Dorsal and Cactus were reduced in animals with knockdown of Akt1 in the muscle. Notably, in some animals expressing $Akt1^{RNAi}$ in the muscle, Dorsal showed an altered intracellular distribution that overlapped with the mislocalized GluRIIA. However, because Dorsal and Cactus mutants are not reported to mislocalize GluRIIA into intracellular bands, Akt1 is likely to have additional downstream targets that influence GluRIIA localization and delivery to the postsynaptic specialization.

Physiological measures of synaptic transmission showed that Akt1 function is required for normal synapse function. Akt1 transheterozygous mutants ($Akt1^{1}/Akt1^{04226}$) showed reduced EJP amplitudes and altered decay kinetics of the EJP. These same phenotypes were observed in animals with muscle-specific inhibition of Akt1 function, with the severity correlating to the degree of Akt1 inhibition. These changes in EJP kinetics were not accompanied by alterations of nonvoltage-dependent membrane capacitance or resistance, suggesting that voltage-gated channels contributing to EJP rise and decay times may be affected by Akt1. These findings contrast published work with Akt1 mutant animals describing changes in long-term depression but not in EJP properties (Guo and Zhong, 2006). However, we note that our physiological studies were conducted at a higher Ca^{2+} concentration, which could account for these different measures of EJP properties in Akt1 mutants. It is important to point out that the physiological changes we document were observed in both Akt1 mutant larvae as well as animals with RNA interference of Akt1 in the muscle cell. The physiological changes we observed in Akt1 compromised animals are logical consequences of observed changes in NMJ composition. Loss of GluRIIA-containing receptors and an overall decrease in functional GluRs at the synapse could decrease the EJP amplitude. The altered EJP decay pattern in animals with reduced Akt1 is consistent with the involvement of Gtaxin, as we have documented here. Gtaxin mutants showed similar changes in EJP decay, indicating that this feature of Akt1 mediated physiological change is associated with the consequences of compromising the function of this t-SNARE.

There is a precedent for Akt-mediated regulation of neurotransmitter receptor localization to the cell surface. The NMDA receptor subunit NR2C is developmentally regulated in cerebellar granule cells and Akt-mediated phosphorylation is critical for cell surface expression of NR2C-containing receptors (Chen, 2009). Akt has also proven to be important in the elaboration of dendritic complexity in Drosophila sensory neurons, suggesting that this kinase is of general importance in the control of nervous system receptive fields (Parrish et al., 2009). Selective control of Akt or its downstream targets could provide a powerful method of influencing synaptic transmission and the receptive properties of neurons.

We are grateful to Aaron DiAntonio, David Featherstone, Mani Ramaswami, Steven Wasserman, Vivian Budnick, Fumiko Kawasaki, Richard Ordway, and Melissa Rolls as well as to the Bloomington Drosophila stock center and Vienna Drosophila RNAi Center for Drosophila stocks and antibodies. We also acknowledge Missy Hazen for technical assistance with electron microscopy and Claire Reynolds for critical reading of the manuscript. Our study was supported by grants from USDD, Martin Lenz Harrison Endowed Chair (Department of Pediatrics, University of Minnesota), and The Pennsylvania State University.

REFERENCES

Bae SS, Cho H, Mu J, Birnbaum MJ. 2003. Isoform-specific regulation of insulin-dependent glucose uptake by Akt/protein kinase B. J Biol Chem 278:49530–49536.

Besse F, Mertel S, Kittel R, Wichmann C, Rasse T, Sigrist S, Ephrussi A. 2006. Basigin controls neuromuscular junction growth and synaptic vesicle distribution and release. J Neurogenet 20:86–87.

Besse F, Mertel S, Kittel RJ, Wichmann C, Rasse TM, Sigrist SJ, Ephrussi A. 2007. The Ig cell adhesion molecule Basigin controls compartmentalization and vesicle

release at Drosophila melanogaster synapses. J Cell Biol 177:843–855.

Brand AH, Perrimon N. 1993. Targeted gene-expression as a means of altering cell fates and generating dominant phenotypes. Development 118:401–415.

Broadie K, Bate M. 1993. Innervation directs receptor synthesis and localization in Drosophila embryo synaptogenesis. Nature 361:350–353.

Brunner A, Okane CJ. 1997. The fascination of the Drosophila NMJ. Trends Genet 13:85–87.

Budnik V, Koh YH, Guan B, Hartmann B, Hough C, Woods D, Gorczyca M. 1996. Regulation of synapse structure and function by the Drosophila tumor suppressor gene dlg. Neuron 17:627–640.

Chen B-S. 2009. Growth factor-dependent trafficking of cerebellar NMDA receptors via protein kinase B/Akt phosphorylation of NR2C. Neuron 62:471–478.

Chen K, Merino C, Sigrist SJ, Featherstone DE. 2005. The 4.1 protein coracle mediates subunit-selective anchoring of Drosophila glutamate receptors to the postsynaptic actin cytoskeleton. J Neurosci 25:6667–6675.

Chen KY, Featherstone DE. 2005. Discs-large (DLG) is clustered by presynaptic innervation and regulates postsynaptic glutamate receptor subunit composition in Drosophila. BMC Biol 3:1 doi:10.1186/1741-7007-3-1.

Chen WS, Xu PZ, Gottlob K, Chen ML, Sokol K, Shiyanova T, Roninson I, et al. 2001. Growth retardation and increased apoptosis in mice with homozygous disruption of the akt1 gene. Genes Dev 15:2203–2208.

Cho H, Mu J, Kim JK, Thorvaldsen JL, Chu QW, Crenshaw EB, Kaestner KH, et al. 2001. Insulin resistance and a diabetes mellitus-like syndrome in mice lacking the protein kinase Akt2 (PKB beta). Science 292:1728–1731.

Collins CA, DiAntonio A. 2007. Synaptic development: Insights from Drosophila. Curr Opin Neurobiol 17:35–42.

Dan HC, Cooper MJ, Cogswell PC, Duncan JA, Ting JPY, Baldwin AS. 2008. Akt-dependent regulation of NF-kappa B is controlled by mTOR and Raptor in association with IKK. Genes Dev 22:1490–1500.

Datta SR, Brunet A, Greenberg ME. 1999. Cellular survival: A play in three Akts. Genes Dev 13:2905–2927.

DiAntonio A. 2006. Glutamate receptors at the Drosophila neuromuscular junction. In: Fly Neuromuscular Junction: Structure and Function, 2nd ed. Vivian Budnik and Catalina Ruiz-Canada: Elsevier Academic Press Inc., pp 165–179.

DiAntonio A, Petersen SA, Heckmann M, Goodman CS. 1999. Glutamate receptor expression regulates quantal size and quantal content at the Drosophila neuromuscular junction. J Neurosci 19:3023–3032.

Dietzl G, Chen D, Schnorrer F, Su KC, Barinova Y, Fellner M, Gasser B, et al. 2007. A genome-wide transgenic RNAi library for conditional gene inactivation in Drosophila. Nature 448:151–156.

Dimitroff B, Howe K, Watson A, Campion B, Lee HG, Zhao N, O'Connor MB, et al. 2012. Diet and energy-sensing inputs affect TorC1-mediated axon misrouting but not TorC2-directed synapse growth in a Drosophila

model of tuberous sclerosis. PLoS ONE 7(2): e30722.doi:10.1371/journal.pone.0030722.

Dudek H, Datta SR, Franke TF, Birnbaum MJ, Yao RJ, Cooper GM, Segal RA, et al. 1997. Regulation of neuronal survival by the serine-threonine protein kinase Akt. Science 275:661–665.

Easton RM, Cho H, Roovers K, Shineman DW, Mizrahi M, Forman MS, Lee VMY, et al. 2005. Role for Akt3/Protein kinase B gamma in attainment of normal brain size. Mol Cell Biol 25:1869–1878.

Featherstone DE, Rushton E, Broadie K. 2002. Developmental regulation of glutamate receptor field size by nonvesicular glutamate release. Nat Neurosci 5:141–146.

Featherstone DE, Rushton E, Rohrbough J, Liebl F, Karr J, Sheng Q, Rodesch CK, et al. 2005. An essential Drosophila glutamate receptor subunit that functions in both central neuropil and neuromuscular junction. J Neurosci 25:3199–3208.

Franke TF. 2008. PI3K/Akt: Getting it right matters. Oncogene 27:6473–6488.

Gonzalez E, McGraw TE. 2006. Insulin signaling diverges into Akt-dependent and -independent signals to regulate the recruitment/docking and the fusion of GLUT4 vesicles to the plasma membrane. Mol Biol Cell 17:4484–4493.

Gorczyca D, Ashley J, Speese S, Gherbesi N, Thomas U, Gundelfinger E, Gramates LS, et al. 2007. Postsynaptic membrane addition depends on the discs-large-interacting t-SNARE gtaxin. J Neurosci 27:1033–1044.

Gramates LS, Budnik V. 1999. Assembly and maturation of the Drosophila larval neuromuscular junction. Int Rev Neurobiol 43:93–117.

Grider MH, Park D, Spencer DM, Shine HD. 2009. Lipid Raft-targeted Akt promotes axonal branching and growth cone expansion Via mTOR and Rac1, respectively. J Neurosci Res 87:3033–3042.

Grillo CA, Piroli GG, Hendry RM, Reagan LP. 2009. Insulin-stimulated translocation of GLUT4 to the plasma membrane in rat hippocampus is PI3-kinase dependent. Brain Res 1296:35–45.

Guan B, Hartmann B, Kho YH, Gorczyca M, Budnik V. 1996. The Drosophila tumor suppressor gene, dig, is involved in structural plasticity at a glutamatergic synapse. Curr Biol 6:695–706.

Guo HF, Zhong Y. 2006. Requirement of Akt to mediate long-term synaptic depression in Drosophila. J Neurosci 26:4004–4014.

Heckscher ES, Fetter RD, Marek KW, Albin SD, Davis GW. 2007. NF-kappa B, I kappa B, and IRAK control glutarnate receptor density at the Drosophila NMJ. Neuron 55:859–873.

Hou Q, Zhang D, Jarzylo L, Huganir RL, Man HY. 2008. Homeostatic regulation of AMPA receptor expression at single hippocampal synapses. Proc Natl Acad Sci USA 105:775–780.

Jan LY, Jan YN. 1976. Properties of larval neuromuscular-junction in Drosophila melanogaster. J Physiol 262:189–214.

Jia XX, Gorczyca M, Budnik V. 1993. Ultrastructure of neuromuscular-junctions in Drosophila—Comparison of

wild-type and mutants with increased excitability. J Neurobiol 24:1025–1044.

Karr J, Vagin V, Chen KY, Ganesan S, Olenkina O, Gvozdev V, Featherstone DE. 2009. Regulation of glutamate receptor subunit availability by microRNAs. J Cell Biol 185:685–697.

Kittel RJ, Wichmann C, Rasse TM, Fouquet W, Schmidt M, Schmid A, Wagh DA, et al. 2006. Bruchpilot promotes active zone assembly, Ca^{21} channel clustering, and vesicle release. Science 312:1051–1054.

Kumar V, Fricke R, Bhar D, Reddy-Alla S, Krishnan KS, Bogdan S, Ramaswami M. 2009. Syndapin promotes formation of a postsynaptic membrane system in Drosophila. Mol Biol Cell 20:2254–2264.

Lahey T, Gorczyca M, Jia XX, Budnik V. 1994. The Drosophila tumor-suppressor gene Dlg is required for normal synaptic bouton structure. Neuron 13:823–835.

Lauterborn JC, Rex CS, Kramar E, Chen LY, Pandyarajan V, Lynch G, Gall CM. 2007. Brain-derived neurotrophic factor rescues synaptic plasticity in a mouse model of fragile 3 syndrome. J Neurosci 27:10685–10694.

Lee C-C, Huang C-C, Hsu K-S. 2011. Insulin promotes dendritic spine and synapse formation by the PI3K/Akt/mTOR and Rac1 signaling pathways. Neuropharmacology 61:867–879.

Manning BD, Cantley LC. 2007. AKT/PKB signaling: Navigating downstream. Cell 129:1261–1274.

Marrus SB, Portman SL, Allen MJ, Moffat KG, DiAntonio A. 2004. Differential localization of glutamate receptor subunits at the Drosophila neuromuscular junction. J Neurosci 24:1406–1415.

McCurdy CE, Cartee GD. 2005. Akt2 is essential for the full effect of calorie restriction on insulin-stimulated glucose uptake in skeletal muscle. Diabetes 54: 1349–1356.

Mozden SM, Rubin GM. 1999. The Berkeley Drosophila genome project gene disruption project: Single P-element insertions mutating 25% of vital Drosophila genes. Genetics 153:1491–1491.

Nakatani K, Sakaue H, Thompson DA, Weigel RJ, Roth RA. 1999. Identification of a human Akt3 (protein kinase B gamma) which contains the regulatory serine phosphorylation site. Biochem Biophys Res Commun 257:906–910.

Parrish JZ, Xu PZ, Kim CC, Jan LY, Jan YN. 2009. The microRNA bantam functions in epithelial cells to regulate scaling growth of dendrite arbors in Drosophila sensory neurons. Neuron 63:788–802.

Petersen SA, Fetter RD, Noordermeer JN, Goodman CS, DiAntonio A. 1997. Genetic analysis of glutamate receptors in Drosophila reveals a retrograde signal regulating presynaptic transmitter release. Neuron 19:1237–1248.

Pielage J, Fetter RD, Davis GW. 2006. A postsynaptic spectrin scaffold defines active zone size, spacing, and efficacy at the Drosophila neuromuscular junction. J Cell Biol 175:491–503.

Pratt KG, Zimmerman EC, Cook DG, Sullivan JM. 2011. Presenilin 1 regulates homeostatic synaptic scaling through Akt signaling. Nat Neurosci 14:1112–1114.

Qin G, Schwarz T, Kittel RJ, Schmid A, Rasse TM, Kappei D, Ponimaskin E, et al. 2005a. Four different subunits are essential for expressing the synaptic glutamate receptor at neuromuscular junctions of Drosophila. J Neurosci 25:3209–3218.

Qin Y, Zhu YH, Baumgart JP, Stornetta RL, Seidenman K, Mack V, van Aelst L, et al. 2005b. State-dependent Ras signaling and AMPA receptor trafficking. Genes Dev 19:2000–2015.

Rasse TM, Fouquet W, Schmid A, Kittel RJ, Mertel S, Sigrist CB, Schmidt M, et al. 2005. Glutamate receptor dynamics organizing synapse formation in vivo. Nat Neurosci 8:898–905.

Rawson JM, Lee M, Kennedy EL, Selleck SB. 2003. Drosophila neuromuscular synapse assembly and function require the TGF-beta type I receptor saxophone and the transcription factor mad. J Neurobiol 55:134–150.

Ruiz-Canada C, Budnik V. 2006. Introduction on the use of the Drosophila embryonic/larval neuromuscular junction as a model system to study synapse development and function, and a brief summary of pathfinding and target recognition. Int Rev Neurobiol 75:1–31.

Salinas PC. 2003. Synaptogenesis: Wnt and TGF-beta take centre stage. Curr Biol 13:R60–R62.

Schuster CM. 2006. Glutamatergic synapses of Drosophila neuromuscular junctions: A high-resolution model for the analysis of experience-dependent potentiation. Cell Tissue Res 326:287–299.

Serantes R, Arnalich F, Figueroa M, Salinas M, Andres-Mateos E, Codoceo R, Renart J, et al. 2006. Interleukin-1 beta enhances GABA(A) receptor cell-surface expression by a phosphatidylinositol 3-kinase/Akt pathway—Relevance to sepsis-associated encephalopathy. J Biol Chem 281:14632–14643.

Sigrist SJ, Thiel PR, Reiff DF, Schuster CM. 2002. The postsynaptic glutamate receptor subunit DGluR-IIA mediates long-term plasticity in Drosophila. J Neurosci 22:7362–7372.

Staveley BE, Ruel L, Jin J, Stambolic V, Mastronardi FG, Heitzler P, Woodgett JR, et al. 1998. Genetic analysis of protein kinase B (AKT) in Drosophila. Curr Biol 8:599–602.

Stewart BA, Atwood HL, Renger JJ, Wang J, Wu CF. 1994. Improved stability of Drosophila larval neuromuscular preparations in haemolymph-like physiological solutions. J Comp Physiol A 175:179–191.

Thomas U, Ebitsch S, Gorczyca M, Koh YH, Hough CD, Woods D, Gundelfinger ED, et al. 2000. Synaptic targeting and localization of discs-large is a stepwise process controlled by different domains of the protein. Curr Biol 10:1108–1117.

Tschopp O, Yang ZZ, Brodbeck D, Dummler BA, Hemmings-Mieszczak M, Watanabe T, Michaelis T, et al. 2005. Essential role of protein kinase B gamma (PKB gamma/Akt3) in postnatal brain development but not in glucose homeostasis. Development 132:2943–2954.

Wagh DA, Rasse TM, Asan E, Hofbauer A, Schwenkert I, Durrbeck H, Buchner S, et al. 2006. Bruchpilot, a protein with homology to ELKS/CAST, is required for structural

integrity and function of synaptic active zones in Drosophila. Neuron 49:833–844.

Watson RT, Pessin JE. 2006. Bridging the GAP between insulin signaling and GLUT4 translocation. Trends Bio- chem Sci 31:215–222.

Zeidler MP, Tan C, Bellaiche Y, Cherry S, Hader S, Gayko U, Perrimon N. 2004. Temperature-sensitive control of protein activity by conditionally splicing inteins. Nat Biotechnol 22:871–876.

Zhang H, Zha XM, Tan Y, Hornbeck PV, Mastrangelo AJ, Alessi DR, Polakiewicz RD, et al. 2002. Phospho- protein analysis using antibodies broadly reactive against phosphorylated motifs. J Biol Chem 277:39379–39387.